AD_____

Award Number: DAMD17-02-1-0451

TITLE: Adenovirus-Mediated p202 Gene Transfer in Breast Cancer Gene Therapy

PRINCIPAL INVESTIGATOR: Yi Ding, M.D., Ph.D.

CONTRACTING ORGANIZATION: The University of Texas M.D. Anderson Cancer Center
Houston, TX 77030

REPORT DATE: May 2005

TYPE OF REPORT: Final

20060215 096

PREPARED FOR: U.S. Army Medical Research and Materiel Command
Fort Detrick, Maryland 21702-5012

DISTRIBUTION STATEMENT: Approved for Public Release;
Distribution Unlimited

The views, opinions and/or findings contained in this report are those of the author(s) and should not be construed as an official Department of the Army position, policy or decision unless so designated by other documentation.

REPORT DOCUMENTATION PAGE

Form Approved
OMB No. 0704-0188

Public reporting burden for this collection of information is estimated to average 1 hour per response, including the time for reviewing instructions, searching existing data sources, gathering and maintaining the data needed, and completing and reviewing this collection of information. Send comments regarding this burden estimate or any other aspect of this collection of information, including suggestions for reducing this burden to Department of Defense, Washington Headquarters Services, Directorate for Information Operations and Reports (0704-0188), 1215 Jefferson Davis Highway, Suite 1204, Arlington, VA 22202-4302. Respondents should be aware that notwithstanding any other provision of law, no person shall be subject to any penalty for failing to comply with a collection of information if it does not display a currently valid OMB control number. **PLEASE DO NOT RETURN YOUR FORM TO THE ABOVE ADDRESS.**

1. REPORT DATE *(DD-MM-YYYY)*
01-05-2005

2. REPORT TYPE
Final

3. DATES COVERED *(From - To)*
1 May 2002 – 30 Apr 2005

4. TITLE AND SUBTITLE
Adenovirus-Mediated p202 Gene Transfer in Breast Cancer Gene Therapy

5a. CONTRACT NUMBER

5b. GRANT NUMBER
DAMD17-02-1-0451

5c. PROGRAM ELEMENT NUMBER

5d. PROJECT NUMBER

5e. TASK NUMBER

5f. WORK UNIT NUMBER

6. AUTHOR(S)
Yi Ding, M.D., Ph.D.

E-mail: yiding@mdanderson.org

7. PERFORMING ORGANIZATION NAME(S) AND ADDRESS(ES)

The University of Texas M.D. Anderson
Cancer Center
Houston, TX 77030

8. PERFORMING ORGANIZATION REPORT NUMBER

9. SPONSORING / MONITORING AGENCY NAME(S) AND ADDRESS(ES)
U.S. Army Medical Research and Materiel Command
Fort Detrick, Maryland 21702-5012

10. SPONSOR/MONITOR'S ACRONYM(S)

11. SPONSOR/MONITOR'S REPORT NUMBER(S)

12. DISTRIBUTION / AVAILABILITY STATEMENT
Approved for Public Release; Distribution Unlimited

13. SUPPLEMENTARY NOTES
Original contains color plates: All DTIC reproductions will be in black and white.

14. ABSTRACT
Abstract follows.

15. SUBJECT TERMS
Ad-p202, IFIX, HIN-200 family, gene therapy, p53, HDM2

16. SECURITY CLASSIFICATION OF:			17. LIMITATION OF ABSTRACT	18. NUMBER OF PAGES	19a. NAME OF RESPONSIBLE PERSON
a. REPORT	b. ABSTRACT	c. THIS PAGE			19b. TELEPHONE NUMBER *(include area code)*
U	U	U	UU	85	

ABSTRACT

The main goal of this project is to study the anti-tumor activity of p202 (aim 1), the potential application to breast cancer gene therapy (aim 2) and the anti-tumor activity of IFIX (aim 3). Our studies show that Ad-p202 infection induces growth inhibition and sensitize breast cancer cells to TNF-α induced apoptosis. In addition, we demonstrate for the first time that Ad-p202 infection induces apoptosis. More impoetantly, we show the efficacy of Ad-p202 treatment on breast cancer xenograft models.

In search for the potential human ortholog of mouse p202, we identified a new human HIN-200 gene , IFIX (IFN-Inducible protein X). We found that the expression of IFIX is reduced in breast tumor tissues and breast cancer cell lines and that the enforced expression of IFIX in breast cancer cell lines reduces their growth and tumorigenicity. We also demonstrate the treatment efficacy of an IFIX-based gene therapy in an orthotopic breast cancer model.

To investigate the mechanism of the IFIX α1-mediated tumor suppression, we found a novel interaction between IFIX α1 and HDM2. Importantly, IFIXα1 destabilizes HDM2 leading to increased p53 stability and enhanced p53-mediated transcriptional activity. Furthermore, we showed that IFIXα1 promotes the ubiquitination of HDM2. Our data suggest that IFIXα1 functions as a tumor suppressor by negatively regulating HDM2. They also suggest that IFIXα1 mediates a novel crosstalk between IFN signaling pathway and HDM2-p53 auto-regulatory loop, and that may contribute in part to the IFN-induced anti-tumor activity in certain cancers.

Table of Contents

Cover.....1

SF 298.....2

Table of Contents.....3

Introduction.....4

Body.....4

Key Research Accomplishments.....5

Reportable Outcomes.....6

Conclusions.....6

References.....7

Appendices.....9

Introduction

The hematopoietic interferon (IFN) inducible nuclear protein (HIN-200) family are IFN-inducible proteins that share a signature 200-amino acid motif of type *a* and/or *b*. Three human (IFI16, MNDA and AIM2) and four mouse (p202, p203, p204, and D3) HIN-200 family proteins have been identified. (1-4). Genes encoding HIN-200 family proteins in both mouse and human are located at chromosome 1q21-23 and form a gene cluster (1, 3). HIN-200 proteins are primarily nuclear proteins involved in transcriptional regulation of genes important for cell cycle control, differentiation, and apoptosis (1, 3, 4). Our previous studies have shown that p202 suppressed tumor growth, reduced tumorigenicity, and suppressed metastasis and tumor angiogenesis of many human cancer cell lines (5-7).

This project is to study the anti-tumor activity of p202 (aim1) and its potential application to breast cancer gene therapy (aim2). Aim 3 is based on our recent discovery of a novel human HIN-200 gene, IFIX (IFN-Inducible protein X). In search for the potential human ortholog of mouse p202, we cloned a new member of the human HIN-200 protein family, IFIX, and show that IFIX-α1, the longest isoform of IFIX, function as a tumor suppressor.

Body

A. Objectives (New objective 3 has been added)

1) Determine the Ad-p202-mediated anti-tumor activities *in vitro*.
2) Determine the Ad-p202-mediated anti-tumor activities *in vivo*.
3) Determine the anti-tumor activity of IFIX.

B. Studies and results

In the past 3 years, we demonstrated the anti-tumor activity of Ad-p202 *in vitro* and in *vivo* (Clinical Cancer Res., 8:3290-3297, 2002). In addition, we identified a new member of the human HIN-200 protein family, IFIX (IFN-Inducible protein X), and demonstrated its anti-tumor activity in breast cancer (Oncogene, 23:4556-4566, 2004). Furthermore, we found that IFIX-α1 up-regulates p53 by promoting HDM2 destabilization (please see the attached manuscript).

The progress of each objective is discussed below:

Objective 1: Determine the Ad-p202-mediated anti-tumor activities *in vitro*.

We found that Ad-p202 infection induces growth inhibition and sensitize breast cancer cells to TNF-α induced apoptosis. In addition, we demonstrate for the first time that Ad-p202 infection induces apoptosis and that activation of caspases is required for the full apoptotic affect. (Clinical Cancer Res., 8:3290-3297, 2002).

Objective 2: Determine the Ad-p202-mediated anti-tumor activities *in vivo*.

To test the efficacy of Ad-p202 *in vivo*, we performed *in vivo* tumorigenesis on female nude mice. The tumor bearing mice were treated with Ad-p202 via intra-tumor or tail vein injection. Our results showed Ad-p202 treatment by either route yielded significant efficacy. The therapeutic effect was associated with an increased apoptosis in Ad-p202-treated tumors

and that is consistent to what has been observed *in vitro*. Together, our results confirm the feasibility of using Ad-p202 as a therapeutic agent in breast cancer treatment. (Clinical Cancer Res., 8:3290-3297, 2002.)

Objective 3: Determine the anti-tumor activity of IFIX.

We identified IFIX as a new member of HIN-200 family. Six different alternatively spliced forms of mRNA are transcribed from the IFIX gene. The IFIX proteins are primarily localized in the nucleus. They share a common N-terminal region that contains a predicted pyrin domain and a putative nuclear localization signal. Interestingly, the expression of IFIX was reduced in most human breast tumors and breast cancer cell lines. Expression of IFIXα1, the longest isoform of IFIX, in human breast cancer cell lines reduced their anchorage-dependent and -independent growth *in vitro* and tumorigenicity in nude mice. Moreover, a liposome-mediated IFIXα1 gene transfer suppressed the growth of already-formed tumors in a breast cancer xenograft model. IFIXα1 appears to suppress the growth of breast cancer cells in a pRB- and p53-independent manner by increasing the expression of the cyclin-dependent kinase inhibitor $p21^{CIP1}$, which leads to the reduction of the kinase activity of both Cdk2 and $p34^{Cdc2}$. Our results show that IFIXα1 possesses a tumor suppressor activity (Oncogene, 23:4556-4566, 2004).

To understand how IFIX α1 function as a tumor suppressor, we searched IFIX α1 interacting proteins and found that IFIXα1 binds and destabilizes HDM2, a principal negative regulator of p53. The HDM2 RING finger domain, which possesses E3 ligase activity, is required for the IFIXα1-mediated HDM2 destabilization. This result is supported by the observation that IFIXα1 induces the ubiquitination of HDM2. As expected, the down regulation of HDM2 by IFIXα1 leads to induction of p53 and activation of p53 target gene (e.g., $p21^{CIP1}$). Moreover, the positive regulation of p53 by IFIXα1 can be observed only in p53-/- MEF but not in p53-/-, mdm2-/- double knockout MEF. Together, these results suggest that IFIXα1 function as a tumor suppressor by negatively regulating HDM2.

Key Research Accomplishments:

*Ad-p202-mediated anti-tumor activities *in vitro*: Ad-p202 infection induces growth inhibition and sensitize breast cancer cells to TNF-α induced apoptosis; Ad-p202 infection induces apoptosis (Clinical Cancer Res., 8:3290-3297, 2002.)

*Ad-p202-mediated anti-tumor activities *in vivo*: we performed *in vivo* tumorigenesis on female nude mice. The tumor bearing mice were treated with Ad-p202 via intra-tumor or tail vein injection. Our results showed Ad-p202 treatment by either route yielded significant efficacy (Clinical Cancer Res., 8:3290-3297, 2002.)

*Anti-tumor activity of IFIX:

1. Cloning of a new HIN-200 family member, IFIX.
2. IFIX is down-regulated in breast tumors.
3. IFN-γ treatment suppresses the growth of MCF-7 and MDA-MB-468 breast cancer cells, which correlated with the induction of IFIX.
4. Expression of IFIX reduces anchorage-dependent and -independent cell growth *in vitro* and suppresses tumorigenicity *in vivo*.

5. Liposome-mediated IFIX gene transfer suppresses the growth of already-formed tumors in a breast cancer xenograft model.
6. IFIX-α 1 up-regulate p21.
7. IFIXα1 binds and destabilizes HDM2, the HDM2 RING finger domain, which possesses E3 ligase activity, is required for the IFIXα1-mediated HDM2 destabilization.
8. IFIXα1 induces the ubiquitination of HDM2.
9. The down regulation of HDM2 by IFIXα1 leads to induction of p53 and activation of p53 target gene (e.g., $p21^{CIP1}$).
10. The positive regulation of p53 by IFIXα1 can be observed only in p53-/- MEF but not in p53-/-, mdm2-/- double knockout MEF.

#1-6: Oncogene, 23:4556-4566, 2004.
#7-10: please see the attached manuscript.

Reportable Outcomes:

1. Publications:

Yi Ding, Yong Wen, Bill Spohn, Li Wang, Weiya Xia, Ka Yin Kwong, Ruping Shao, Zheng Li, Gabriel N. Hortobagyi, Mien-Chie Hung, and Duen-Hwa Yan. Proapoptotic and antitumor activities of Adenovirus-mediated p202 gene transfer. Clin. Cancer Res. 8:3290-3297, 2002.

Yi Ding, Li Wang, Li-Kuo Su, Jennifer A. Frey, Ruping Shao, Kelly K. Hunt, and Duen-Hwa Yan. Anti-tumor activity of IFIX, a novel interferon-inducible HIN-200 gene, in breast cancer. Oncogene 23: 4556-4566, 2004.

2. Manuscript:

Yi Ding, Jin-Fong Lee, Hua Lu, and Duen-Hwa Yan. Interferon-inducible protein IFIXα1 function as a negative regulator of HDM2 (Submitted).

3. US Patent pending

Title: IFIX, a novel HIN-200 protein, for cancer therapy.
Inventors: Duen-Hwa Yan, **Yi Ding**, Li Wang, and Mien-Chie Hung.

Training accomplishments:
1) A poster presentation (Abstract No. 3511) at 95th AACR meeting, Orlando, FL.
2) A poster presentation at Trainee Recognition 2004, U. T. M. D. Anderson Cancer center.
3) Attended department seminars (12:00 am-1:00pm, Wednesday), institutional seminars (12:00 am-1:00pm, Friday) and other seminars.

Conclusions:

Our studies show that Ad-p202 infection induces growth inhibition and sensitize breast cancer cells to TNF-α induced apoptosis. In addition, we demonstrate for the first time that Ad-p202 infection induces apoptosis and that activation of caspases is required for the full apoptotic affect. More impoetantly, we show the efficacy of Ad-p202 treatment on breast

cancer xenograft models. Together, our results confirm the feasibility of using Ad-p202 as a therapeutic agent in breast cancer treatment.

In search for the potential human ortholog of mouse p202, we identified a new member of the human HIN-200 protein family, IFIX (IFN-Inducible protein X). We found that the expression of IFIX is reduced in breast tumor tissues and breast cancer cell lines and that the enforced expression of IFIX in breast cancer cell lines reduces their growth and tumorigenicity. We also demonstrate the treatment efficacy of an IFIX-based gene therapy in an orthotopic breast cancer model.

To investigate the mechanism of the IFIXα1-mediated tumor suppression, we found a novel interaction between IFIXα1 and HDM2. Importantly, IFIXα1 destabilizes HDM2 leading to increased p53 stability and enhanced p53-mediated transcriptional activity. Furthermore, we showed that IFIXα1 promotes the ubiquitination of HDM2, thus, providing a plausible mechanism for the up regulation of p53 and the down regulation of HDM2 by IFIXα1. Our data suggest that IFIXα1 functions as a tumor suppressor by negatively regulating HDM2. They also suggest that IFIXα1 mediates a novel crosstalk between IFN signaling pathway and HDM2-p53 auto-regulatory loop, and that may contribute in part to the IFN-induced anti-tumor activity in certain cancers.

Together, our data suggest that both Ad-p202 and IFIX may be further developed into efficient therapeutic agents for human cancer gene therapy.

References:

1. Lengyel, P., Choubey, D., Li, S.-J., & Datta, B. (1995) *Semi Virol* **6,** 203-213.
2. Landolfo, S., Gariglio, M., Gribaudo, G. & Lembo, D. (1998) *Biochimie* **80,** 721-728.
3. Johnstone, R. W. & Trapani, J. A. (1999) *Mol Cell Biol* **19,** 5833-5838.
   Choubey, D. (2000) *J Biol Regul Homeost Agents* **14,** 187-192.
4. Yan, D.-H., Wen, Y., Spohn, B., Choubey, D., Gutterman, J. U., & Hung, M.-C. (1999) Oncogene**18**, 807-811.
5. Wen, Y., Yan, D.-H., Wang, B., Spohn, B., Ding, Y., Shao, R., Zhou, Y., Xie, K. &Hung, M-C. (2001) Cancer Res **61**, 7142-7147.
6. Wen, Y., Yan, D. H., Spohn, B., Deng, J., Lin, S. Y. & Hung, M. C. (2000) Cancer Res **60**, 42-46.
7. Xian-Yong Ma, Hong Wang, Bo Ding, Haihong Zhong, Sankar Ghosh, and Peter Lengyel. (2003) J.Biol.Chem. **278**, 23008-23019.

List of personnel receiving pay from this research effort:

Yi Ding

Appendices

1. Publications:

Yi Ding, Yong Wen, Bill Spohn, Li Wang, Weiya Xia, Ka Yin Kwong, Ruping Shao, Zheng Li, Gabriel N. Hortobagyi, Mien-Chie Hung, and Duen-Hwa Yan. Proapoptotic and antitumor activities of Adenovirus-mediated p202 gene transfer. Clin. Cancer Res. 8:3290-3297, 2002.

Yi Ding, Li Wang, Li-Kuo Su, Jennifer A. Frey, Ruping Shao, Kelly K. Hunt, and Duen-Hwa Yan. Anti-tumor activity of IFIX, a novel interferon-inducible HIN-200 gene, in breast cancer. Oncogene 23: 4556-4566, 2004.

2. Manuscript:

Yi Ding, Jin-Fong Lee, Hua Lu, and Duen-Hwa Yan. Interferon-inducible protein IFIXα1 function as a negative regulator of HDM2 (Submitted).

Proapoptotic and Antitumor Activities of Adenovirus-mediated p202 Gene Transfer[1]

Yi Ding, Yong Wen, Bill Spohn, Li Wang, Weiya Xia, Ka Yin Kwong, Ruping Shao, Zheng Li, Gabriel N. Hortobagyi, Mien-Chie Hung, and Duen-Hwa Yan[2]

Departments of Molecular and Cellular Oncology [Y. D., Y. W., B. S., L. W., W. X., K. Y. K., R. S., Z. L., M-C. H., D-H. Y.], Breast Medical Oncology [G. N. H.], and Surgical Oncology [M-C. H., D-H. Y.]. The University of Texas M. D. Anderson Cancer Center, Houston, Texas 77030

ABSTRACT

Purpose and Experimental Design: **p202, a mouse IFN-inducible protein, is a member of the 200-amino acid repeat family. Enforced p202 expression in stable cancer cell lines resulted in growth inhibition *in vitro* and tumor suppression *in vivo*. However, to study the immediate effect of p202 and test the potential efficacy of p202 treatment, an efficient gene delivery system for p202 is required. For these purposes, an adenoviral vector expressing the p202 gene (Ad-p202) was generated. We examined the effects of Ad-p202 infection on human breast cancer cells. Furthermore, we tested the efficacy of Ad-p202 treatment on breast and pancreatic cancer xenograft models.**

Results: **We found that Ad-p202 infection induces growth inhibition and sensitizes the otherwise resistant cells to tumor necrosis factor α-induced apoptosis. In addition, we demonstrated for the first time that Ad-p202 infection induces apoptosis and that activation of caspases is required for the full apoptotic effect. More importantly, we showed the efficacy of Ad-p202 treatment on breast cancer xenograft models, and this antitumor effect correlated well with enhanced apoptosis in Ad-p202-treated tumors.**

Conclusions: **We conclude that Ad-p202 is a potent growth-inhibitory, proapoptotic, and tumor-suppressing agent. Ad-p202 may be further developed into an efficient therapeutic agent for human cancer gene therapy.**

INTRODUCTION

IFN is known to exert antiproliferative and antiviral actions. It has both direct and indirect (immunological) antitumor activity in several human malignancies, including leukemia and lymphomas as well as solid tumors. Aside from the therapeutic effects of IFN in certain clinical settings, there are also undesirable side effects (*e.g.,* fever, chills, anorexia, and anemia) associated with the high-dose IFN treatment that is often required to obtain a significant response (1, 2). This has hampered IFN as an effective anticancer agent. In an attempt to circumvent this potential drawback and maintain the benefit of IFN-mediated antitumor activity, we have begun to explore the possibility of using an IFN-inducible protein, p202, as a potential therapeutic agent (3–5). p202 is a mouse IFN-inducible, chromatin-associated protein. It belongs to the 200-amino acid repeat family (6, 7). The unique feature of p202 is illustrated by its ability to interact with several important transcriptional regulators that include E2Fs, Rb, pocket proteins p130 and p107, Fos/Jun, c-Myc, NF-κB,[3] and p53BP-1 (reviewed in Ref. 8), resulting in transcriptional repression of genes that are upregulated by these transcriptional regulators. The exact role of p202 in the IFN-mediated signal pathway is not well defined. However, consistent with the multiple antitumor activities of IFN (9), enforced expression of p202 in stable murine fibroblasts and human cancer cell lines leads to retardation of cell growth and suppression of transformation phenotype (3, 5, 10, 11). Furthermore, breast cancer cells stably transfected with p202 are sensitized to TNF-α-induced apoptosis (5), and that effect is associated with inactivation of the TNF-α-induced NF-κB via p202-NF-κB interaction. We postulated that p202 sensitizes cancer cells to TNF-α-induced apoptosis by inactivating NF-κB, which, in turn, turns off NF-κB-activated antiapoptotic gene expression, leading to enhanced TNF-α-induced cell killing (5).

To generate a p202-based therapeutic agent for efficacy study in animal models and a tool to study the biological function of p202, we constructed Ad-p202. In this study, we

Received 1/22/02; revised 6/26/02; accepted 6/27/02.

The costs of publication of this article were defrayed in part by the payment of page charges. This article must therefore be hereby marked *advertisement* in accordance with 18 U.S.C. Section 1734 solely to indicate this fact.

[1] Supported by the University Cancer Foundation at the University of Texas M. D. Anderson Cancer Center, Department of Defense Grant DAMD17-99-1-9270, and Texas Advanced Technology Program under Grant 003657-0082-1999 (to D-H. Y.); NIH Grant CA77858 and Department of Defense Grants DAMD17-00-1-0312 and DAMD17-01-1-0071 (to M-C. H.); the Breast Cancer Research Foundation/Estee Lauder Foundation (G. N. H. and M-C. H.); and Cancer Center Core Grant 16672. Y. W. is a recipient of a predoctoral fellowship from the Department of Defense Breast Cancer Research Training Grant DMAD17-99-1-9264.

[2] To whom requests for reprints should be addressed, at Department of Molecular and Cellular Oncology, The University of Texas M. D. Anderson Cancer Center, 1515 Holcombe Boulevard, Houston, TX 77030. Phone: (713) 792-3677; Fax: (713) 794-0209; E-mail: dyan@mdanderson.org.

[3] The abbreviations used are: NF-κB, nuclear factor κB; TNF-α, tumor necrosis factor α; i.t., intratumor; CMV, cytomegalovirus; GFP, green fluorescence protein; MTT, 3-(4,5-dimethylthiazol-2-yl)-2,5-diphenyltetrazolium bromide; MOI, multiplicity of infection; PARP, poly-(ADP-ribose) polymerase; pfu, plaque-forming unit(s); TUNEL, terminal deoxynucleotidyl transferase-mediated dUTP nick end labeling; PI, postinfection; fmk, fluoromethyl ketone; Z-VAD, N-benzyloxycarbonyl-Val-Ala-Asp; Z-DEVD, N-benzyloxycarbonyl-Asp-Glu-Val-Asp.

show that Ad-p202 infection of breast cancer cells resulted in growth inhibition and sensitization to TNF-α-induced apoptosis. Interestingly, we found that Ad-p202 infection alone induces apoptosis in breast cancer cells, and the activation of caspases is critical for this process. More importantly, we demonstrated the efficacy of Ad-p202 treatment in human breast cancer xenograft models through either i.t. or i.v. injection. This antitumor activity correlated well with p202 expression and apoptosis in Ad-p202-treated tumors. Together, our results suggest that Ad-p202 is a potent growth-inhibitory, proapoptotic, antitumor agent that could be further developed to become an effective therapeutic agent for cancer gene therapy treatment.

MATERIALS AND METHODS

Generation of Ad-p202. Ad-p202 was constructed according to the protocol described previously (12). p202 cDNA (11) was subcloned into an adenovirus vector (pAdTrack-CMV) that carries a CMV promoter-driven GFP. A separate CMV promoter directs p202 cDNA. A control virus, an adenoviral vector expressing luciferase gene and GFP (Ad-Luc), was likewise generated. The expression of GFP gene enabled us to monitor the infection efficiency by direct observation using a fluorescence microscope.

***In Vitro* Growth Assays.** MDA-MB-468 human breast cancer cells were maintained in DMEM/Ham's F-12 (HyClone Laboratories, Inc.) supplemented with 10% (v/v) fetal bovine serum. MTT is a pale yellow substrate that can be cleaved by living cells (but not dead cells) to yield a dark blue formazan product. The extent of MTT cleavage determined colorimetrically (at 570 nm) can be used to measure cell proliferation. Briefly, 2×10^3 cells were plated in 96-well culture plates in 0.1 ml of culture medium. Ad-p202 or Ad-Luc was added at a MOI of 200 on the next day. At the different times indicated, 20 μl of MTT (5 mg/ml stock solution) were added to each well. Cells were cultured for an additional 2 h, and then 100 μl of lysis buffer [20% SDS in 50% *N,N*-dimethylformamide (pH 4.7)] were added to each well, followed by 5 h of incubation, and then absorbance was measured at 570 nm. [^{3}H]Thymidine incorporation assay was performed as described previously (13).

Apoptosis Assays. For flow cytometry analysis, cells were collected at the indicated times PI, washed once with PBS, and suspended in 0.5 ml of PBS containing 0.1% (v/v) Triton X-100 for nuclei preparation. The suspension was filtered through a nylon mesh and then adjusted to a final concentration of 0.1% (w/v) RNase and 50 μg/ml propidium iodide. Apoptotic cells were quantified by FACScan cytometer. The DNA fragmentation assay was carried out as described previously (13).

Western Blot Analysis. MDA-MB-468 cells treated with or without TNF-α (R&D Systems, Inc., Minneapolis, MN) were infected with Ad-p202 or Ad-Luc at a MOI of 200. Seventy-two h PI, cells were lysed with radioimmunoprecipitation assay lysis buffer. The protein extracts were subjected to SDS-PAGE followed by Western blotting according to the procedure described previously (5). Goat anti-p202 polyclonal antibody and anti-PARP antibody were obtained from Santa Cruz Biotechnology (Santa Cruz, CA) and BD Transduction Laboratories (Lexington, KY), respectively. Caspase inhibitors Z-VAD and Z-DEVD-fmk were purchased from Enzyme Systems Products (Livermore, CA).

Gel-Shift Assay. The NF-κB gel-shift assay was performed as described previously (13).

Ad-p202 Gene Therapy in Human Cancer Xenograft Models. For the orthotopic breast cancer xenograft model, MDA-MB-468 cells (2×10^6 cells) were implanted in mammary fat pads (2 tumors/mouse) of female nude mice. Tumor-bearing mice were divided into two treatment groups: group 1, Ad-Luc; and group 2, Ad-p202. For i.t. injection, 1×10^9 pfu viruses/treatment was administered. Treatment started when tumor reached 0.3 cm in diameter with a treatment schedule of twice a week for 7 weeks and once a week thereafter. For tail vein injection, 5×10^8 pfu viruses/treatment were administered. Treatment started when tumor reached 0.5 cm in diameter with a treatment schedule of twice a week for 5 weeks and once a week thereafter.

Immunohistochemical Analysis of p202 Expression and Apoptosis. Mice were sacrificed 24 h after the last treatment. Tumors obtained from Ad-p202- or Ad-Luc-treated mice bearing either breast or pancreatic tumors were then excised and fixed with formalin and embedded in paraffin. Immunohistochemical analysis of p202 protein expression was performed according to the protocol described previously (14). Tumor sections were incubated with goat polyclonal antibody specific for p202 (Santa Cruz Biotechnology) followed by incubation with biotinylated rabbit antigoat IgG and subsequent incubation with avidin-biotin peroxidase before visualization. TUNEL assay was performed to detect the ends of degraded DNA fragments induced by apoptosis according to the protocol described previously (15).

RESULTS

Ad-p202 Mediates p202 Expression in Breast Cancer Cells. To test the efficiency and monitor the expression of p202 protein by Ad-p202 infection, we infected MDA-MB-468 breast cancer cells with either Ad-p202 or Ad-Luc followed by fluorescence microscopy and Western blot analysis, respectively. As shown in Fig. 1*A*, Ad-p202 and Ad-Luc infection at a MOI of 200, at 24-h PI, exhibited >90% infection efficiency as indicated by the GFP-positive cells shown in a representative field (Fig. 1*A*, *right panels*). The same cells are shown in phase-contrast images (Fig. 1*A*, *left panels*). The mock-infected cells (*Control*) showed no GFP expression. In addition to MDA-MB-468, we found that Ad-p202 could infect a panel of other human breast cancer cell lines (*e.g.*, MDA-MB-453, MDA-MB-435, MDA-MB-231, and MCF-7), albeit with various infection efficiency rates (data not shown). We chose the MDA-MB-468 cell line for subsequent studies because it is tumorigenic in the mouse xenograft model and has relatively high infection efficiency by Ad-p202. The expression of p202 protein in Ad-p202-infected cells was further analyzed by Western blot using p202-specific antibody. Fig. 1*B* shows that whereas the mock- and Ad-Luc-infected cells have no p202 expression, Ad-p202 infection efficiently directed p202 expression in MDA-MB-468 cells in a dose-dependent manner. These results clearly demonstrate that Ad-p202 infection adequately directs p202 expression in MDA-MB-468 cells.

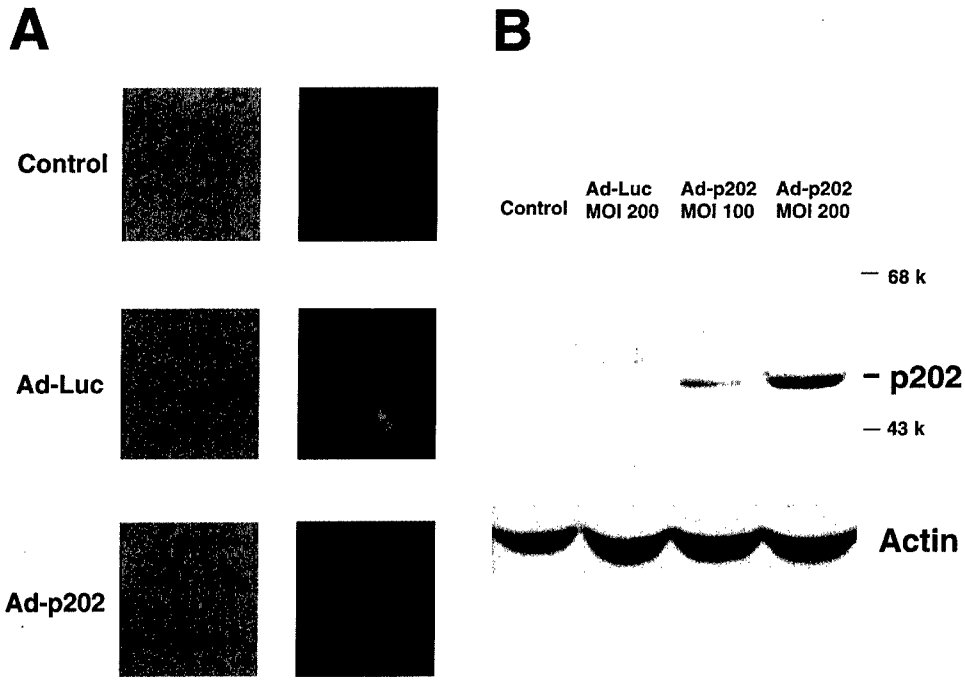

Fig. 1 Ad-p202 construction, p202 expression, and infection efficiency. *A,* Ad-p202 was generated according to the protocol described previously (12). The pAdTrack-CMV vector contains two independent CMV promoter-driven transcription units, one for GFP and one for p202 cDNA. MDA-MB-468 human breast cancer cells were infected by Ad-Luc or Ad-p202 at a MOI of 200. Twenty-four h PI, >90% of cells were found to be GFP positive as visualized by fluorescence microscopy (*right panels*), indicating that the infection efficiency is >90%. *Left panels,* phase-contrast microscopy. *Control,* mock-infected cells. *B,* p202 protein is expressed in Ad-p202 infected cells. MDA-MB-468 cells infected with Ad-Luc or Ad-p202 for 72 h were analyzed for p202 protein expression by Western blot. *Control,* mock-infected cells. Actin protein was used as an equal loading control.

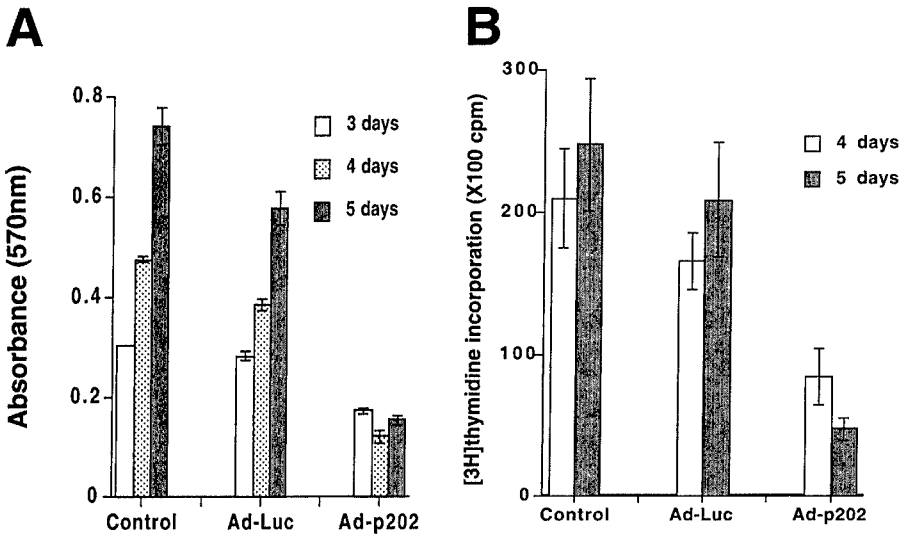

Fig. 2 Ad-p202 infection inhibits cell proliferation. MDA-MB-468 cells were infected with Ad-Luc or Ad-p202 at a MOI of 200. Cell growth was monitored at the indicated PI time (3–5 days) by (*A*) MTT assay [means ± SD (n = 3)] or (*B*) [^{3}H]thymidine incorporation assay; data are presented as the means of quadruplicates.

Ad-p202 Infection Reduces Breast Cancer Cell Growth. To assess the effect of Ad-p202 infection on cell growth, we infected MDA-MB-468 cells with either Ad-p202 or Ad-Luc followed by *in vitro* growth assays such as the MTT assay and [^{3}H]thymidine incorporation assay at different time points, *i.e.*, 3–5 days PI. As shown in Fig. 2, whereas the mock infection (*Control*) and Ad-Luc infection have no growth-inhibitory effect on MDA-MB-468 cells, Ad-202 infection significantly hampered cell growth (Fig. 2*A*) and DNA synthesis rates (Fig. 2*B*). This observation strongly indicates that Ad-p202 infection inhibits cell growth in breast cancer cells and is congruent with our previous findings using stable cancer cell lines (3, 5).

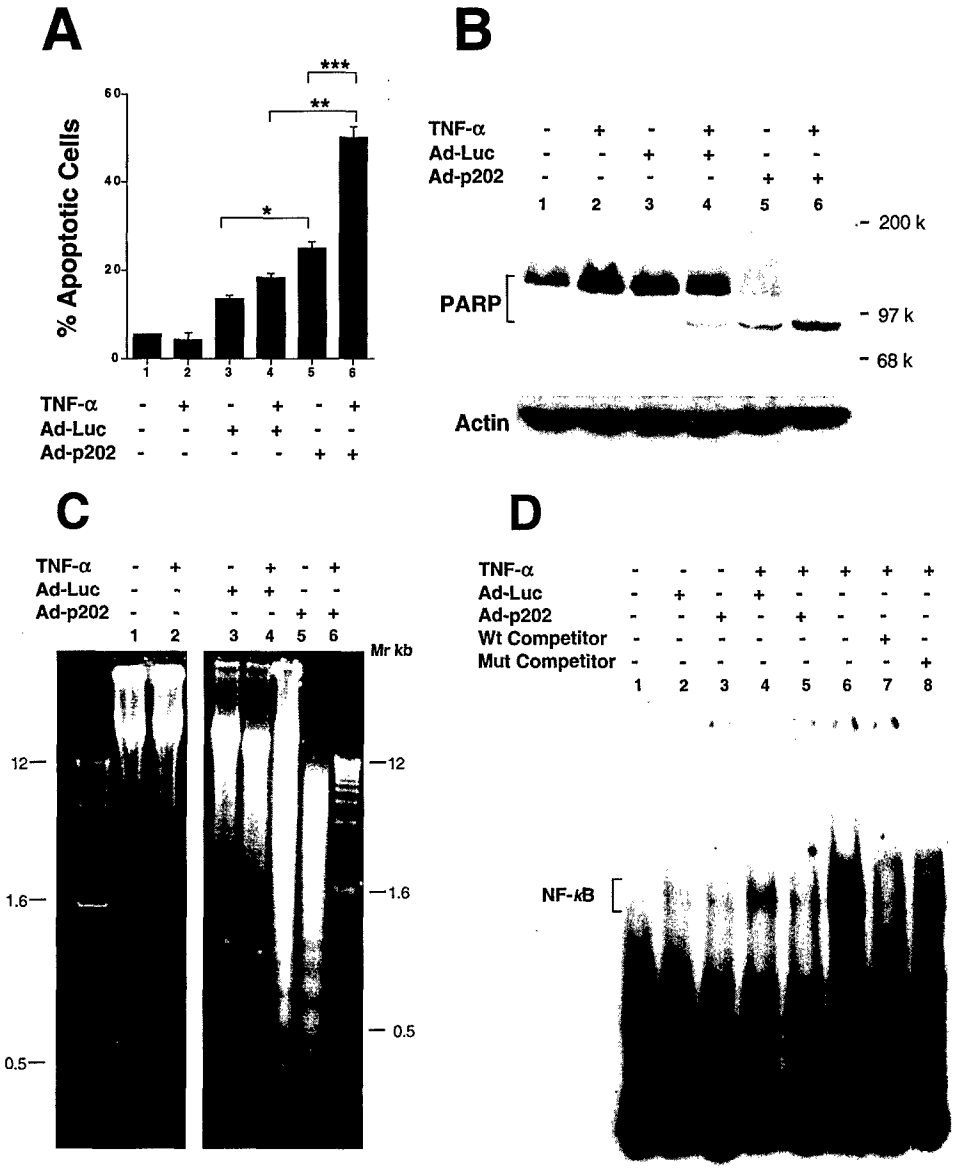

Fig. 3 Ad-p202 infection induces apoptosis and sensitizes cells to apoptosis induced by TNF-α. MDA-MB-468 cells were infected with Ad-Luc or Ad-p202 at a MOI of 200. *A*, 24 h PI, TNF-α (50 ng/ml) was added to the medium and incubated for 48 h (72 h PI). Apoptosis was then monitored by flow cytometry analysis (done in triplets; *bars*, SD). *t* test: *, $P < 0.001$; **, $P < 0.0002$; and ***, $P < 0.0005$. *B*, PARP cleavage assay. Twenty-four h PI, TNF-α (50 ng/ml) was added to the medium and incubated for 24 h. Treated cells were harvested 48 h PI. The PARP protein (M_r 116,000) was cleaved into M_r 85,000 product in the event of apoptosis. *C*, DNA fragmentation assay. Twenty-four h PI, TNF-α (50 ng/ml) was added to the medium and incubated for 24 h. Treated cells were harvested 48 h PI. *D*, Ad-p202 infection inhibits TNF-α-induced NF-κB DNA binding activity. MDA-MB-468 cells were infected with Ad-p202 or Ad-Luc in the presence or absence of TNF-α (50 ng/ml) 24 h PI for 30 min. The nuclear extracts were then isolated and incubated with a radioactive-labeled oligonucleotide containing NF-κB binding site (13). The excess cold wild-type or mutant NF-κB binding site was added to the incubation to demonstrate the specific NF-κB DNA binding activity. The NF-κB-DNA complex is indicated.

Ad-p202 Infection Induces Apoptosis in Breast Cancer Cells. Without stress signals, the p202 stable cancer cell lines do not exhibit apoptotic phenotype (3, 5). It is possible that p202 stable cell lines isolated after a vigorous selection process may possess a physiologically tolerant level of p202. The fact that only a small number of p202 stable cell lines were obtained by colony-forming assay (3, 5) raises the possibility that p202 expression alone may induce apoptosis. To test that possibility, we infected MDA-MB-468 cells with Ad-p202 or Ad-Luc followed by flow cytometry analysis at 72-h PI to detect apoptosis by measuring the cell population in the sub-G_1 phase of cell cycle. As shown in Fig. 3*A*, although Ad-Luc infection induced modest apoptosis (compare *Lane 1* with *Lane 3*), Ad-p202 infection (*Lane 5*) caused significantly more apoptosis (>20%) than Ad-Luc infection (*Lane 3*; $P < 0.001$, *t* test). That observation was further confirmed by two other apoptosis assays: (*a*) the PARP cleavage assay, in which full-length PARP (M_r 116,000) is cleaved by caspases into a fragment of approximately M_r 85,000 (Fig. 3*B*); and (*b*) a DNA fragmentation assay that is based on the activated endonucleases during apoptosis (Fig. 3*C*). Ad-p202 infection resulted in a marked increase of the PARP cleavage product (M_r 85,000; Fig. 3*B*, *Lane 5* and Fig. 4*A*, *Lane 3*) and an enhancement of DNA fragmentation (Fig. 3*C*, *Lane 5*). In contrast, Ad-Luc infection yielded a minimum amount of M_r 85,000 PARP cleavage product (Fig. 3*B*, *Lane 3* and Fig. 4*A*, *Lane 2*) as well as a near basal level of DNA fragmentation (Fig. 3*C*, compare *Lanes 1* and *3*). Together, our results strongly indicate that Ad-p202 alone induces apoptosis in MDA-MB-468 cells. Given that the MDA-MB-468 cell line harbors mutant p53 (16), Ad-p202-mediated apoptosis thus appears to be independent of p53 status.

p202-mediated Apoptosis Is Caspase-dependent. Because caspases are activated during apoptosis and have a variety

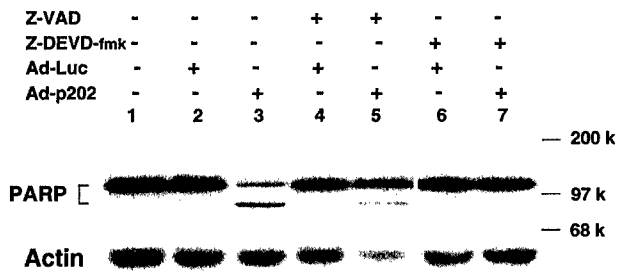

Fig. 4 The activation of caspases is critical for Ad-p202-mediated apoptosis. Z-VAD (100 μM) and Z-DEVD-fmk (80 μM) inhibit Ad-p202-mediated apoptosis in MDA-MB-468 cells. Western blot analysis of PARP cleavage and actin expression was performed 48 h PI. The intensity of full-length PARP and PARP cleavage product bands was measured using NIH Image 1.62 software.

of substrates including PARP (17), the cleavage of PARP in Ad-p202-infected cells suggests that the activation of caspase may be involved in Ad-p202-induced apoptosis. To test that hypothesis, we infected MDA-MB-468 cells with Ad-p202 or Ad-Luc in the presence or absence of a pan-caspase inhibitor, Z-VAD. At 48 h PI, the intensity of full-length PARP and PARP cleavage product bands on Western blot was measured using NIH Image 1.62 software. The percentage of M_r 85,000 product was calculated by setting the total intensity of both M_r 116,000 and M_r 85,000 bands in each lane at 100%. As shown in Fig. 4, the addition of Z-VAD attenuates Ad-p202-induced apoptosis, as indicated by the reduced (but not completely eliminated) level of PARP M_r 85,000 cleavage product from 57.4% (*Lane 3*) to 13.3% (*Lane 5*), whereas Z-VAD has no effect on PARP cleavage in Ad-Luc-infected cells (*Lane 4*). This result supports the idea that the activation of caspases, at least in part, is required for Ad-p202 to induce full apoptotic effect. Because PARP is also a substrate for caspase-3, which is considered to be a crucial enzyme commonly activated during apoptosis (17), we examined whether the activation of caspase-3 plays a role in Ad-p202-induced apoptosis. To that end, we infected MDA-MB-468 cells with either Ad-p202 or Ad-Luc in the presence of a caspase-3-specific inhibitor, Z-DEVD-fmk (18). As shown in Fig. 4, the level of PARP cleavage product in Ad-p202-infected MDA-MB-468 cells is significantly reduced to 8.9% (*Lane 7*) with Z-DEVD-fmk treatment as compared with that without Z-DEVD-fmk (57.4%; *Lane 3*). As a control, no detectable PARP cleavage was observed in Ad-Luc-infected cells treated with Z-DEVD-fmk (*Lane 6*). Thus, this result suggests that the activation of caspase-3 is critical for Ad-p202-mediated apoptosis. To further confirm this observation, we infected a caspase-3-null breast cancer cell line, MCF-7 (19), with Ad-p202 or Ad-Luc, followed by flow cytometry analysis. We observed that although p202 was readily expressed as determined by Western blot, the Ad-p202-infected MCF-7 cells yielded the similar level of apoptosis as that of the controls, *i.e.*, mock and Ad-Luc infection (data not shown). Therefore, our data suggest that the activation of caspases is critical for Ad-p202 to exert full apoptotic effect.

Ad-p202 Infection Sensitizes Breast Cancer Cells to TNF-α-induced Apoptosis. We tested whether Ad-p202 infection could also sensitize breast cancer cells to TNF-α-induced apoptosis (5). Although MDA-MB-468 cells appear to be resistant to TNF-α (50 ng/ml; added at 24 h PI for 48 h)-induced apoptosis (Fig. 3*A*, *Lanes 1* and *2*; Fig. 3*B*, *Lanes 1* and *2*; and Fig. 3*C*, *Lanes 1* and *2*), the combination of TNF-α and Ad-p202 induced massive cell killing [compare Fig. 3*A*, *Lanes 5* and *6* ($P < 0.0005$); Fig. 3*B*, *Lanes 5* and *6*; and Fig. 3*C*, *Lanes 5* and *6*]. These results suggest that Ad-p202 infection sensitizes MDA-MB-468 cells to TNF-α-induced apoptosis. In contrast, the apoptosis resulting from the combined treatment of TNF-α and Ad-Luc (Fig. 3*A*, *Lane 4*) was significantly less than that from combined treatment with TNF-α and Ad-p202 (Fig. 3*A*, *Lane 6*; $P < 0.0002$). This observation was confirmed by PARP cleavage and DNA fragmentation assays (Fig. 3*B*, *Lanes 4* and *6*; Fig. 3*C*, *Lanes 4* and *6*). These data indicate that the sensitization to TNF-α-induced apoptosis is specific to p202 expression. Because p202-mediated sensitization to TNF-α-induced apoptosis correlated with the inactivation of NF-κB, specifically, via the loss of NF-κB DNA binding activity (5), we next tested whether Ad-p202 infection affects TNF-α-induced NF-κB DNA binding activity. At 24 h PI, TNF-α was added for 30 min, and the nuclear extract was then isolated and subsequently incubated with a radioactive-labeled oligonucleotide containing the NF-κB binding sites. A gel-shift assay was then performed to detect the NF-κB DNA binding activity. As shown in Fig. 3*D*, we observed a complete abolishment of TNF-α-induced NF-κB DNA binding activity in Ad-p202-infected MDA-MB-468 cells (Fig. 3*D*, compare *Lanes 1, 3, 5,* and *6*). As controls, TNF-α-induced NF-κB DNA binding activity (*Lane 6*) can be readily competed by cold wild-type NF-κB DNA binding site (*Lane 7*) and, to a lesser extent, by cold mutant probe (*Lane 8*). Ad-Luc infection also reduces the TNF-α-induced NF-κB DNA binding activity somewhat, but to a lesser extent than Ad-p202 (*Lanes 4* and *5*). Together, our data suggest that Ad-p202 infection could sensitize otherwise resistant MDA-MB-468 cells to apoptosis induced by TNF-α, which correlates with a loss of TNF-α-induced NF-κB DNA binding activity.

Antitumor Activity of Ad-p202 in Cancer Xenograft Models. To test the efficacy of Ad-p202 treatment in an orthotopic breast cancer xenograft model, we implanted MDA-MB-468 cells (2×10^6 cells) into mammary fat pads of female nude mice. Treatment began when tumor size reached ~0.5 cm in diameter (about 2 weeks after implantation). We then treated tumor-bearing mice (7 tumors/treatment group) with either Ad-p202 or control virus Ad-Luc (1×10^9 pfu/treatment) via i.t. injection. Treatments were administered twice per week for 7 weeks and once a week thereafter. Tumor size was measured by using the following formula: tumor size = $1/2 \times L \times S^2$, where L and S are the longest and shortest diameters measured, respectively. The tumor size distribution with Ad-p202 or Ad-Luc treatment at two time points (day 25 and day 67) is presented. Whereas there was little difference at the early stage of treatment (Fig. 5*A*, day 25; $P = 0.13$), the Ad-p202-treated tumors grew significantly slower than those treated with Ad-Luc on day 67 ($P = 0.04$). This result supports the idea of a p202-based gene therapy in breast cancer treatment. Because breast cancer is a metastatic disease, it is critical to develop a systemic delivery system for p202 gene transfer. Although the antitumor effect by i.t. treatment is encouraging, no report has shown a therapeutic effect by systemic administration of p202 in a cancer xenograft model. We then performed systemic gene therapy

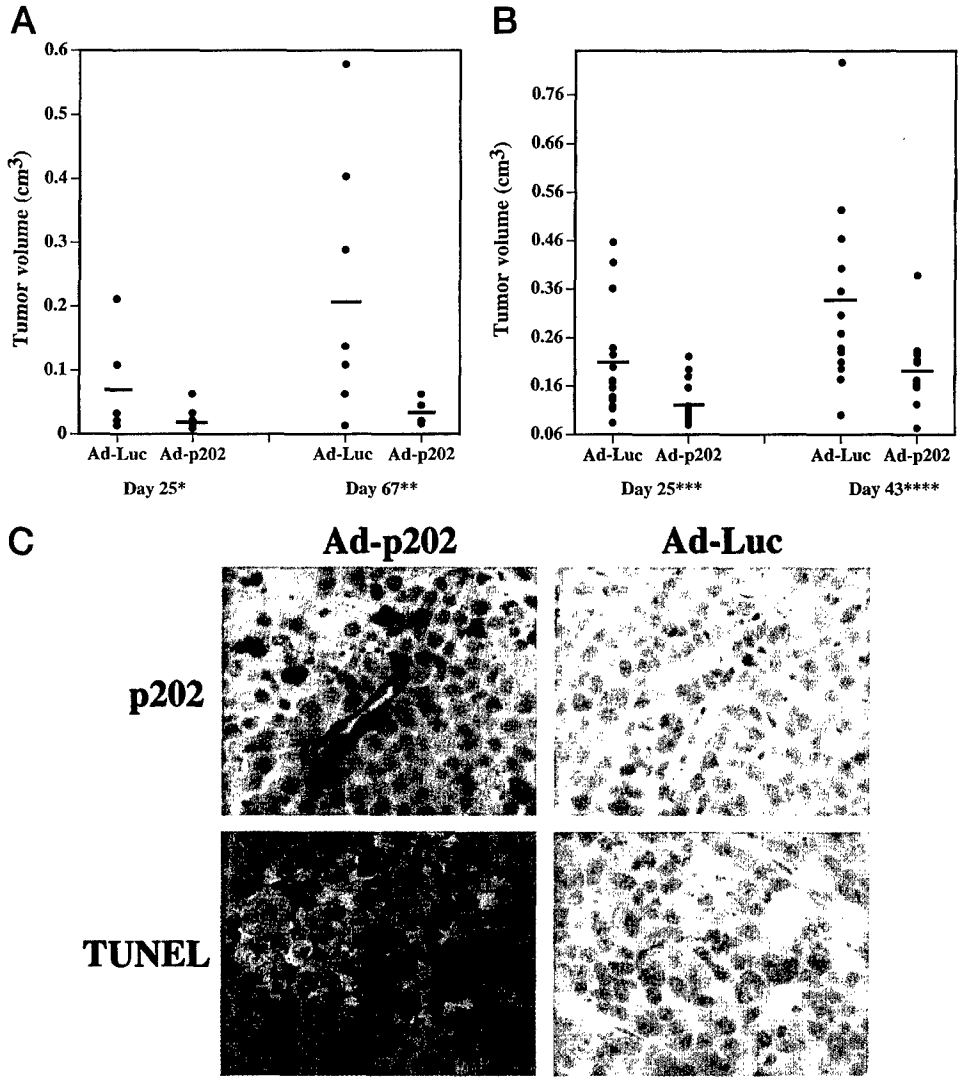

Fig. 5 Antitumor effect by systemic delivery of Ad-p202 in an orthotopic breast cancer xenograft model. *A,* Ad-p202-mediated antitumor effect on breast cancer xenografts by i.t. treatment. MDA-MB-468 cells (2×10^6 cells) were implanted in mammary fat pads of each female nude mouse. Tumor-bearing mice were divided into two treatment groups, Ad-Luc (total, 7 tumors) and Ad-p202 (total, 7 tumors), at 1×10^9 pfu/treatment via i.t. injection. Treatment started when tumor reached 0.3 cm in diameter with a treatment schedule of twice a week for 7 weeks and once a week thereafter. Tumor size in each treatment group was presented at the indicated time, *i.e.*, day 25 and day 67. *t* test: *, $P = 0.13$; and **, $P = 0.04$. *B,* Ad-p202-mediated antitumor effect on breast cancer xenografts by systemic treatment. MDA-MB-468 cells (2×10^6 cells) were implanted in mammary fat pads (2 tumors/mouse) of female nude mice. Tumor-bearing mice were divided into two treatment groups, Ad-Luc (total, 14 tumors) and Ad-p202 (total, 14 tumors), at 5×10^8 pfu via tail vein injection. Treatment started when tumor reached 0.5 cm in diameter with a treatment schedule of twice a week for 5 weeks and once a week thereafter. Tumor size in each treatment group was presented at the indicated time, *i.e.*, day 25 and day 43. *t* test: ***, $P = 0.0097$; and ****, $P = 0.014$. *C,* apoptosis correlates with p202 expression in Ad-p202-treated breast tumors. Mice were sacrificed 24 h after the last systemic treatment as described above. Tumors were then excised and fixed for the subsequent immunohistochemical analysis. p202 expression was analyzed by using an antibody specific for p202 on tumor samples obtained from Ad-p202- or Ad-Luc-treated mice (14). The TUNEL assay was also performed to detect apoptotic cells in these tumors (15). The *arrows* indicate the representatives of apoptotic cells.

experiments by treating tumor-bearing mice with Ad-p202 or Ad-Luc (5×10^8 pfu/treatment, 14 tumors/group) through tail vein injection. Treatments were administered twice per week for 5 weeks and once a week thereafter. As shown in Fig. 5*B*, Ad-p202-treated mice had a significantly reduced tumor growth rate as compared with the Ad-Luc-treated mice on day 25 ($P = 0.0097$) and day 43 ($P = 0.014$). The above-mentioned observation strongly suggests the feasibility of using a systemic p202-based gene therapy treatment for breast cancer. Because Ad-p202 induces apoptosis *in vitro* (Fig. 3), it is likely that the observed antitumor activity may correlate with enhanced apoptosis in Ad-p202-treated tumors. To test this possibility, we examined the presence of apoptosis in breast tumors treated systemically with Ad-p202. Immunostaining for p202 protein and apoptotic cells were performed 24 h after the last Ad-p202 and Ad-Luc treatment. As shown in Fig. 5*C*, p202 expression was readily detected by immu-

nohistochemical staining in Ad-p202-treated tumors but not in tumors treated with Ad-Luc. Interestingly, strong p202 expression was found in endothelial cells of a tumor blood vessel. It may be due to systemic delivery of Ad-p202. As predicted, apoptosis, as determined by TUNEL assay, is prevalent in Ad-p202-treated tumors but not in Ad-Luc-treated tumors (Fig. 5*C*). The *arrows* indicate the representatives of apoptotic cells. This observation is consistent with our *in vitro* data showing that p202 expression induces apoptosis (Fig. 3). We have also performed a similar Ad-p202 preclinical gene therapy treatment in a human pancreatic cancer xenograft model (4). Consistent with the data presented here, Ad-p202 treatment (by i.t. injection) inhibited tumor growth and induced apoptosis in tumors (data not shown). Taken together, the above-mentioned observations strongly indicate that p202 is a potent tumor-suppressing agent, and its apoptosis-inducing activity contributes to the multiple p202-mediated antitumor activities.

DISCUSSION

In this report we showed that, consistent with our previous findings using p202 stable breast cancer cell lines (5), Ad-p202 infection in MDA-MB-468 breast cancer cells resulted in growth inhibition and sensitization to TNF-α-induced apoptosis. Importantly, we demonstrated for the first time that Ad-p202 infection alone induces apoptosis *in vitro*. The correlation between p202 expression and enhanced apoptosis observed in Ad-p202-treated tumors also supports the *in vitro* observation. However, it is possible that the apoptosis could be the result of an artifact caused by coexpression of p202 and adenoviral proteins. We ruled out that possibility because Ad-Luc infection of a p202 stable cell line, 453-p202 (5), did not result in enhanced apoptosis as compared with that of the vector control cells infected by Ad-Luc (data not shown). This result thus strongly suggests that the Ad-p202-induced apoptosis is not likely due to cooperation between p202 and certain adenoviral proteins during infection. Rather, it indicates that a certain cellular apoptotic pathway was activated by p202 expression. Indeed, as shown in Fig. 4, Ad-p202-induced apoptosis requires caspase-3 activation to achieve a full apoptotic effect.

Here, we demonstrated the feasibility of using Ad-p202 in preclinical gene therapy settings. In particular, Ad-p202 treatment by i.t. or i.v. injection resulted in significant tumor suppression in an orthotopic breast cancer xenograft model. Our data are consistent with that reported previously using p202 delivery systems other than adenoviral vector, *i.e.*, polymer and liposome (4, 5). The efficacy of systemic Ad-p202 treatment is encouraging because it shows that Ad-p202 had overcome immunological (nude mice possess immune response, albeit much reduced), physiological, and structural barriers inside and outside the blood vessels to reach tumor cells and unloads the p202 therapeutic gene (20). This result is the first demonstration of efficacy by systemic treatment of p202. It is possible that the systemic Ad-p202 treatment may affect normal tissues the same way it affects tumor tissues. One way to minimize the potential cytotoxicity of the p202 effect on normal tissues is to develop a tumor-specific p202 expression system using a breast cancer-specific promoter to direct p202 expression. This effort is currently in progress. Although toxicity, if any, associated with Ad-p202 treatment remains to be determined, our results nevertheless raise the possibility of using p202-based gene therapy in systemic cancer treatment. In Ad-p202-treated tumors, we also found a reduced level of an angiogenic marker, vascular endothelial growth factor (data not shown). This observation is consistent with the ability of p202 to inhibit angiogenesis (4).

In addition to prostate (data not shown) and breast cancer xenograft models (this study and Ref. 5), the fact that Ad-p202 treatment resulted in an antitumor effect on a pancreatic cancer xenograft model (data not shown; Ref. 4) suggests a general application of p202-based gene therapy in cancer treatment. In addition, because p202 sensitizes cells to TNF-α-induced apoptosis (this study and Ref. 5), our data further support the possible use of Ad-p202/TNF-α combined therapy to achieve better efficacy, especially for cancer cells that are resistant to TNF-α therapy. Experiments are under way to test this possibility in animal models. Taken together, the data we present here strongly suggest that Ad-p202 is a potent therapeutic agent suitable for further development in cancer gene therapy.

REFERENCES

1. Ahre, A., Bjorkholm, M., Osterberg, A., Brenning, G., Gahrton, G., and Gyllenhammar, H. High doses of natural α interferon in the treatment of multiple myeloma: a pilot study from the myeloma group of central Sweden. Eur. J. Hematol., *41:* 123–130, 1988.

2. Kirkwood, J., Harris, J., Vera, R., Sandler, S., Fischer, D., and Khanderkar, J. A randomized study of low and high doses of leukocyte α-interferon in metastatic renal cell carcinoma: the American Cancer Society collaborative trial. Cancer Res., *45:* 863–871, 1985.

3. Yan, D-H., Wen, Y., Spohn, B., Choubey, D., Gutterman, J. U., and Hung, M-C. Reduced growth rate and transformation phenotype of the prostate cancer cells by an interferon-inducible protein, p202. Oncogene, *18:* 807–811, 1999.

4. Wen, Y., Yan, D-H., Wang, B., Spohn, B., Ding, Y., Shao, R., Zhou, Y., Xie, K., and Hung, M-C. p202, an interferon-inducible protein, mediates multiple anti-tumor activities in human pancreatic cancer xenograft models. Cancer Res., *61:* 7142–7147, 2001.

5. Wen, Y., Yan, D. H., Spohn, B., Deng, J., Lin, S. Y., and Hung, M. C. Tumor suppression and sensitization to tumor necrosis factor α-induced apoptosis by an interferon-inducible protein, p202, in breast cancer cells. Cancer Res., *60:* 42–46, 2000.

6. Landolfo, S., Gariglio, M., Gribaudo, G., and Lembo, D. The Ifi 200 genes: an emerging family of IFN-inducible genes. Biochimie (Paris), *80:* 721–728, 1998.

7. Johnstone, R. W., and Trapani, J. A. Transcription and growth regulatory functions of the HIN-200 family of proteins. Mol. Cell. Biol., *19:* 5833–5838, 1999.

8. Choubey, D. p202: an interferon-inducible negative regulator of cell growth. J. Biol. Regul. Homeost. Agents, *14:* 187–192, 2000.

9. Ferrantini, M., and Belardelli, F. Gene therapy of cancer with interferon: lessons from tumor models and perspectives for clinical applications. Semin. Cancer Biol., *10:* 145–157, 2000.

10. Lembo, D., Angeretti, A., Benefazio, S., Hertel, L., Gariglio, M., Novelli, F., and Landolfo, S. Constitutive expression of the interferon-inducible protein p202 in NIH3T3 cells affects cell cycle progression. J. Biol. Regul. Homeost. Agents, *9:* 42–46, 1995.

11. Choubey, D., Li, S-J., Datta, B., Gutterman, J. U., and Lengyel, P. Inhibition of E2F-mediated transcription by p202. EMBO J., *15:* 5668–5678, 1996.

12. He, T. C., Zhou, S., da Costa, L. T., Yu, J., Kinzler, K. W., and Vogelstein, B. A simplified system for generating recombinant adenoviruses. Proc. Natl. Acad. Sci. USA, *95:* 2509–2514, 1998.

13. Shao, R., Karunagaran, D., Zhou, B. P., Li, K., Lo, S-S., Deng, J., Chiao, P., Hung, M-C. Inhibition of nuclear factor-κB activity is in-

volved in E1A-mediated sensitization of radiation-induced apoptosis. J. Biol. Chem., *272:* 32739–32742, 1997.

14. Xia, W., Lau, Y. K., Zhang, H. Z., Xiao, F. Y., Johnston, D. A., Liu, A. R., Li, L., Katz, R. L., and Hung, M. C. Combination of EGFR, HER-2/neu, and HER-3 is a stronger predictor for the outcome of oral squamous cell carcinoma than any individual family members. Clin. Cancer Res., *5:* 4164–4174, 1999.

15. Shao, R., Hu, M. C., Zhou, B. P., Lin, S. Y., Chiao, P. J., von Lindern, R. H., Spohn, B., and Hung, M. C. E1A sensitizes cells to tumor necrosis factor-induced apoptosis through inhibition of IκB kinases and nuclear factor κB activities. J. Biol. Chem., *274:* 21495–21498, 1999.

16. Hunt, K. K., Deng, J., Liu, T. J., Wilson-Heiner, M., Swisher, S. G., Clayman, G., and Hung, M. C. Adenovirus-mediated overexpression of the transcription factor E2F-1 induces apoptosis in human breast and ovarian carcinoma cell lines and does not require p53. Cancer Res., *57:* 4722–4726, 1997.

17. Thornberry, N. A., and Lazebnik, Y. Caspases: enemies within. Science (Wash. DC), *281:* 1312–1316, 1998.

18. Pastorino, J. G., Chen, S. T., Tafani, M., Snyder, J. W., and Farber, J. L. The overexpression of Bax produces cell death upon induction of the mitochondrial permeability transition. J. Biol. Chem., *273:* 7770–7775, 1998.

19. Janicke, R. U., Sprengart, M. L., Wati, M. R., and Porter, A. G. Caspase-3 is required for DNA fragmentation and morphological changes associated with apoptosis. J. Biol. Chem., *273:* 9357–9360, 1998.

20. Nishikawa, M., and Huang, L. Nonviral vectors in the new millennium: delivery barriers in gene transfer. Hum. Gene Ther., *12:* 861–870, 2001.

Oncogene (2004) 23, 4556–4566
© 2004 Nature Publishing Group All rights reserved 0950-9232/04 $30.00
www.nature.com/onc

Antitumor activity of IFIX, a novel interferon-inducible HIN-200 gene, in breast cancer

Yi Ding[1], Li Wang[1], Li-Kuo Su[1,3], Jennifer A Frey[1,3], Ruping Shao[1], Kelly K Hunt[2] and Duen-Hwa Yan*[,1,2,3]

[1]*Department of Molecular and Cellular Oncology, The University of Texas, MD Anderson Cancer Center, 1515 Holcombe Blvd., Houston, TX 77030, USA;* [2]*Department of Surgical Oncology, The University of Texas, MD Anderson Cancer Center, 1515 Holcombe Blvd., Houston, TX 77030, USA;* [3]*The University of Texas Graduate School of Biomedical Sciences at Houston, USA*

We identified IFIX as a new member of the hematopoietic interferon (IFN)-inducible nuclear protein with the 200-amino-acid repeat (HIN-200) family. Six different alternatively spliced forms of mRNA are transcribed from the IFIX gene, which are predicted to encode six different isoforms of IFIX proteins (IFIXα1, α2, β1, β2, γ1, and γ2). The IFIX proteins are primarily localized in the nucleus. They share a common N-terminal region that contains a predicted pyrin domain and a putative nuclear localization signal. Unlike IFIXα and IFIXβ, IFIXγ isoforms do not have the 200-amino-acid signature motif. Interestingly, the expression of IFIX was reduced in most human breast tumors and breast cancer cell lines. Expression of IFIXα1, the longest isoform of IFIX, in human breast cancer cell lines reduced their anchorage-dependent and -independent growth *in vitro* and tumorigenicity in nude mice. Moreover, a liposome-mediated IFIXα1 gene transfer suppressed the growth of already-formed tumors in a breast cancer xenograft model. IFIXα1 appears to suppress the growth of breast cancer cells in a pRB- and p53-independent manner by increasing the expression of the cyclin-dependent kinase inhibitor p21^{CIP1}, which leads to the reduction of the kinase activity of both Cdk2 and p34^{Cdc2}. Together, our results show that IFIXα1 possesses a tumor-suppressor activity and suggest IFIXα1 may be used as a therapeutic agent in cancer treatment.
Oncogene (2004) **23,** 4556–4566. doi:10.1038/sj.onc.1207592
Published online 3 May 2004

Keywords: IFIX; interferon; HIN-200; p21^{CIP1}; breast cancer

*Correspondence: D-H Yan, Department of Molecular and Cellular Oncology, The University of Texas, MD Anderson Cancer Center, 1515 Holcombe Blvd., Houston, Texas 77030, USA. Tel: 713-792-3677, Fax: 713-794-0209; E-mail: dyan@mdanderson.org
Received 16 July 2003; revised 30 October 2003; accepted 29 January 2004; Published online 3 May 2004

Introduction

The interferon (IFN) family of cytokines is known for its growth-inhibitory activity, which plays an important role in IFN-mediated antitumor activity (Kimchi *et al.*, 1988). Proteins induced by IFN are thought to play important roles in mediating the antitumor activity of IFN (Lengyel, 1993). HIN-200 family proteins are IFN-inducible proteins that share a 200-amino-acid signature motif of type *a* and/or *b*. Three human (IFI16, MNDA, and AIM2) and five mouse (p202*a*, p202*b*, p203, p204, and D3) HIN-200 family proteins have been identified (Johnstone and Trapani, 1999; Choubey, 2000). Genes encoding HIN-200 family proteins are located at chromosome 1q21–23 and form a gene cluster in both mouse and human (Johnstone and Trapani, 1999). HIN-200 proteins are primarily nuclear proteins involved in the transcriptional regulation of genes important for cell cycle control, differentiation, and apoptosis (Johnstone and Trapani, 1999; Choubey, 2000). The antitumor activity of HIN-200 proteins has been demonstrated. In particular, we have shown that p202*a* suppressed tumor growth, reduced tumorigenicity, induced apoptosis, and suppressed metastasis and tumor angiogenesis of human cancer cells (Wen *et al.*, 2000, 2001; Ding *et al.*, 2002). The amino-acid sequence identity between the three human HIN-200 family proteins and the mouse p202*a* are 40% or less, thus none of these human proteins appears to be the ortholog of p202*a*. In a search for potential new human HIN-200 proteins, we have identified a new member of the human HIN-200 protein family, IFN-inducible protein X (IFIX). There are at least six IFIX isoforms encoded by alternatively spliced mRNAs (Figures 1a and 2a). We show here that the mRNA level of IFIX is reduced in breast tumor tissues and breast cancer cell lines and that expression of IFIXα1 reduces growth and tumorigenicity of breast cancer cell lines that have undetectable levels of IFIX expression. We also demonstrate the treatment efficacy of an IFIXα1-based gene therapy in an orthotopic breast cancer model. Together, our data suggest that IFIXα1 functions as a tumor suppressor and may be developed as a therapeutic agent in breast cancer treatment.

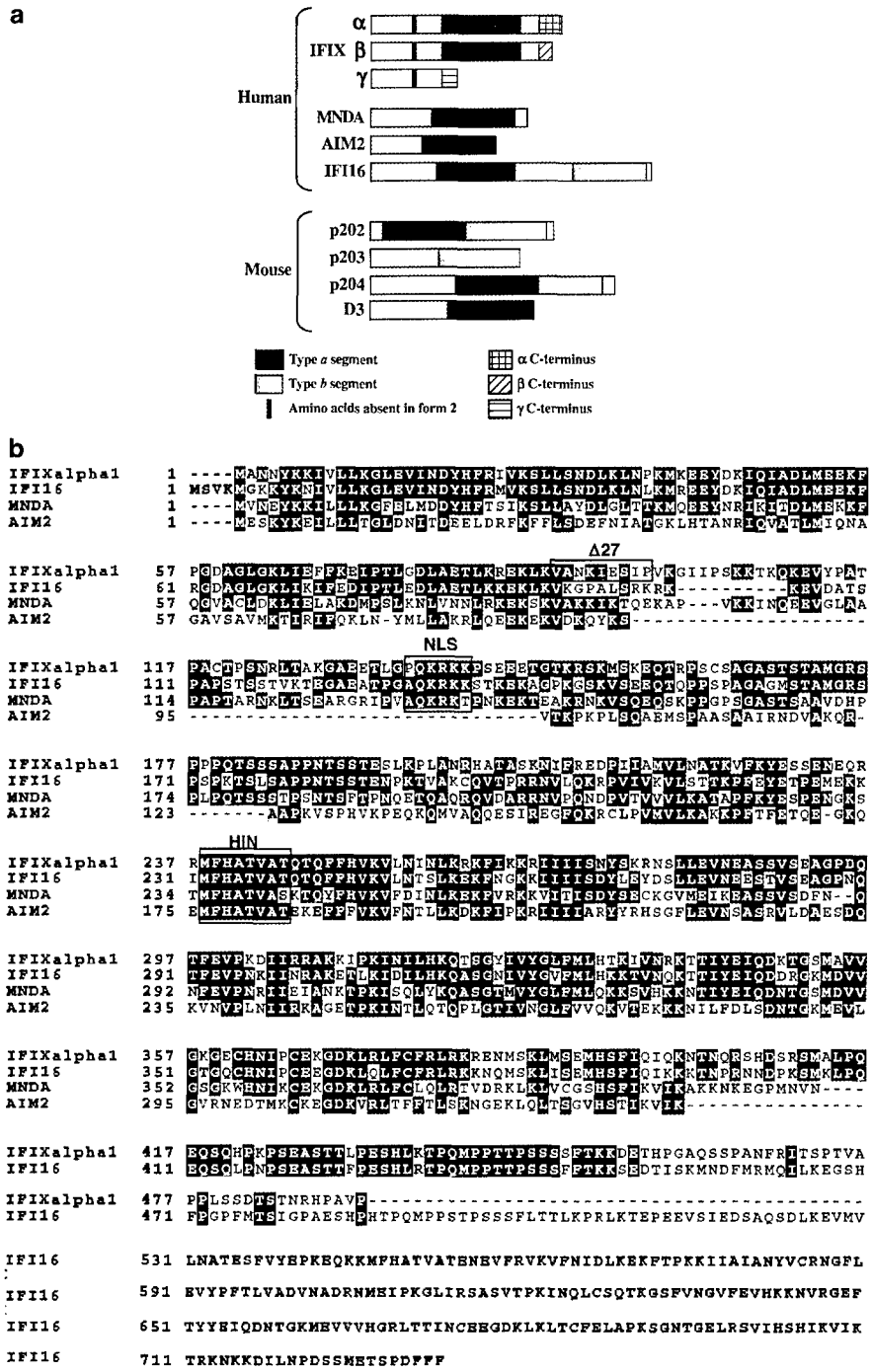

Figure 1 Characterization of IFIX. (**a**) Structural comparison among HIN-200 proteins. Black and gray bars indicate the type *a* and type *b* 200-amino-acid signature motifs of HIN-200 proteins, respectively. Different patterns of the C-terminus of IFIX isoforms indicate different amino-acid sequences of their C-terminal S/T/P-rich domains. The nine amino acids absent in α2, β2, and γ2 isoforms are indicated. (**b**) Amino-acid sequence comparison among human HIN-200 proteins. Amino acids identical or similar in at least two sequences are highlighted with black or gray background, respectively. Dashes indicate gaps introduced in the sequence to obtain the best alignment. The putative nuclear localization signal (NLS) and the nine-amino-acid deletion (Δ27) are indicated. The common MFHATVAT (HIN) in the 200-amino-acid signature motif of the human HIN-200 proteins is indicated

Results

IFIX is a novel human HIN-200 gene

To identify potential new human HIN-200 proteins, we used the amino-acid sequence of p202*a* to query human-specific nr, est, and htgs databases at National Center for Biotechnology Information (http://www.ncbi.nlm.nih.gov/) by using the tblastn protocol. These queries identified a new gene IFIX in addition to three previously known human HIN-200 family members, MNDA, IFI16, and AIM2. The IFIX gene is located between MNDA and IFI16 at chromosome 1q21–23.

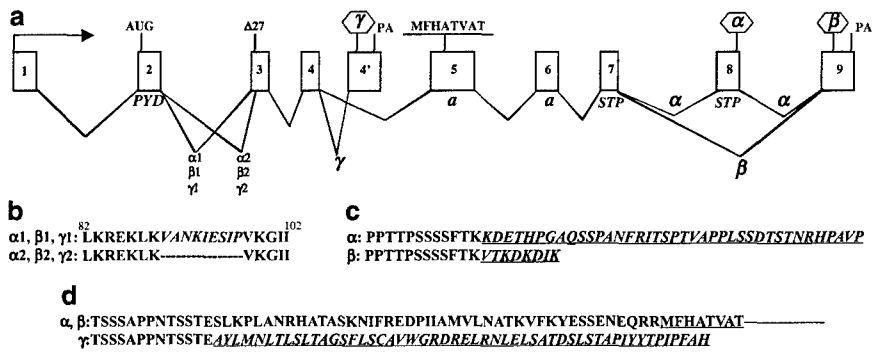

Figure 2 Structures of IFIX isoforms. *a*. Schematics of the *IFIX* gene. Exons of the *IFIX* gene are shown as open boxes and the exon numbers are indicated, the size of exons and introns are not drawn to scale. Alternative splicing events that result in various IFIX isoforms are indicated. Arrow indicates a putative transcriptional start site determined by 5′ rapid amplification of cDNA ends. AUG: the translation initiation codon; *PYD*: the putative pyrin domain; Δ27: the 27 bp absent in the α2, β2, and γ2 isoforms; the hexagons: stop codons of the α, β, and γ isoforms; PA: polyadenylation signal; MFHATVAT: an amino-acid sequence shared among HIN-200 proteins. *a*: the type *a* 200-amino-acid repeat; *STP*: serine/threonine/proline-rich region. The predicted size of each isoform is as follows: α1, 492 aa, α2, 483 aa, β1, 461 aa, β2, 452 aa, γ1, 246 aa, and γ2, 237 aa. *b*: The nine amino acids (VANKIESIP) absent in isoforms α2, β2, and γ2 are italicized. *c*: The C-terminal amino-acid sequences of isoforms α and β. Amino acids different between isoforms α and β are italicized and underlined. *d*: The unique C-terminal amino-acid sequence of the γ isoforms. Amino acids of γ isoforms different from isoforms α and β are italicized and underlined. The MFHATVAT signature motif of HIN-200 proteins in α and β isoforms is underlined

The IFIX cDNAs were obtained by RT–PCR using total RNA isolated from IFN-α-treated Daudi cells. Each cDNA clone was confirmed by DNA sequencing. We identified at least six IFIX isoforms (α1, α2, β1, β2, γ1, and γ2) that are homologous to other human and mouse HIN-200 proteins (Figure 1a). The identity between the amino-acid sequence of IFIXα1 and other members of human HIN-200 family is: IFI16, 67%; MNDA, 53%; and AIM2, 31% (Figure 1b). IFIX is unlikely to be the human ortholog of p202*a* because the similarity between the amino-acid sequences of IFIX and p202*a* is only limited to the type *a* 200-amino-acid signature motif (Figure 1a). The IFIX isoforms are likely derived from the alternative splicing based on the comparison between the cDNA sequences and the genomic sequence (Figure 2a). IFIXα2, β2, and γ2 have a deletion of identical nine amino acids, that is, ^{89}VANKIESIP (resulting from alternative splicing), in their N-terminal region when compared to IFIXα1, β1, and γ1 (Figure 2b). The α and β isoforms contain a type *a* 200-amino-acid signature motif of HIN-200 proteins whereas γ isoforms do not have this motif. The C-termini of α, β, and γ isoforms are diverse due to alternative splicing (Figure 2c and d). The IFIX isoforms share a common N-terminal region, which contains a predicted pyrin domain (amino acids 3–88), a protein–protein interaction module involved in apoptotic and inflammatory signaling pathways (Fairbrother *et al.*, 2001; Martinon *et al.*, 2001; Staub *et al.*, 2001). In addition, the N-terminal region also contains a putative nuclear localization signal, ^{134}LGPQKRKK (Figure 1b, Dawson and Trapani, 1995). Consistent with that prediction, we found the stably transfected IFIXα1 as well as the EGFP-tagged IFIXα1, β1, and γ1 fusion proteins are localized in the nucleus (Figure 8a and b). Interestingly, while IFIXα1 and IFIXβ1 are primarily localized in the nucleoplasm, IFIXγ1 forms a speckled nuclear pattern (Figure 8b). This observation suggests that, like most of the HIN-200 proteins, the IFIX proteins are primarily nuclear proteins. Consistent with the notion that HIN-200 genes are IFN inducible, the IFIX mRNA levels are characteristically induced by IFN-α and IFN-γ in several human cancer cell lines of hematopoietic origin (Figure 3a). A tissue distribution study showed that IFIX mRNA (~2.4 kb) is readily detected in the spleen, lymph node, and peripheral blood leukocyte, but to a less extent in thymus, bone marrow, and fetal liver (Figure 3b). No detectable level of IFIX mRNA was found in adult brain, heart, skeletal muscle, colon, kidney, liver, small intestine, placenta, and lung (data not shown). These results suggest that IFIX expression may be involved in immune response.

IFIX is downregulated in human breast cancers

AIM2 has been suggested to play a role in tumorigenesis (De Young *et al.*, 1997). We therefore investigated whether the expression of IFIX was altered in human cancers. We examined the expression of IFIX using a panel of commercially available human cDNAs derived from 12 normal breast tissues (normal) and 12 breast carcinoma tissues (tumor) (Origene Technologies, Inc. Rockville, MD, USA see Materials and methods) by PCR using primers specific to IFIXα. As shown in Figure 4a, IFIXα expression is detectable in 10 out of 12 normal breast tissue samples. In contrast, only two out of 12 breast carcinoma tissues have detectable IFIXα expression. This result suggests IFIX is downregulated in breast tumors. We further tested this correlation in the matched normal and tumor tissues collected from five breast cancer patients by RT–PCR using primers specific to IFIXα. The expression of IFIXα was detected in all tissues examined however, the level of IFIXα in tumor tissue was lower than that in the normal tissue of each patient (Figure 4b). We also examined the

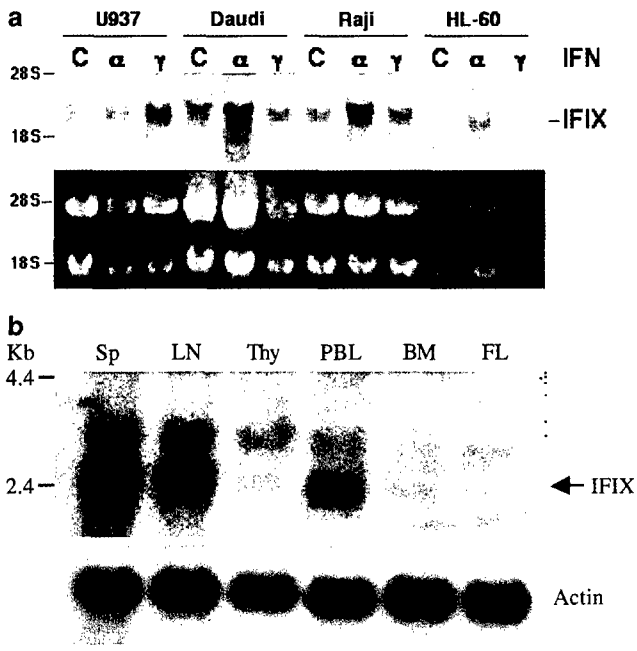

Figure 3 (**a**) Induction of IFIX expression by IFN. The IFIX mRNA in the indicated cell lines without treatment (c) or treated with 100 U/ml of IFNα (α) or IFNγ (γ) was detected by Northern blot analysis. The 18S and 28S rRNAs serve as loading controls. (**b**) IFIX expresses mainly in the secondary lymphoid organs. The Multiple Tissue Northern blot (BD Biosciences) was hybridized with an IFIXα1 cDNA probe. The IFIX mRNA (IFIX) band is indicated. The actin mRNA served as the loading control. Sp: spleen; LN: lymph node; PBL: peripheral blood leukocyte; Thy: thymus; BM: bone marrow; FL: fetal liver. The molecular weight markers (Kb) are indicated

expression of IFIX in a panel of human breast epithelial cell lines. IFIX expression was detected in all the three nontumorigenic cell lines. In contrast, seven out of nine breast cancer cell lines did not express detectable IFIX (Figure 4c and 7a). These data show that the expression of IFIX is reduced in breast cancer and suggest IFIX may function as a tumor suppressor. To determine the identity of IFIX isoforms in the IFIX-expressing cell lines, we performed RT–PCR using specific primers for these isoforms. As shown in Figure 4d (top and middle panels), the IFIXα, β, and γ isoforms are present in these cell lines, although the 27-bp deletion in the 'form 2' isoforms cannot be distinguished at this gel resolution.

To further determine the presence of the 'form 2' isoforms, we designed primers that flank the Δ27 region (Figure 1b and 2a) followed by RT–PCR. Consistent with the fact that the 'form 2' isoforms were isolated from Daudi cells, the expression of 'form 2' isoforms is detectable in Daudi cells, but the expression levels are much lower than that of the 'form 1' isoforms with the 27-bp region (Figure 4d, bottom panel). However, under

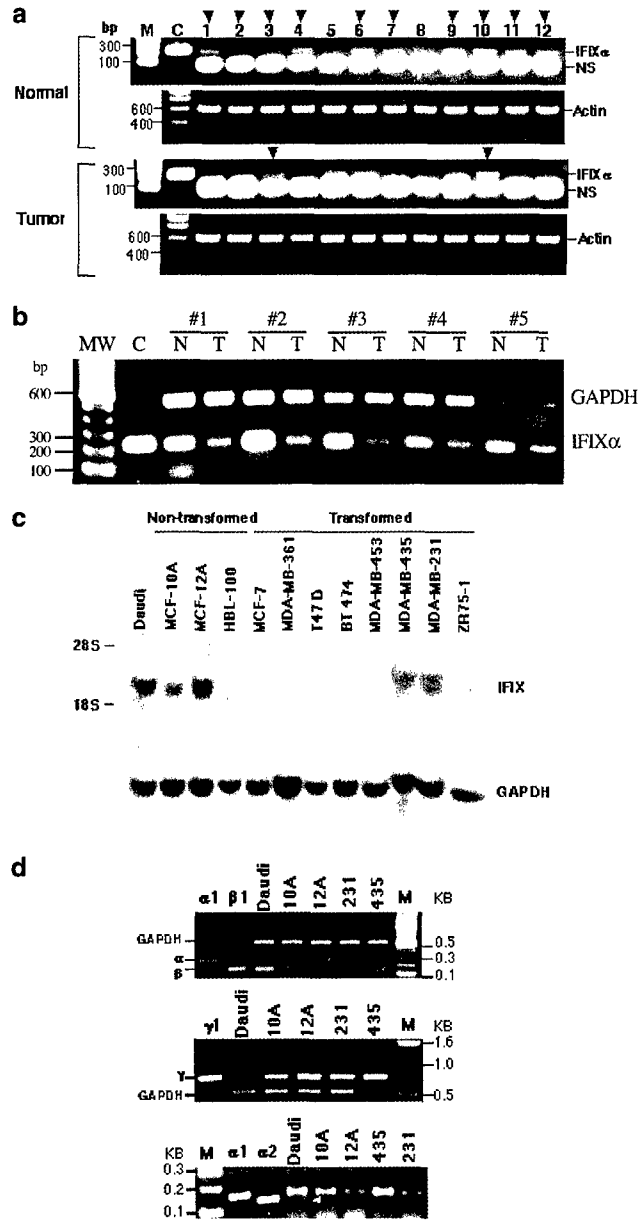

Figure 4 Reduced expression of IFIX in human breast tumor and breast cancer cell lines. (**a**) Reduced expression of IFIX in human breast tumors. The commercially available human cDNAs derived from 12 normal breast tissues (normal) and 12 breast carcinoma tissues (tumor) (Origene Technologies, Inc.) were analysed for IFIX expression by PCR using primers specific to IFIXα. The IFIXα1 cDNA was used as a control (C). Molecular weight markers (M) are indicated. The IFIXα and β-actin specific bands are indicated. NS: nonspecific PCR products. Samples positive for IFIXα expression are indicated by solid triangles. (**b**) Reduction of IFIXα mRNA levels in breast cancer. The IFIXα mRNA levels in normal breast (N) and breast cancer (T) tissues from five breast cancer patients were determined by RT–PCR using primers specific to IFIXα. C, an IFIXα1 cDNA clone used as the template in PCR. RT–PCR of GAPDH was used as a control for the RNA quality and quantity. (**c**) Reduction of IFIX mRNA levels in breast cancer cell lines. IFIX mRNA in 20 μg of total RNA isolated from indicated cell lines was determined using Northern blot analysis. GAPDH mRNA on the same blot was subsequently detected to serve as an RNA-loading control. (**d**) The presence of IFIX isoforms in the IFIX-expressing cell lines. RT–PCR was performed using primers specific for IFIXα, β, (top panel) or γ (middle panel), and the 'form 2' (indicated by an arrowhead, bottom panel) in Daudi, MCF-10A (10A), MCF-12A (12A), MDA-MB-231 (231), and MDA-MB-435 (435). The IFIXα1, α2, β1, and γ1 cDNAs were used as controls

our experimental conditions, the 'form 2' isoforms appeared to be not expressed or undetectable in other IFIX-expressing cell lines.

IFIX α1 suppresses breast cancer cell growth and tumorigenicity

As the first step to investigate the potential role of IFIX in tumor suppression in breast cancer, we use IFIXα1 for subsequent studies because it is the longest isoform of IFIX and possesses the most structural features among IFIX isoforms (Figure 1a and 1b). IFIXα1 is predicted to contain 492 amino acids with an apparent molecular weight of ~53 kDa. To investigate the possible tumor-suppressor function of IFIXα1, we employed two human breast cancer cell lines, MCF-7 and MDA-MB-468, which express very low levels of endogenous IFIX (Figure 4c, 5a, and 7b). Consistent with a previous report (Gooch *et al.*, 2000), we showed that IFN-γ treatment suppressed the growth of these breast cancer cells (Figure 5a, top panel), which correlated with the induction of IFIX (Figure 5a, bottom panel). To determine whether IFIX could suppress cell growth, we stably expressed IFIXα1 in MDA-MB-468 and MCF-7 cells (Figure 5b). Examination of the growth rates of the control cell lines (parental (P) and empty vector stable cell line (V)) and two independent IFIXα1-expressing cell lines (X-1 and X-2) derived from MDA-MB-468 and MCF-7 cells showed that the expression of IFIXα1 reduced the growth of breast cancer cells (Figure 5c). The soft agar assay was used to determine the effect of IFIXα1 on the *in vitro* transformation property. As shown in Figure 5d, the number of foci of IFIXα1-expressing derivatives (X-1 and X-2) was reduced as compared with the control cell lines (P and V). This result indicated that IFIXα1 suppressed the transformation phenotype of breast cancer cells and predicted a loss of tumorigenicity of IFIXα1-expressing breast cancer cells. To test that possibility, the tumorigenicity of the IFIXα1-expressing derivative 468-X-2 was then investigated by implanting 468-X-2 and the control, MDA-MB-468 cells into the mammary fat pad (MFP) of 6-week-old female nude mice. As shown in Figure 5e, while MDA-MB-468 cells (P) are highly tumorigenic, the tumorigenicity of 468-X-2 cells (X) is significantly reduced. Given that IFN is known to mediate growth inhibition and tumor suppression in breast cancer (Zhang *et al.*, 1996; Coradini *et al.*, 1998; Gooch *et al.*, 2000), our data suggest that IFIXα1 is a major mediator of the tumor-suppressor activity of IFN.

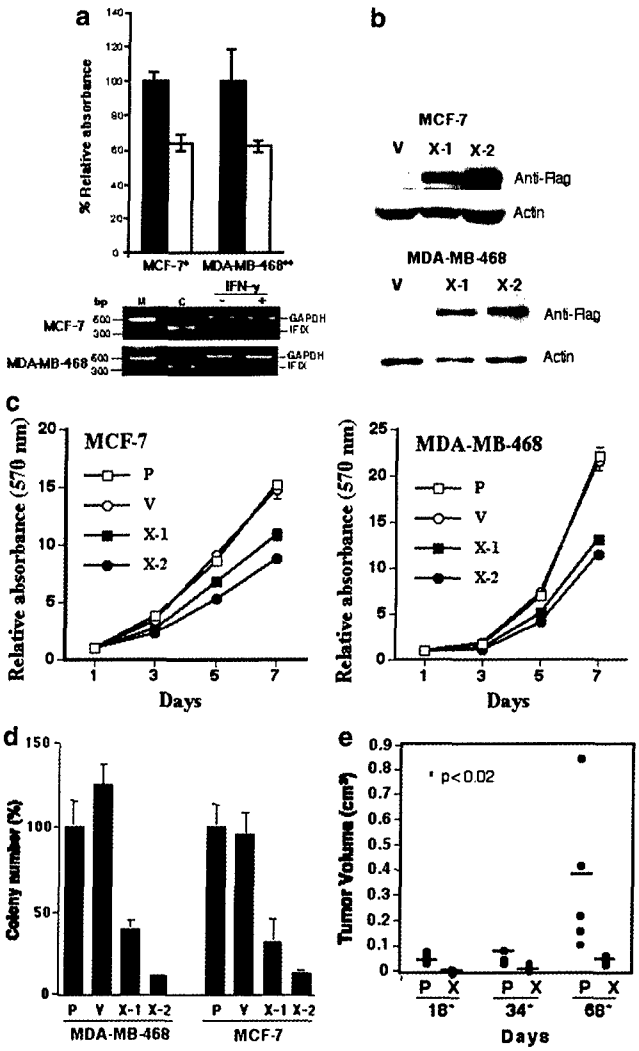

Figure 5 Suppression of the growth and tumorigenicity of breast cancer cells by IFIXα1. (**a**) IFN-γ induces IFIX expression in breast cancer cells. Top panel: MCF-7 and MDA-MB-468 cells were treated with (open bars) or without (solid bars) IFN-γ (1000 U/ml) in DMEM/F12 media containing 0.25% fetal calf serum for 48 h. The growth of the cells was measured by MTT assay. The experiment was run in triplicate and represented as the mean ± s.d. The asterisks represent the statistically significant differences due to the IFN-γ treatment. $*P<0.0005$, $**P<0.036$. Bottom panel: Total RNAs isolated from MCF-7 and MDA-MB-468 cells treated with or without IFN-γ (1000 U/ml) under the same condition as described above were analysed for IFIX expression by RT–PCR. GAPDH was used as an internal control. The IFIXα1 cDNA was used as a specificity control (C). Molecular weight markers (M) are indicated. (**b**) Expression of exogenous IFIXα1 in breast cancer cell lines. The Flag-tagged IFIXα1 in lysates from clones expressing Flag-tagged IFIXα1 (X-1 and X-2) and the empty vector (pCMV-Tag2B) (V) control clones were detected by Western blot using an anti-Flag antibody. The actin protein levels serve as loading controls. (**c**) Reduced growth rates in IFIXα1 stable cell lines. The growth rate of IFIXα1-expressing clones (X-1 and X-2), the parental (P) and the empty vector (V) control clones was measured by MTT assay. Each measurement was made in quadruplicate. The relative absorbance at 570 nm was determined by setting the absorbance on day 1 at 1. The range of variation at some data points is too small to be seen. (**d**) Suppression of *in vitro* transformation by IFIX. The parental (P), the empty vector (V), or IFIXα1 stable cell lines (X-1 and X-2) derived from MDA-MB-468 or MCF-7 cells were seeded in soft agar and the colony number was scored at 3 weeks after seeding. The relative colony numbers of IFIXα1-expressing clones are compared with that of their parental cells (100%). (**e**) Suppression of tumorigenicity by IFIXα1. 468-X-2 and the control, MDA-MB-468 (P) cells were implanted into the MFP of 6-week-old female nude mice at two sites per mouse, three mice per group. The actual size of each tumor at the indicated time points after implantation is presented. Horizontal bars indicate the average tumor size. *t*-test: $*P<0.02$

IFIXα1 treatment results in therapeutic efficacy

To rule out the possibility that the reduced tumorigenicity of 468-X-2 was due to clonal variation (Figure 5e) and to test whether IFIXα1 could suppress breast tumor growth, we performed a preclinical gene therapy experiment using an orthotopic breast cancer xenograft model. Female nude mice were inoculated with MDA-MB-468 cells into their MFP and tumors were allowed to grow to 0.5 cm in diameter. Tumors were then injected with the liposome SN2 complexed with either an IFIXα1-expression vector (CMV-IFIXα1) or an empty vector (pCMV-Tag2B). SN2 was selected as the gene delivery system because it is a nonviral, stable liposome-forming cationic lipid formulation and has been proven to be highly efficient in gene delivery (Zou *et al.*, 2002). As shown in Figure 6, the CMV-IFIXα1/SN2 (X) treatment yielded significant antitumor activity as compared to the pCMV-Tag2B/SN2 (V) treatment. This observation suggests that the reduced tumorigenicity seen in 468-X-2 (Figure 5e) is likely caused by IFIX expression and not by clonal variation. More importantly, this result indicates that IFIXα1 possesses antitumor activity and shows the feasibility of an IFIX-based gene therapy for breast cancer treatment.

IFIXα1 upregulates p21^{cip1}

IFN-induced growth arrest is known to be associated with an elevated level of the cyclin-dependent kinase inhibitor (CKI) p21^{CIP1} (Naldini *et al.*, 2002; Zhou *et al.*, 2002). As the expression of IFIXα1 is induced by IFN (Figure 3a and 5a), we therefore investigated the mRNA and protein levels of p21^{CIP1} in IFIXα1 stable transfectants. As shown in Figure 7a and b, both p21^{CIP1} protein and mRNA levels are upregulated in IFIXα1 stable cell lines (X-1 and X-2) as compared with the control cell lines (P and V). However, there are no detectable changes in the expression of other CKIs, such as p27^{KIP1}, p57^{KIP2}, and p16^{INK4a} in IFIXα1-expressing derivatives (data not shown). Since p21^{CIP1} is a universal CKI, upregulation of p21^{CIP1} should inactivate the kinase activity of Cdk2 in IFIXα1 stable cells. Therefore, we used an immunocomplex kinase assay to determine the Cdk2 kinase activity in IFIXα1 stable cell lines and control cells. As expected, Cdk2 activity is reduced in 468-X-2 and MCF-X-2 as compared to their respective parental cells (Figure 7c). Western blot indicates that there are comparable amounts of Cdk2 protein used in the kinase assay. However, since MDA-MB-468 cells lack pRB and express mutant p53 (Yin *et al.*, 2001), inhibition of MDA-MB-468 cell growth by IFIXα1 cannot simply be attributed to the inactivation of Cdk2 leading to G1/S-phase arrest (MacLachlan *et al.*, 1995). One possible explanation was that p21^{CIP1} also inhibits p34^{Cdc2}, a G2/M-phase Cdk (Yu *et al.*, 1998). We examined the p34^{Cdc2} kinase activity in IFIXα1-expressing MDA-MB-468 cells and found that it was much lower than that of the control cells (Figure 7c). This result suggests that inactivation of p34^{Cdc2} may contribute to the IFIXα1-mediated growth inhibition in MDA-MB-468 cells. To further confirm this observation, we performed a flow cytometry analysis to determine any changes in the cell cycle distributions caused by the expression of IFIX. As shown in Figure 7d, a significant G1-phase accumulation and S-phase reduction was observed in MCF-X-2 cells. In contrast, 468-X-2 cells exhibited a significant S- and G2/M-phase accumulation. This observation not only provides an explanation for the slower growth rate of IFIX stable cell lines (Figure 5c) but also correlates with the inactivation of Cdk2, leading to G1-phase accumulation in MCF-7 in which pRB/E2F pathway is intact and the inactivation of p34^{Cdc2}, resulting in a blockage of G2/M-phase entry in MDA-MB-468 in which pRB/E2F pathway is defective. Together, the data suggest that the p53/pRB-independent p21^{CIP1} upregulation contributes to IFIXα1-mediated antitumor activity in breast cancer cells. To test the ability of different IFIX isoforms to induce p21^{CIP1}, we transiently transfected MCF-7 cells with the plasmids encoding EGFP-tagged IFIXα1, β1, or γ1 fusion protein followed by immunostaining with the p21^{CIP1}-specific antibody. As shown in Figure 8b, the expression of IFIXα1 or β1 mainly coincides with the expression of p21^{CIP1} in the nucleus (64 and 52%, respectively). In contrast, like the empty vector (EGFP) control, the expression of IFIXγ1 has little effect on the expression of p21^{CIP1} (0.95 and 2%, respectively). Together with a unique speckled nuclear pattern, our observations indicate that IFIXγ1 may function differently from IFIXα1/β1, and it also suggests that the

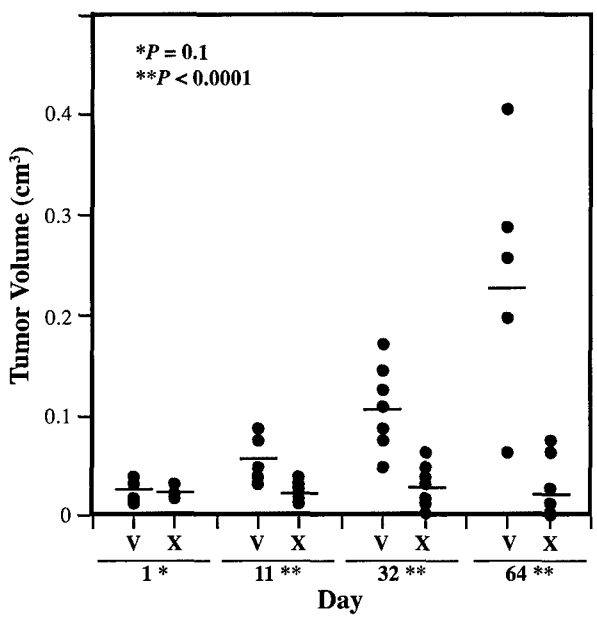

Figure 6 The antitumor effect of IFIXα1/SN2 liposome treatment in an orthotopic breast cancer xenograft model. Orthotopic breast tumors were established by inoculating MDA-MB-468 cells into the MFP of nude mice and the treatments began at tumors about 0.5 cm in diameter. Tumors were treated twice weekly with SN2 mixed with either CMV-IFIXα1 (X) or pCMV-Tag2B (V). The actual size of each tumor at the indicated time points after treatments begun is presented. Horizontal bars indicate the average tumor size. *t*-test: $*P=0.1$, $**P<0.0001$

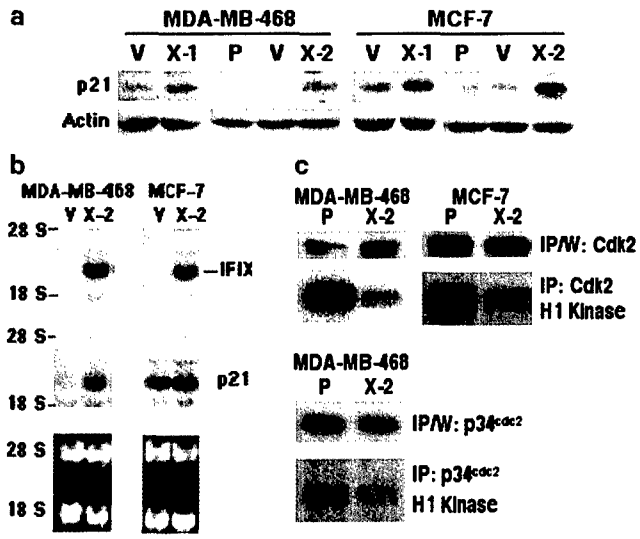

d

		G1 (%)	S (%)	G2/M (%)
MCF-7	V	46.35±1.35	45.70±0.30	7.95±1.05
	X-2	68.35±2.45	24.40±2.20	7.25±0.25
MDA-MB-468	V	54.25±3.95	30.50±3.10	15.25±0.85
	X-2	34.35±1.35	43.65±0.55	22.00±1.90

Figure 7 Upregulation of $p21^{CIP1}$ by IFIXα1. (**a**) Increased $p21^{CIP1}$ protein levels in MDA-MB-468 and MCF-7 IFIXα1 stable cells. Cell lysates isolated from 468-X-1, 468-X-2, MCF-X-1, MCF-X-2, and the control parental (P) and empty vector (V) cell lines were analysed by Western blot using an anti-$p21^{CIP1}$ antibody. Actin served as the loading control. (**b**) Increased $p21^{CIP1}$ mRNA levels in MDA-MB-468 and MCF-7 IFIXα1 stable cells. Total RNA (20 μg) isolated from 468-X-2, MCF-X-2, and the corresponding empty vector (V) control cell lines were analysed by Northern blot using an IFIXα1 or $p21^{CIP1}$ probe as indicated. The 18S and 28S rRNA bands on the membrane after transfer stained by ethidium bromide serve as loading control. (**c**) Inhibition of the kinase activity of Cdk2 and $p34^{Cdc2}$ by IFIXα1. Cell lysates isolated from 468-X-2, MCF-X-2, and the parental (P) control cell lines were immunoprecipitated by Cdk2 (or $p34^{Cdc2}$)-specific antibody followed by Histone H1 (H1) kinase assay. Immunoprecipitation followed by Western blot (IP/W) with Cdk2 or $p34^{Cdc2}$ antibody served as the loading control. (**d**) IFIX expression affects cell cycle distribution. The IFIX-expressing cells (X-2) and the empty vector control cells (V) derived from MCF-7 and MDA-MB-468 cells were subjected to flow cytometry analysis. The percentage of each cell line in G1, S, and G2/M phases was calculated. This result was obtained from two independent experiments

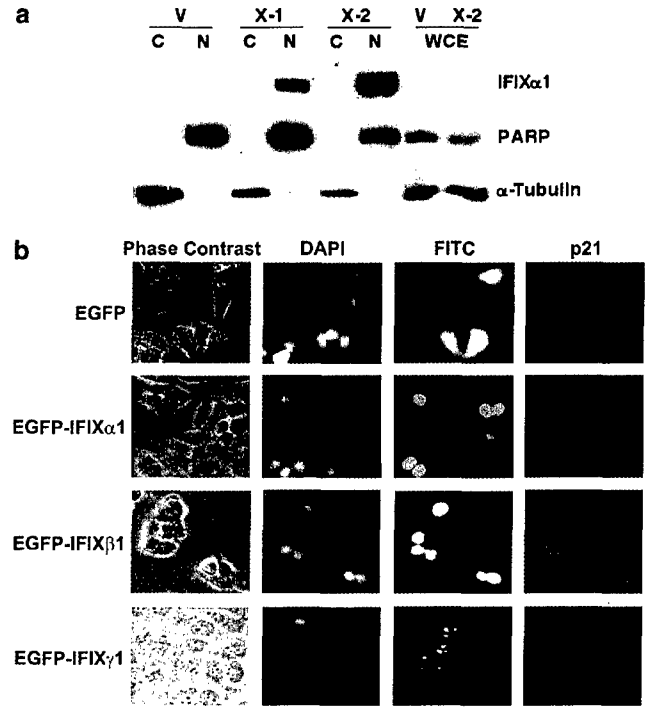

Figure 8 IFIX proteins are localized in the nucleus. (**a**) The stably transfected IFIXα1 protein is localized in the nucleus. Cytoplasmic (C), nuclear (N), or whole cell extracts (WCE) isolated from MCF-X-1, MCF-X-2, or the MCF-7 empty vector control cells (V) were analysed for IFIXα1 expression by Western blot using an anti-Flag antibody. The same blot was used to verify the quality of the extracts using the antibodies against the nuclear protein, PARP, and the cytoplasmic protein, α-Tubulin. (**b**) The transiently transfected IFIXα1 protein is localized in the nucleus. MCF-7 cells were transfected with the plasmid encoding EGFP-tagged IFIXα1, β1, or γ1 protein. The EGFP-expression vector serves as a control. Phase contrast, nuclear staining (DAPI), green fluorescence (FITC), and Texas Red for $p21^{CIP1}$ staining (p21) of each transfection are shown. At 48 h after transfection, the percentage of $p21^{CIP1}$-positive in EGFP-positive cells was counted for each transfection: EGFP (0.95%, 1/105), IFIXα1 (64%, 68/107), IFIXβ1 (52%, 55/106), and IFIXγ1 (2%, 2/100). Cells were examined at ×60 magnification

200-amino-acid domain may be responsible for the upregulation of $p21^{CIP1}$.

Discussion

We identified IFIX as a new member of the human HIN-200 protein family. At least six isoforms were identified in Daudi cells. Interestingly, while the 'form 1' isoforms are present in IFIX-expressing cells such as MCF-10A, MCF-12A, MDA-MB-231, and MDA-MB-435, the 'form 2' isoforms were either missing or undetectable in these cells. A systematic analysis on the expression of 'form 2' isoforms is required to determined whether 'form 2' expression is specific in hematopoietic cells and/or caused by IFN treatment. Using a commercial cDNA expression panel, we found that IFIXα was detectable in only two out of 12 breast carcinomas, whereas most (10 out of 12) of the normal breast tissues have detectable IFIXα expression (Figure 4a). This result was consistent with that of five pairs of matched normal versus tumor samples we collected from patients in which IFIXα expression is downregulated in all tumor samples as compared with that of the matched normal breast tissue samples (Figure 4b). Furthermore, seven out of nine breast cancer cell lines examined in this study have no detectable IFIX, while IFIX expression is readily detectable in the nontransformed breast cell lines (Figure 4c). Although it is possible that the signals on the northern blots may come from other HIN-200 genes due to sequence homology, we consider the IFIXα1

cDNA probe used in these experiments is quite specific based on the size and the tissue distribution patterns of IFIX mRNA. First, the size of IFIX mRNA (including all isoforms) is ~2.4 kb (between 28S and 18S) (Figure 3a and b), which would effectively rule out the HIN-200 genes MNDA (2.0 kb, at 18S) and AIM2 (1.8 kb, below 18S) (De Young *et al.*, 1997). However, the size of IFI16 mRNA is ~2.7 kb, it is possible that it may migrate closely with IFIX mRNA. Second, in contrast to the expression of IFI16 mRNA in lymphoid tissues such as spleen, thymus, and peripheral blood leukocyte, and many other organs (Wei *et al.*, 2003), the expression of IFIX mRNA is clearly restricted to the secondary lymphoid organs such as spleen, lymph nodes, and peripheral blood leukocyte but not the primary lymphoid organs such as thymus and bone marrow (Figure 3b). Thus, based on the size and tissue distribution patterns of different HIN-200 mRNAs, we believe that, under our experimental conditions, the signals in the Northern blots are mainly generated from the probe hybridizing with IFIX mRNA. Albeit, we cannot rule out the possibility that the additional weak band detected above the IFIX signals in Figure 3b is IFI16 mRNA based on its slightly higher molecular weight and its expression in the thymus. The IFIX-specific antibodies are being generated to detect IFIX proteins by Western blot and immunostaining. Once these critical reagents are available, a more systematic analysis of IFIX protein expression on the breast and normal tumor tissues will be performed to confirm the RT–PCR and Northern blot data presented in this study, and to further investigate the diagnostic and prognostic values of IFIX expression in breast cancer. To understand how IFIX is downregulated in certain breast tumors or breast cancer cell lines but not in others (Figure 4a and c), further genetic and biochemical analysis is necessary.

The expression of HIN-200 was originally identified in hematopoietic cells and was thought to be restricted in this cell type (Dawson and Trapani, 1996). However, recent reports have shown that IFI16 is expressed in epithelial cells in addition to lymphoid cells (Gariglio *et al.*, 2002; Wei *et al.*, 2003). Our finding that IFIX expresses in normal breast tissues (Figure 4a and b) and nontransformed breast epithelial cell lines (Figure 4c) supports the notion that HIN-200 expression is not restricted in hematopoietic cells. Taken together, these observations suggest that IFIX may play a role in maintaining the normal growth of epithelial cells and the downregulation of IFIX expression may contribute to the uncontrolled cell growth and leads to tumorigenesis. It is intriguing that the two breast cancer cell lines that express IFIX, that is, MDA-MB-435 and MDA-MB-231, are metastatic in experimental systems (Price *et al.*, 1990; Zhang *et al.*, 1991). This observation raises a possible link between IFIX expression and metastatic potential of breast cancer cells. However, this possibility is not supported by the available information. (The manufacturer did not provide the metastasis status of patient samples used in Figure 4a.) Of the five breast tumors we collected from patients, all expressed reduced levels of IFIX (Figure 4b), including two recurrent metastatic breast tumors in the chest wall (#1 and #2) and three primary breast tumors (#3, #4, and #5). Moreover, except the BT-474 cell line which was isolated from a solid invasive ductal carcinoma, all breast cancer cell lines used for Northern blot analysis shown in Figure 4c were isolated from metastatic breast tumors: MCF-7, T47-D, MDA-MB-435, MDA-MB-231, and MDA-MB-468 (pleural effusion); MDA-MB-361 (brain metastasis); MDA-MB-453 (effusion); and ZR-75-1 (ascitic effusion). Thus, there is no clear correlation between the expression of IFIX and the metastatic potential of breast cancer in human patients.

Compared to the control MDA-MB-468 cells (P and V), MDA-MB-468 derivatives that expressed exogenous IFIXα1 formed fewer colonies in soft agar and resulted in tumors that grew slower in mice, suggesting that IFIXα1 suppresses tumorigenicity (Figure 5d and e). However, the differences between IFIXα1-expressing derivatives and their parental cells could be due to clonal difference. Moreover, although stably expressing IFIXα1 in breast cancer cell lines are appropriate for proof-of-principle experiments, it is inappropriate for predicting treatment outcome in patients. We therefore performed an IFIXα1-based gene therapy to determine if it would yield efficacy in an orthotopic breast cancer xenograft model. As shown in Figure 6, direct injection of IFIXα1 complexed with the liposome SN2 into tumors yielded a significant antitumor activity as compared to the empty vector control. This result supports the notion that the reduced tumorigenicity of 468-X-2 (Figure 5e) is caused by IFIXα1 expression and not by clonal difference. Importantly, it clearly demonstrates a feasibility of using IFIXα1 as a potential antitumor agent. Since breast cancer is a metastatic disease, this observation should set the stage for testing the therapeutic efficacy of IFIXα1 in systemic treatments delivered by either SN2 liposome (Zou *et al.*, 2002) or viral vectors (Ding *et al.*, 2002).

IFN has been shown to increase the expression of $p21^{CIP1}$ and this is critical for IFN to suppress the anchorage-independent growth of breast cancer cells (Gooch *et al.*, 2000). Consistent to that observation, the expression of IFIXα1, an IFN-inducible protein (Figure 3a and 5a), reduces the growth of breast cancer cells in soft agar (Figure 5d) and increases the expression of $p21^{CIP1}$ (Figure 7a and b). This observation suggests that IFIXα1 may mediate $p21^{CIP1}$ upregulation in response to IFN. The result that IFIXα1 is able to upregulate $p21^{CIP1}$ in MDA-MB-468 cells, which express only mutant p53, indicates the upregulation of $p21^{CIP1}$ by IFIXα1 is independent of p53. The p53-independent upregulation of $p21^{CIP1}$ has been well documented (Cox, 1997; Nadal *et al.*, 1997; Fang *et al.*, 2000; Hingorani *et al.*, 2000). In particular, our observation is reminiscent of a previous finding that overexpression of a mouse HIN-200 protein, that is, p202*a*, also resulted in a p53-independent upregulation of $p21^{CIP1}$ (Gutterman and Choubey, 1999). Since the regulation of $p21^{CIP1}$ expression could take place on transcriptional and/or posttranscriptional levels (Funk and Galloway, 1998; Dotto, 2000), further

determination of the half-life of $p21^{CIP1}$ mRNA and protein, and the effect on the $p21^{CIP1}$ transcriptional activity by IFIX will be necessary to elucidate the mechanism underlying the IFIX-mediated $p21^{CIP1}$ upregulation. As expected, the upregulation of $p21^{CIP1}$ leads to hypo-phosphorylation of pRB in IFIX-expressing MCF-7 cells (data not shown). However, since MDA-MB-468 cells lack pRB (Yin *et al.*, 2001), the inhibition of E2F/pRB pathway by $p21^{CIP1}$ cannot account for the mechanism for IFIX-mediated growth inhibition of MDA-MB-468 cells. Our finding that the kinase activity of $p34^{Cdc2}$ is reduced in IFIXα1-expressing MDA-MB-468 cells (Figure 7c) suggests that IFIXα1 may suppress the growth of MDA-MB-468 cells through the inhibition of $p34^{Cdc2}$ kinase activity at the G2/M phase of the cell cycle by $p21^{CIP1}$. This interpretation is further supported by the results of flow cytometry analysis (Figure 7d) that show G1 arrest in IFIXα1-expressing MCF-7 cells in which pRB/E2F pathway is intact because $p21^{CIP1}$ upregulation leads to inactivation of Cdk2 and the subsequent activation of pRB, resulting in a blockage at the G1/S-phase transition (Dotto, 2000). In the case of IFIXα1-expressing MDA-MB-468 cells, although Cdk2 is inactivated, cells progress through G1/S-phase because pRB/E2F pathway is absent. However, the upregulation of $p21^{CIP1}$ also leads to inactivation of $p34^{Cdc2}$, a critical Cdk controlling G2/M transition (Doree and Hunt, 2002), resulting in S- and G2/M-phase accumulation.

Although it has been shown that two copies of the 200-amino-acid motif of a mouse HIN-200 protein are required for growth inhibition (Gribaudo *et al.*, 1999), a more recent study showed that the overexpression of a human HIN-200 protein, AIM2, which has only one copy of the type *a* 200-amino-acid motif, is sufficient to suppress cell growth (Choubey *et al.*, 2000). Thus, our findings support the notion that, at least in human HIN 200 proteins, a single 200-amino-acid motif is sufficient for growth suppression. Interestingly, IFIXγ does not have the characteristic 200-amino-acid signature motif of the HIN-200 family proteins (Figure 1a and 2d) and forms a speckled nuclear pattern (Figure 8b). Thus, it is likely that IFIXγ plays a distinct functional role from α and β isoforms. Indeed, we showed that, while IFIXα1 or IFIXβ1 induced $p21^{CIP1}$ expression, IFIXγ1 did not (Figure 8b). This result also suggests the 200-amino-acid signature motif may be required for $p21^{CIP1}$ upregulation and, possibly, growth suppression. Given that the pyrin domains are known to be involved in protein–protein interactions (Fairbrother *et al.*, 2001; Martinon *et al.*, 2001; Staub *et al.*, 2001), it is possible that IFIXγ may function as a dominant-negative protein by interacting with IFIXα/β or other pyrin domain-containing proteins.

In summary, IFIX, a newly identified HIN-200 gene, is downregulated in breast cancer. The data presented here indicate that IFIXα1 expression is associated with growth retardation, loss of tumorigenicity, and $p21^{CIP1}$ upregulation in breast cancer. Moreover, efficacy of an IFIXα1-based gene therapy is demonstrated, raising the possibility of using IFIXα1 as a therapeutic agent in breast cancer treatment.

Materials and methods

Cell lines and plasmids

MCF-10A and MCF-12A cells were maintained in DMEM/F12 media containing 5% horse serum, 10 μg/ml bovine insulin, 20 ng/ml epidermal growth factor, 100 ng/ml cholera toxin, 0.5 μg/ml hydrocortisone, and 250 ng/ml fungizone. Daudi, Raji, HL-60, and U937 cells were grown in RPMI medium containing 10% fetal bovine serum. All other cell lines were cultured in DMEM/F12 media containing 10% fetal bovine serum. The IFIXα1 expression vector CMV-IFIXα1 was constructed by inserting IFIXα1 cDNA into pCMV-Tag2B (Flag) (Stratagene, La Jolla, CA, USA). To generate IFIXα1 stable cell lines, CMV-IFIXα1 was transfected into MDA-MB-468 or MCF-7 cells. After 3 weeks of G418 selection (500 μg/ml), the G418-resistant colonies were screened for IFIXα1 expression by Western blot using an anti-Flag antibody (M5, Sigma, St Louis, MO, USA). Control derivatives of MDA-MB-468 and MCF-7 that carry pCMV-Tag2B were similarly established. The EGFP-IFIX expression vectors were constructed by inserting IFIXα1, β1, and γ1 cDNAs into pEGFP-C vectors (BD Biosciences).

Identification and cloning IFIX gene

To identify a new human HIN-200 gene that might be the ortholog of mouse p202, we first used the amino-acid sequence of p202 to query human specific nr, est, and htgs database in the National Center for Biotechnology Information (NCBI) using the tblstn protocol and identified a potential new gene located between MNDA and IFI16 at chromosome 1. As the predicted amino-acid sequence of the new gene appeared to be more homologous to human HIN-200 members than to mouse p202, we then used the IFI16 amino-acid sequence to query these same databases using tblastn. This query allowed us to extend the length of this new gene. Primers were then designed according to the sequences of this potential gene to isolate cDNA by RT–PCR.

Determination of gene expression

The expression of IFIX in cell lines was determined by using Northern blot analysis performed as previously described (Wen *et al.*, 2001). The expression of GAPDH was used as a control for RNA loading. Human cDNAs derived from 12 normal breast tissues (normal) and 12 breast carcinoma tissues (tumor) (Human Breast Cancer Rapid-Scan™ Gene Expression Panel, Origene Technologies, Inc. Rockville, MD, USA) were analysed for IFIX expression by PCR using primers specific to IFIXα under the condition suggested by the manufacturer. The IFIXα1 cDNA was used as a DNA template for the IFIXα-specific positive control. β-actin specific primers (provided by the manufacturer) were used to amplify the β-actin-specific band as an internal control. We used RT–PCR to determine the expression of IFIXα in normal and cancerous breast tissues from five patients with various stages of breast cancer including one with only ductal carcinoma *in situ*. Total RNA was isolated from tissues using Atlas Pure Total RNA Labeling System (BD Biosciences) and reverse transcription was performed using SuperScript First-strand Synthesis System (Invitrogen, Carlsbad, CA, USA). PCR was performed for 35 cycles at 94°C for 40 s, 56°C for 1 min, and 72°C for 40 s. Primers 5′-GGAACAGAGTCAG CATCC-3′ (exon 7) and 5′-CTGCTGGATGGCGGTTGG-3′ (exon 8) were used to amplified a 224 bp fragment specific to IFIXα (Figure 4a and b).

In addition, to detect both IFIXα (265 bp) and β (140 bp) isoforms in cell lines (Figure 4d), the following primers are used: 5′-GGAACAGAGTCAGCATCC-3′ (exon 7) and 5′-GTTATTTGATATCCTTGTCC-3′ (exon 9). To detect IFIXγ isoforms (γ1, 744 bp and γ2, 717 bp), the following primers are used: 5′-TTAGAGATGGCAAATAACTAC-3′ (exon 2) and 5′-TTAGTGAGCAAAGGGAATG-3′ (exon 4′). To detect the expression of the 'form 2' isoforms ('form 1', 161 bp and 'form 2', 134 bp), the following primers are used: 5′-TTGGGC AAACTAATAGAATTC-3′ (exon 2) and 5′-GCAGGATA CACTTCTTTCTG-3′ (exon 3). As a control for the quality of the RNA samples, an ~600 bp GAPDH cDNA fragment was amplified using primers 5′-TGAAGGTCGGAGTCAACG GA-3′ and 5′-GGCATGGACTGTGGTCATGA-3′. To detect all IFIX isoforms (~350 bp) (Figure 5a, bottom panel), the following primers are used: 5′-TGATGGAGGAAAAGTT CC-3′ (exon 2) and 5′-TGCTGGCTCCTGCAGAGC-3′ (exon 4).

Determination of growth, in vitro *transformation and* in vivo *tumorigenicity of breast cancer cells*

MTT and soft agar assays were used to determine the anchorage-dependent and -independent *in vitro* cell growth, respectively, and were performed as previously described (Shao, 1997). To measure the effect of IFN-γ on cell growth (Gooch *et al.*, 2000), MCF-7 and MDA-MB-468 cells were planted in 24-well plates (18,000 cells/well) in DMEM/F12 media supplemented with 10% fetal calf serum. The next day, cells were washed in 1 × PBS and grown in serum-free DMEM/F12 media overnight. The serum-free media was replaced with DMEM/F12 media containing 0.25% fetal calf serum. IFN-γ (1000 U/ml) was added. The growth of the cells was measured by MTT assay at 48 h. To determine tumorigenicity, 1×10^6 cells were injected into the MFP of 6-week-old female nude mice and the growth of tumors was monitored weekly. For each experiment, a cell line was injected into three mice with each mouse injected at 2 MFP.

IFIX α1 gene therapy

One million MDA-MB-468 cells in 200 μl of PBS were injected into a MFP of 4–5-week old female nude mice. Each cell line was injected into 5 mice with each mouse injected at 2 MFP. After the tumors grew to 0.5 cm in diameter, mice were treated twice a week by intratumoral injection. Tumor-bearing mice were randomly divided into two equal treatment groups with each tumor injected with 22.5 μl of the liposome SN2 in 50 μl of PBS (Zou *et al.*, 2002) mixed with 15 μg of either CMV-IFIXα1 or a control vector pCMV-Tag2B (100 μl total injection volume).

Histone H1 kinase assay

Cells were lysed with RIPA-B buffer (20 mM Na_2PO_4 (pH 7.4), 150 mM NaCl, 1% Triton X-100, 100 mM NaF, 2 mM Na_3VO_4, 5 mM phenylmethylsulfonyl fluoride, 1% aprotinin). Lysate containing 200–400 μg of protein was incubated at 4°C for 1 h with 2 μg of anti-Cdk2 antibody (Santa Cruz Biotechnology, Inc. Santa Cruz, CA, USA) or 1.5 μg anti-$p34^{Cdc2}$ antibody (Santa Cruz Biotech.), followed by incubation with Protein A-agarose for 2 h. The immunoprecipitates were washed twice with PBS, once with kinase buffer (10 mM Tris (pH 7.4), 150 mM NaCl, 10 mM $MgCl_2$, and 0.5 mM dithiothreitol), and then resuspended in 40 μl of kinase buffer containing 2 μg of histone H1 (Sigma), 25 μM ATP, and 5 μM γ-^{32}P ATP. The kinase reaction was terminated by adding 40 μl of SDS–PAGE loading buffer after a 15 min incubation at room temperature (Cdk2) or 30 min incubation at 30°C ($p34^{Cdc2}$). Samples were resolved by SDS–PAGE and the phosphorylated Histone H1 was visualized by autoradiography.

Western blot

The standard procedure has been described previously (Wen *et al.*, 2001). The antibodies used in this study are anti-Flag (Sigma, M5), anti-β-actin (Sigma), anti-$p21^{CIP1}$ (Santa Cruz Biotech.), anti-poly-(ADP-ribose) polymerase (PARP) (BD Biosciences), and anti-α-Tubulin (Sigma). The cytoplasmic and nuclear extracts were isolated according to the protocol described previously (Xie and Hung, 1994).

Immunostaining

MCF-7 cells (1×10^4 in 0.5 ml). were cultured in a four-well glass chamber overnight. Cells were then transfected with 1 μg of the plasmid encoding EGFP-tagged IFIXα1, β1, or γ1 fusion protein. The EGFP expression vector serves as a control. At 48 h after transfection, cells were washed with PBS and fixed with 3% paraformaldehyde in PBS for 20 min at room temperature followed by PBS wash. The primary $p21^{CIP1}$ monoclonal antibody (Santa Cruz Biotech.) (1 : 100) was incubated with the cells at 37°C for 1 h. Cells were then washed with PBS, followed by incubation with the rabbit anti-mouse secondary antibody conjugated with Texas Red (1 : 200) at 37°C for 45 min. After incubation, cells were washed briefly with PBS and air-dried, followed by incubation with the blue fluorescent dye DAPI (1 : 100 in 50% glycerol/PBS). A cover slip was placed on top of the slide for visualization by microscopy.

GenBank Accession numbers

IFIXα1 (AY185344), IFIXα2 (AY185345), IFIXβ1 (AY185346), IFIXβ2 (AY185347), and IFIXγ1 (XM086611).

Note Added In Proof

During the preparation of this manuscript, a partial amino acid sequence of the N-terminal domain of IFIX protein (referred to as IFI16-like protein 1) was published (Liepinsh *et al.*, 2003).

Acknowledgements
We thank Drs Mien-Chie Hung, Funda Meric, Naoto Ueno, Dihua Yu, Mong-Hong Lee, and Nancy Poindexter for providing the reagents used in this study. This work was supported in part by grants from the Department of Defense (DAMD17- 99-1-9270), Texas Advanced Technology Program (003657-0082-1999), and an Institutional Research Grant from The University of Texas, MD Anderson Cancer Center (to DHY), and Cancer Center Core Grant CA16672 from the NIH. YD is the recipient of a post-doctoral fellowship from the Department of Defense (DAMD17-02-1-0451).

References

Choubey D. (2000). *J. Biol. Regul. Homeost. Agents*, **14,** 187–192.
Choubey D, Walter S, Geng Y and Xin H. (2000). *FEBS Lett.*, **474,** 38–42.
Coradini D, Pellizzaro C, Biffi A, Lombardi L, Pirronello E, Riva L and Di Fronzo G. (1998). *Anticancer Res.*, **18,** 177–182.
Cox LS. (1997). *J. Pathol.*, **183,** 134–140.
Dawson MJ and Trapani JA. (1995). *J. Cell. Biochem.*, **57,** 39–51.
Dawson MJ and Trapani JA. (1996). *J. Leukotr. Biol.*, **60,** 310–316.
De Young KL, Ray ME, Su YA, Anzick SL, Johnstone RW, Trapani JA, Melzer PS and Trent JM. (1997). *Oncogene*, **15,** 453–457.
Ding Y, Wen Y, Spohn B, Wang L, Xia W, Kwong KY, Shao R, Li Z, Hortobagyi GN, Hung M-C and Yan D-H. (2002). *Clin. Cancer Res.*, **8,** 3290–3297.
Doree M and Hunt T. (2002). *J. Cell Sci.*, **115,** 2461–2464.
Dotto GP. (2000). *Biochim. Biophys. Acta*, **1471,** M43–M56.
Fairbrother WJ, Gordon NC, Humke EW, O'Rourke KM, Starovasnik MA, Yin JP and Dixit VM. (2001). *Protein Sci.*, **10,** 1911–1918.
Fang M, Liu B, Schmidt M, Lu Y, Mendelsohn J and Fan Z. (2000). *Anticancer Res.*, **20,** 103–111.
Funk JO and Galloway DA. (1998). *Trends Biochem. Sci.*, **23,** 337–341.
Gariglio M, Azzimonti B, Pagano M, Palestro G, De Andrea M, Valente G, Voglino G, Navino L and Landolfo S. (2002). *J. Interferon Cytokine Res.*, **22,** 815–821.
Gooch JL, Herrera RE and Yee D. (2000). *Cell Growth Differ.*, **11,** 335–342.
Gribaudo G, Riera L, De Andrea M and Landolfo S. (1999). *FEBS Lett.*, **456,** 31–36.
Gutterman JU and Choubey D. (1999). *Cell Growth Differ.*, **10,** 93–100.
Hingorani R, Bi B, Dao T, Bae Y, Matsuzawa A and Crispe IN. (2000). *J. Immunol.*, **164,** 4032–4036.
Johnstone RW and Trapani JA. (1999). *Mol. Cell. Biol.*, **19,** 5833–5838.
Kimchi A, Resnitzky D, Ber R and Gat G. (1988). *Mol. Cell. Biol.*, **8,** 2828–2836.
Lengyel P. (1993). *Proc. Natl. Acad. Sci. USA*, **90,** 5893–5895.
Liepinsh E, Barbals R, Dahl E, Sharipo A, Staub E and Otting G. (2003). *J. Mol. Biol.*, **332,** 1155–1163.
MacLachlan TK, Sang N and Giordano A. (1995). *Crit. Rev. Eukaryot. Gene Express.*, **5,** 127–156.
Martinon F, Hofmann K and Tschopp J. (2001). *Curr. Biol.*, **11,** R118–R120.
Nadal A, Jares P, Cazorla M, Fernandez PL, Sanjuan X, Hernandez L, Pinyol M, Aldea M, Mallofre C, Muntane J, Traserra J, Campo E and Cardesa A. (1997). *J. Pathol.*, **183,** 156–163.
Naldini A, Carney DH, Pucci A and Carraro F. (2002). *J. Cell. Physiol.*, **191,** 290–297.
Price JE, Polyzos A, Zhang RD and Daniels LM. (1990). *Cancer Res.*, **50,** 717–721.
Shao R, Karunagaran D, Zhou BP, Li K, Lo S-S, Deng J, Chiao P and Hung M-C. (1997). *J. Biol. Chem.*, **272,** 32739–32742.
Staub E, Dahl E and Rosenthal A. (2001). *Trends Biochem. Sci.*, **26,** 83–85.
Wei W, Clarke CJP, Somers GR, Cresswell KS, Loveland KA, Trapani JA and Johnstone RW. (2003). *Histochem. Cell. Biol.*, **119,** 45–54.
Wen Y, Yan D-H, Wang B, Spohn B, Ding Y, Shao R, Zhou Y, Xie K and Hung M-C. (2001). *Cancer Res.*, **61,** 7142–7147.
Wen Y, Yan DH, Spohn B, Deng J, Lin SY and Hung MC. (2000). *Cancer Res.*, **60,** 42–46.
Xie Y and Hung MC. (1994). *Biochem. Biophys. Res. Commun.*, **203,** 1589–1598.
Yin F, Giuliano AE, Law RE and Van Herle AJ. (2001). *Anticancer Res.*, **21,** 413–420.
Yu D, Jing T, Liu B, Yao J, Tan M, McDonnell TJ and Hung MC. (1998). *Mol. Cell*, **2,** 581–591.
Zhang JF, Hu C, Geng Y, Selm J, Klein SB, Orazi A and Taylor MW. (1996). *Proc. Natl. Acad. Sci. USA*, **93,** 4513–4518.
Zhang RD, Fidler IJ and Price JE. (1991). *Invasion Metastasis*, **11,** 204–215.
Zhou Y, Wang S, Yue BG, Gobl A and Oberg K. (2002). *Cancer Investig.*, **20,** 348–356.
Zou Y, Peng H, Zhou B, Wen Y, Wang SC, Tsai EM and Hung MC. (2002). *Cancer Res.*, **62,** 8–12.

Interferon-inducible protein IFIXα1 functions as a negative regulator of HDM2

Yi Ding[1], Jin-Fong Lee[1], Hua Lu[3], and Duen-Hwa Yan[1, 2]*

[1]Department of Molecular and Cellular Oncology, The University of Texas, M. D. Anderson Cancer Center, 1515 Holcombe Blvd., Houston, Texas 77030, [2]The University of Texas, Graduate School of Biomedical Sciences at Houston, [3]Department of Biochemistry and Molecular Biology, Oregon Health & Science University, 3181 SW Sam Jackson Park Road, Portland, Oregon 97239

Running title: IFIXα1 binds and destabilizes HDM2

*Corresponding author. Mailing address: Department of Molecular and Cellular Oncology, The University of Texas, M. D. Anderson Cancer Center, 1515 Holcombe Blvd., Houston, Texas 77030. Phone: (713) 792-3677. Fax: (713) 794-0209. E-mail: dyan@mdanderson.org

Word count for the "Materials and Methods": 1,386

Combined word count for the "Introduction", "Results", and "Discussion": 5,500

ABSTRACT

IFIX is a new member of the hematopoietic interferon (IFN)-inducible nuclear protein with the 200-amino-acid repeat (HIN-200) gene family. IFIX is often found down regulated in breast tumors and breast cancer cell lines. The expression of the longest isoform of IFIX gene products, IFIXα1, is associated with suppression of growth, transformation, and tumorigenesis. However, the mechanism for the tumor suppressor activity of IFIX is not well understood. Here, we show IFIXα1 binds and destabilizes HDM2, a principal negative regulator of p53. The HDM2 RING finger domain, which possesses E3 ligase activity, is required for the IFIXα1-mediated HDM2 destabilization. This result is supported by the observation that IFIXα1 induces the ubiquitination of HDM2. As expected, the down regulation of HDM2 by IFIXα1 leads to induction of p53 and activation of p53 target gene (e.g., $p21^{CIP1}$). Moreover, the positive regulation of p53 by IFIXα1 can be observed only in p53-/- MEF but not in p53-/-, mdm2-/- double knockout MEF. Together, these results suggest that IFIXα1 positively regulates p53 by acting as a negative regulator of HDM2. Thus, IFIXα1 functions as a tumor suppressor that may contribute to the anti-tumor activity of IFN in certain cancers.

INTRODUCTION

IFNs play an essential role in innate and adaptive immunity and host defense system against viral, bacterial and parasitic infections (46). In addition to viral infection, IFNs have been used as therapeutic agents in treating human solid and haematologic malignancies such as hairy cell leukemia, chronic myelogenous leukemia, follicular (non-Hodgkin's) lymphoma, and malignant melanoma (31, 79). Although the mechanism of the IFN-induced anti-tumor activity is poorly understood, it is widely thought that the IFN-inducible proteins are critically involved in this process (45). Indeed, IFN-inducible genes such as RNase L (70), IFN regulatory factor-1 (IRF-1) (65), and the double-stranded RNA-regulated serine/threonine protein kinase (PKR) (36) have been implicated in tumor suppression.

The IFN-inducible HIN-200 gene family encodes a class of proteins that share a 200-amino acid (HIN) signature motif of type *a* and/or type *b*. Four human (IFI16, MNDA, AIM2, and IFIX) and five mouse (p202*a*, p202*b*, p203, p204, and p205 (or D3)) HIN-200 family proteins have been identified (2, 51). HIN-200 genes are located at chromosome 1q21-23 as a gene cluster in mouse and human genomes. Most HIN-200 proteins possess two major protein domains: first, except p202*a* and p202*b*, the N-terminal region of HIN-200 proteins contains a highly helical pyrin domain (PYD) (32), which belongs to the death domain-containing protein superfamily involved in apoptosis and inflammation (49, 64, 72). Second, the C-terminal HIN domain consists of two consecutive OB (oligonucleotide/oligosaccharide-binding) folds (1). The OB-fold containing proteins are involved in a variety of biological processes including DNA replication, DNA recombination, DNA repair, and telomere maintenance (6, 76). However, the role of HIN-200 proteins in these biological processes is poorly understood.

The observations that HIN-200 proteins interact with several cellular regulators involved in cell cycle control, differentiation, and apoptosis indicate the physiological role of HIN-200 proteins is clearly beyond the IFN system (2, 51). Moreover, HIN-200, e.g., IFI16, expression is widely expressed in normal human tissues including endothelial and epithelial cells further support this notion (25, 63, 82). Therefore, it is not surprising that loss or reduced expression of HIN-200 genes is associated with human cancers (3, 15-17, 24, 43, 59, 62, 78). These observations suggest HIN-200 proteins may play a role in tumor suppression.

The mouse double-minute gene 2 (mdm2) encodes an oncoprotein (20, 22). Consistently, HDM2, the human homologue of mdm2, is found frequently overexpressed in human cancers including about 50% of breast cancers (30, 52-54, 68). A recent report also showed that HDM2 overexpression in tumors is associated with poor prognosis (57). These results underscore the pivotal involvement of HDM2 in tumorigenesis. Therefore, HDM2 has been an important target for developing cancer therapeutics (23, 42, 69).

The RING finger domain of HDM2 possesses an intrinsic E3 ubiquitin ligase activity (39). The ubiquitinated proteins are targeted for proteasome-mediated degradation. The best-known substrate of the E3 ligase activity of HDM2 is p53 tumor suppressor protein. p53 binds to the N-terminus of HDM2. This interaction allows HDM2 to inhibit p53 in two ways: first, blocking p53's ability to activate transcription of its target genes by binding to the N-terminal transactivation domain of p53 (10, 60); and second, mediating ubiquitination of p53 leading to degradation by proteasome (27, 28, 44). Interestingly, HDM2 is also a substrate of its own E3 ligase activity (21, 33). The intricate regulation of p53 and HDM2 is further demonstrated by that fact that HDM2 is also a p53 responsive gene (4, 61). Thus, these

two molecules link together in a negative feedback loop for the purpose of keeping the cellular p53 at low levels in the absence of stress. The p53-HDM2 auto-regulatory loop is vital as demonstrated by the rescue of embryonic lethality of mdm2-null mice in a p53-null background (41, 58). Therefore, a defective auto-regulatory loop caused by mutations, DNA damage, or oncogenic insult has a profound impact on tumorigenesis (14).

We recently identified IFIX as a novel member of the human HIN-200 gene family (16). The IFIX transcriptional unit expresses at least six IFIX isoforms. IFIX proteins are primarily nuclear and possess a single type *a* HIN motif. Importantly, the expression of IFIX is reduced in majority of breast tumors and breast cancer cell lines. Therefore, IFIX may function as a putative tumor suppressor. Consistently, the expression of IFIXα1, the longest IFIX isoform, leads to suppression of growth and transformation phenotype *in vitro*, and tumorigenicity and tumor growth *in vivo* (16). The growth inhibitory activity of IFIXα1 is associated with an induction of $p21^{CIP1}$, a key cyclin dependent kinase inhibitor (16). However, the mechanism of the IFIXα1 tumor suppressor activity has not been well elucidated. In this report, we show a novel interaction between IFIXα1 and HDM2, which leads to destabilization of HDM2. In turn, p53 is stabilized and its transcriptional activity activated. The novel crosstalk between IFN-IFIX signaling pathway and HDM2-p53 auto-regulatory loop, may contribute to the IFN-induced anti-tumor activity in certain cancers.

MATERIALS AND METHODS

Cell lines, plasmids, and reagents. MCF-7 and its FLAG-tagged IFIXα1 derivatives, X-1 and X-2, as well as MDA-MB-468 and its FLAG-tagged IFIXα1 derivatives, X-1 and X-2, have been described previously (16). The corresponding control cell lines are the pooled stable clones transfected with the empty vector (pCMV-Tag2B (FLAG), Stratagene, La Jolla, CA) (16). H1299, HCT116 and its p53-null derivative, HCT116 (p53-/-) (8), 293 and its large-T derivative, 293T, and p53-/- and p53-/-, mdm2-/- double knockout (DKO) MEFs were grown in Dulbecco's modified Eagle's medium containing 10% fetal calf serum (FCS). Raji and U937 cells treated with or without IFN-α (Hu-IFN-αA) (2000 U/ml) and IFN-γ (1000 U/ml) (Sigma, St. Louis, MO), respectively, were grown in RPMI medium contain 10% or 0.2% FCS for the time described in the text. MG132 (10 μM) (Sigma) treatment was performed for 5 h prior to harvest. The EGFP-tagged IFIXα1 (EGFP-IFIXα1) and IFIXβ1 (EGFP-IFIXβ1) have been previously described (16). The IFIX-N was generated using PCR primer set: forward: 5'-CCGGATCCTTAGAGATGGCAAATAACTAC (containing a Bam HI site) and reverse: 5'-CGGGATCCCTCAGTTGAGGAAGTGTTGG (containing a Bam HI site), to amplify a 579-bp region corresponding to 1-193 amino acid of IFIXα1. The IFIX-HIN was generated using PCR primer set: forward: 5'-CGGAATTCCAGACCTCATCATCAGCTCC (containing an Eco RI site) and reverse: 5'-CGGGATCCTTACTGGATGAAACTATGCATTTC (containing a Bam HI site) to amplify a 654-bp region corresponding to 179-397 amino acid of IFIXα1. Both FLAG-tagged or EGFP-tagged IFIX-N and IFIX-HIN were generated as described before (16). GFP-p53 (gift from Dr. G. Wahl (73)), CMV-HDM2 (gift from Dr. Y. Zhang (37)), and the HDM2 mutants, i.e., HDM2 (Δ150-230) and HDM2 (1-441), have been previously described (38). Plasmid DNA transfection was performed by using FuGENE 6 Transfection Reagent (Roche, Indianapolis, IN) according to the manufacturer's instructions. To

isolate the GFP-positive cells, at 48 h after transfection, cells transfected with EGFP-IFIXα1, EGFP-HIN, or EGFP empty vector were sorted out by BD FACSAria™ Cell Sorting System (Palo Alto, CA).

siRNA transfection. Electroporation was used to transfect siRNAs into cells. The IFIX siRNA, i.e., ^{689}GGAGTAAGATGTCCAAAGA^{707} in exon 4 of IFIXα1 (Dharmacon, Lafayette, CO), was used for transfection. In Fig. 9B, a mixture of four IFIX siRNAs corresponding to 689-707, 1190-1209, 1246-1265, and 1486-1504 sequences of IFIXα1 cDNA (Dharmacon) was used. The non-specific control siRNA is 5'-TAGCGACTAAACACATCAATTdT-3' (Dharmacon). Briefly, cells were suspended in the electroporation buffer (120 nM KCl, 0.15 mM $CaCl_2$, 10 mM K_2HPO_4, 6 mM Glucose, 25 mM Hepes (pH7.6), 2 mM EGTA, and 5 mM $MgCl_2$). The siRNAs (100 nM) were then added to the cell suspension followed by electroporation using Nucleofector™ (Amaxa Biosystems, Koeln, Germany).

Co-immunoprecipitation, western blot, and antibodies. Protein lysates (0.5-1.5 mg) were prepared using RIPA-B lysis buffer as described previously (83). Antibodies (2-4 μg) used in co-IP: anti-HDM2 (D-7 for IP; and D-7 and N-20 for WB, Santa Cruz Biotechnology, Inc. Santa Cruz, CA), anti-FLAG (Sigma, M2 for co-IP and M5 for WB), and anti-GFP (Santa Cruz Biotech.) (Santa Cruz Biotech.). Immune complexes were recovered using 30 μl of protein-G (for monoclonal antibodies) or protein-A (for rabbit polyclonal antibodies) agarose (Roach) overnight at 4°C. Immune complex was then washed with PBS for 4-6 times at 4°C followed by centrifugation and SDS-PAGE. Proteins were then transferred to a nitrocellulose membrane and probed with antibodies as indicated in the text. Other antibodies used in the western blot (WB) include anti-PARP (BD Biosciences, Palo Alto, CA), anti-α-tubulin (Sigma), anti-PKR (Santa Cruz Biotech.), anti-IFI16 (Santa Cruz Biotech.), anti-p53 (NeoMarker, Freemont, CA), and anti-p21^{CIP1} (Santa Cruz Biotech.). The peptide-purified anti-IFIX antibodies (recognizing α, β, and γ isoforms) are rabbit polyclonal antibodies against two overlapping

peptides that corresponding to ^{195}LKPLANRHATASKNIFREDPIIA^{217} in the N-terminal domain of IFIXα1 (16) (Bethyl Laboratories, Inc. Montgomery, TX). The peptide-purified anti-IFIXα antibodies (recognizing α1 and α2 isoforms) are rabbit polyclonal antibodies against a synthetic peptide: ^{468}FRITSPTVAPPLSSDTSTNRHPAVP^{492}, which corresponds to the C-terminal 25 amino acid of IFIXα1 (16) (Bethyl Laboratories). Detection was achieved by incubating the secondary goat anti-rabbit or mouse antibodies coupled with horseradish peroxidase (Pierce, 1:5000) followed by the enhanced chemiluminescence kit (Amersham Pharmacia biotech, Buckinghamshire, UK).

Northern blot analysis. Northern blot analysis was performed as previously described (83).

Luciferase assays. Cells transfected with luciferase reporter gene, PG13-LUC (a Firefly luciferase gene under the control of 13 p53 responsive elements (77)), MG15-LUC (a corresponding construct with mutated p53 responsive elements), or wwp-LUC (a Firefly luciferase gene under the control of p21^{CIP1} promoter region containing 2.4 kb pair upstream sequence (19)) and pRL-TK (for normalizing transfection efficiency) (Promega) were harvested to measure luciferase activity using the Dual Luciferase Reporter Assay System (Promega, Madison, WI) and a illuminometer (TD-20/20, Promega).

Immunofluorescence assay. Cells were cultured in a four-well glass chamber overnight. 24 h after transfection, cells were fixed with 4% paraformaldehyde in PBS for 20 min at room temperature. Cells were then permeabilized with 0.5% Triton X-100 for 15 min at room temperature. Anti-p53 antibody (1:100) (NeoMarker) and anti-IFIXα (1:100) were added to the cells. The p53 and IFIXα1 proteins were visualized using secondary antibodies (1:500) conjugated with Texas Red and fluorescein isothiocyanate (FITC), respectively, (Jackson ImmunoResearch Laboratories, West Grove, PA) for 45 min.

Counterstaining was performed using DAPI (1:1000) to visualize nuclei. A cover slip was placed on top of the slide for visualization by a ZEISS fluorescence microscopy.

ChIP assay. The modified protocol used in this study was based on that previously published (50). Briefly, IFIXα1 stable MCF-7 and the vector control cell lines, X-1, X-2 and V were fixed by 1% formaldehyde for 10 min before cell lysis. Cell lysates were subsequently sonicated followed by centrifugation. The "input" (4% of the supernatant) was used in PCR as a positive control. The supernatant was then pre-cleared using mouse IgG (10 μg) for 1 h at 4°C. Protein G-agarose beads (Roche) (50 μl) was added to the supernatant and incubated for 2 h at 4°C. After centrifugation, the supernatant was then used for immunoprecipitation using anti-p53 antibody (2 μg) (NeoMarker) or an irrelevant antibody, e.g., anti-GFP antibody (2 μg) (Santa Cruz Biotech.) and incubated overnight at 4°C. The protein/DNA complex was subsequently incubated with protein G-agarose beads for 2 h at 4°C. The immune complex was collected by centrifugation and then washed 7 times, 10 min each: twice with 50 mM Tris-HCl (pH 8.0), 150 mM NaCl, 1% NP-40, 0.1% SDS, 0.5% sodium deoxycholae; once with 50 mM Tris-HCl (pH 8.0), 500 mM NaCl, 1% NP-40, 0.1% SDS; twice with 50 mM Tris-HCl (pH 8.0), 250 mM LiCl, 1% NP-40, 0.5% sodium deoxycholae, 1 mM EDTA and twice with TE (pH 8.0) buffer. The immune complex was suspended in TE buffer with 0.25% SDS, protease K (250 μg/ml) and RNase (50 μg/ml) and incubated at 37 °C for 4 h and at 65°C overnight. The DNA was then extracted with phenol-chloroform and precipitated with ethanol in the presence of glycogen (20 μg) as carrier. The precipitate was used as a template for PCR amplification. The primers that specifically amplify a 320-bp region located approximately 0.7-1.0 kb upstream of the human $p21^{CIP1}$ promoter are: forward: 5'-AAACCATCTGCAAATGAGGG, and reverse: 5'-GAACCAATCTCCCTACACC. PCR was

performed in the following condition: 35 cycles at 94°C for 40 second, 56°C for 1 min, and 72°C for 40 seconds.

Mobility shift assay. Nuclear extracts isolated from MCF-7 vector control, the IFIX-α1 stable cell lines (X-1 and X-2), and MCF-7 cells treated with or without ultraviolet light (20 j/m^2) were incubated with ^{32}P-labeled oligonucleotide containing p53-binding sites (p53 Nushift kit, Active Motif, Carlsbad CA) in a binding reaction according to manufacturer's instruction. The binding reaction was run on a 5% native polyacrylamide gel. Supershift assay was performed using the nuclear extract isolated from MCF-7 (X-1) cells incubated with or without the anti-p53 antibody provided by the p53 Nushift kit according to manufacture's protocol.

Cyclohexamide-chase assay. Cells were cultured in 6-well plates overnight. To measure the p53 turnover rate, MCF-7 vector control and the IFIXα1 stable cell lines (X-1 and X-2) were treated with cyclohexamide (100 μg/ml) (Sigma) for the indicated time followed by western blot using anti-p53 antibody. To measure the turnover rate of HDM2 and HDM2 (1-441), H1299 cells were co-transfected with HDM2 or HDM2 (1-441) (0.7 μg) and IFIXα1, IFIX-N, or the vector control, pCMV-Tag2B (FLAG) (1.3 μg) (Stratagene, La Jolla, CA). Forty-eight h after transfection, cells were treated with cyclohexamide (100 μg/ml) for the indicated time followed by WB using anti-HDM2 antibody.

RESULTS

IFIXα1 interacts with HDM2

It is known that HDM2 inhibition resulted in up regulation of $p21^{CIP1}$ in both MCF-7 and MDA-MB-468 breast cancer cell lines (38, 80, 87). Since we found IFIXα1 induces $p21^{CIP1}$ in these two cell lines (16), it is possible that IFIXα1 may do so by targeting HDM2. One way that HDM2 can be inhibited is through protein-protein interaction (35, 74). We then tested a possible interaction between IFIXα1 and HDM2 by co-transfecting 293T cells with HDM2 and IFIXα1 expression vectors. Cells were transfected with HDM2 and an enhanced green fluorescent protein (EGFP) vector (vector), the vector expressing EGFP-IFIXα1 (α1), or EGFP-IFIXβ1 (β1) fusion protein. The protein-protein interaction was examined by immunoprecipitation (IP) using anti-HDM2 antibody and followed by WB using either anti-GFP or anti-HDM2 antibody. A clear HDM2/IFIXα1 or HDM2/IFIXβ1 complex was detected (Fig. 1A). A reciprocal IP/WB experiment using anti-GFP antibody to pull down EGFP-IFIXα1 and EGFP-IFIXβ1 further confirmed the presence of these complexes (Fig. 1B). These data strongly suggest HDM2 interacts with IFIXα1 or IFIXβ1. We have attempted to investigate the possible interaction between HDM2 and the smallest IFIX isoform, IFIXγ1 (16). However, we found IFIXγ1 could only be extracted using SDS-containing lysis buffer (data not shown). Therefore, it is not feasible to detect such an interaction using the standard IP protocol. The IFIXα1-HDM2 interaction was also observed in cells co-transfected with FLAG-tagged IFIXα1 (or the control FLAG vector) and HDM2 into 293T cells followed by IP/WB (Fig. 1C). Consistently, using the IFIXα1 stable MCF-7 cell lines, X-1 and X-2, and the vector control cell (V) for IP/WB analysis, we found IFIXα1 could be brought down by anti-HDM2 antibody in X-1 and X-2 stable cell lines (Fig. 1D). This result again confirms the presence of an IFIXα1-HDM2 protein complex. Importantly, this interaction is also confirmed in the IFN inducible cell systems. We previously showed that the IFIX could be readily induced by IFN-α in Raji cells and by

IFN-γ in U937 cells (16). We then investigated the IFIXα1-HDM2 interaction in these IFN-inducible systems. Based on a time course study, at 48 h of treatment, the expression of IFIXα is readily induced by IFN-α or IFN-γ but the HDM2 levels are not reduced in Raji cells (data not shown). At this time point, we performed IP/WB and show a physiological interaction between IFIXα and HDM2 in both Raji and U937 cells (Fig. 1E). The induction of IFIXα (which may include α1 and α2 isoforms) by IFN-α or IFN-γ correlates well with an increase of IFIXα-HDM2 interaction. IP using IgG serves as a negative control. Together, these results strongly indicate that IFIXα1 interacts with HDM2 in both IFIXα1 overexpression system and IFN-inducible systems.

IFIXα1 binds to the 150-230 region of HDM2

To determine the region of HDM2 responsible for binding to IFIXα1, we co-transfected 293T cells with EGFP-IFIXα1 and a vector expressing HDM2 mutant, e.g., RING finger deletion (1-441) or 150-230 deletion (Δ150-230) (38), followed by IP/WB. As shown in Fig. 2A, like the wild type HDM2 (Fig. 1), HDM2 (1-441) can readily interact with IFIXα1. Since the anti-HDM2 antibody used in IP recognizes the epitope resides within 150-230 aa of HDM2, it is therefore not suitable for HDM2 (Δ150-230) IP. Instead, we co-transfected 293T cells with HDM2 or HDM2 (Δ150-230) and EGFP-IFIXα1 or FLAG-IFIXα1 followed by IP with anti-GFP antibody (Fig. 2B) or anti-FLAG antibody (Fig. 2C), respectively. The HDM2-IFIXα1 interaction serves as a positive control. While HDM2 (Δ150-230) and IFIXα1 are readily detectable by direct western blots, there is no HDM2 (Δ150-230) protein present in the IFIXα1 immunocomplex. This result suggests that the 150-230 region of HDM2 is required for IFIXα1 binding.

The HIN region of IFIXα1 interacts with HDM2

IFIXα1 differs from IFIXβ1 at the C-terminal sequence (16). The observation that both isoforms interact with HDM2 (Fig. 1A-B) suggests the C-terminal region of IFIXα1 is dispensable for HDM2 binding. We then tested the HDM2-binding ability of the N-terminal PYD domain (IFIX-N) and the HIN domain (IFIX-HIN). We first examined the cellular localization of these mutants by transfecting the EGFP fusion proteins, i.e., EGFP-IFIX-N and EGFP-IFIX-HIN into MCF-7 cells. As shown in Fig. 2D, IFIX-N is clearly localized in the nucleus. Surprisingly, IFIX-HIN, which lacks the putative nuclear localization signal (NLS) in the N-terminal domain (16), localizes in both nuclear and cytoplasmic compartments (Fig. 2D). Howbeit, nuclear localization appears dominant (N > C, 92/110 (83.6%); and N = C, 18/110 (16.4%)). To determine the protein-protein interaction, we co-transfected 293T cells with HDM2 and EGFP (V), EGFP-IFIXα1 (α1), EGFP-IFIX-N (N), or EGFP-IFIX-HIN (HIN) followed by IP using anti-GFP antibody and WB with either anti-HDM2 antibody or anti-GFP antibody. As shown in Fig. 2E (left panel), IFIX-HIN, but not IFIX-N, alone is sufficient to bind HDM2. Consistently, IFIX-HIN, but not IFIX-N, interacts with HDM2 in a reverse IP/WB (Fig. 2E, right panel). Together, these results indicate that the HIN domain of IFIXα1 is sufficient to interact with HDM2 (Fig. 2F).

The interaction and the RING finger domain of HDM2 are required for the destabilization of HDM2 by IFIXα1

It is known that HDM2 is a substrate of its own E3 ligase activity leading to its degradation through proteasome-mediated pathway (21, 34). It is possible that IFIXα1 binding may affect the protein stability of HDM2. To test this possibility, we measured the turnover rate of HDM2 protein with or without IFIXα1. H1299 cells were co-transfected with HDM2 and IFIXα1 (FLAG-IFIXα1) (or the empty FLAG vector (V)) followed by a cyclohexamide (CHX) (a protein synthesis inhibitor)-chase assay. As shown in Fig. 3A-B, the 50% turnover rate of HDM2 was increased from >30 min in cells

transfected with empty vector to ~21 min with IFIXα1 transfection. Importantly, the HDM2-binding deficient mutant, i.e., IFIX-N, has little effect on the stability of HDM2 (Fig. 3A). These results suggest that IFIXα1 destabilizes HDM2 and the IFIXα1-HDM2 interaction is required for this activity. It is possible that the E3 ligase activity of RING finger domain plays a role in the IFIXα1-mediated HDM2 destabilization. To test this possibility, we measured the turnover rate of a HDM2 mutant, i.e., 1-441, in which the RING finger domain is deleted, with or without IFIXα1. As shown in Fig. 3C, HDM2 (1-441) is refractory to the destabilizing effect of IFIXα1. This result suggests that the E3 ligase activity is required for the IFIXα1-induced HDM2 destabilization. It also rules out the possibility that IFIXα1 may interact with an unknown E3 ligase protein that could *trans*-ubiquitinate HDM2. Together, our data suggest that both interaction and the E3 ligase activity are required for the destabilization of HDM2 by IFIXα1.

IFIXα1 promotes the ubiquitination of HDM2

Since the E3 ligase activity is required for the IFIXα1-mediated HDM2 destabilization (Fig. 3C), it is possible that IFIXα1 destabilizes HDM2 by promoting its ubiquitination. To test this possibility, we determined the levels of ubiquitinated HDM2 in cells transfected with or without IFIXα1 in the presence of MG132. H1299 cells were co-transfected with HDM2, HA-Ubiqutin, and increasing amount of IFIXα1 followed by IP/WB using anti-HDM2 antibody. As shown in Fig. 3D, the ubiquitinated HDM2 levels increase in an IFIXα1 dose dependent manner. The increase of ubiquitinated HDM2 correlates well with the increase of IFIXα1-HDM2 interaction. The observation that IFIXα1 binds HDM2 and promotes its ubiquitination represents a plausible mechanism by which IFIXα1 destabilizes HDM2.

IFIXα1 induces p53 protein stability

HDM2 is the major negative regulator of p53 through ubiquitination-proteasome pathway (7, 35, 56). We show IFIXα1 destabilizes HDM2 (Fig. 3A). It predicts p53 induction in IFIXα1-expressing cells. To test this possibility, we performed a western blot analysis on the p53 protein expression in the IFIXα1 stable MCF-7 cells (which express wild type p53), i.e., X-1 and X-2, and the vector control (V) (16). Indeed, the p53 protein levels are increased in the X-1 and X-2 cells as compared with that in the vector control cells (Fig. 4A). It is possible that the observed p53 increase may be an inadvertent event due to clonal heterogeneity (albeit, two independent clones exhibit p53 induction). To rule out this possibility, we transiently transfected MCF-7 cells with EGFP vector or EGFP-IFIXα1 followed by FACS. Cell lysates isolated from the GFP-positive cells were then subjected to WB analysis to examine the p53 expression. Consistent with the stable cell line data (Fig. 4A), IFIXα1 expression is associated with an increase of endogenous p53 (Fig. 4B). This result suggests that clonal heterogeneity is not the cause for the p53 increase in the IFIXα1 stable cell lines. The causative effect of IFIXα1 on p53 induction was confirmed by an IFIXα1 knockdown experiment using a small inhibitory RNA (siRNA) specific for IFIX (Dharmacon). We chose MCF-7 (X-1) for the IFIXα1 knockdown study because it is a low IFIXα1 expresser as compared with MCF-7 (X-2) (Fig. 4A). As shown in Fig. 4C, the IFIX siRNA transfection specifically reduces p53 protein levels in MCF-7 (X-1) cells as compared with that transfected with the non-specific scramble control (NS) siRNA. This result strongly suggests that the expression of IFIXα1 is primarily responsible for the increase of p53 protein levels in the IFIXα1 stable cell lines. We previously showed that IFIXα1 expression is associated with $p21^{CIP1}$ induction in MCF-7 cells (16). As expected, reduced expression of p53 by IFIX siRNA (Fig. 4C) also leads to decreased expression of its transcriptional target gene, $p21^{CIP1}$ (Fig. 4D). Importantly, there is little change on the p53 mRNA levels with or without IFIXα1 expression (Fig. 4E). This observation strongly suggests that p53 induction by IFIXα1 is regulated post-transcriptionally. To test this possibility, we performed a

CHX-chase experiment to measure the p53 protein turnover rates in IFIXα1 stable (X-1 and X-2) and vector (V) control cells. We found that the half-life of p53 is significantly increased in X-1 and X-2 cells (>30 min) as compared with that in the control cells (<15 min) (Fig. 4F). This result suggests that IFIXα1 induces p53 expression by increasing its protein stability.

IFIXα1 activates the p53-mediated transcription

The induction of p53 by IFIXα1 coincides with an increase of the steady state mRNA levels of HDM2 and $p21^{CIP1}$ (Fig. 4E, (16)). Since both HDM2 and $p21^{CIP1}$ are p53 responsive genes, it is possible that IFIXα1 activates the p53-mediated transcription. To test that possibility, we transfected a human non-small cell lung carcinoma cell line, H1299 (which is p53-null) (85) with PG13-LUC, a luciferase reporter construct containing multiple p53 binding sites (77), or MG15-LUC, a corresponding construct containing mutated p53 binding sites. As shown in Fig. 5A, IFIXα1 increases the p53-mediated transcriptional activity of PG13-LUC (but not MG15-LUC) in a dose-dependent manner. This result indicates IFIXα1 can activate the p53-mediated transcription. We then tested the possibility that IFIXα1-mediated p53 transcriptional activation correlates with an increase of p53 DNA binding activity. We employed a mobility-shift assay in which the ^{32}p-labeled oligonucleotides containing p53 DNA binding sites were incubated with the nuclear extracts (NE) isolated from the IFIXα1 stable cell lines (X-1 and X-2) and the vector control (V) cells. The p53/DNA complex was resolved by a native gel electrophoresis. As shown in Fig. 5B (top panel), the p53 DNA binding activity is strongly enhanced in X-1 and X-2 cells as compared with that in the control cells. The p53 DNA binding activity induced by DNA damaging agent such as ultraviolet light (UV) serves as a positive control. The protein/DNA complex (indicated by an arrow) is p53 specific since incubation of anti-p53 antibody in the X-1 nuclear extract diminishes the complex. The increase of p53 DNA binding activity correlates well with an

increase of p53 in the nuclear extracts isolated from the X-1 and X-2 cells (Fig. 5B, bottom panel). To determine the effect of IFIXα1 on $p21^{CIP1}$ transcription, we co-transfected the wild type p53-expressing cell lines, MCF-7 and HCT116 (a human colorectal carcinoma cell line), with a luciferase reporter gene driven by a $p21^{CIP1}$ promoter (wwp-LUC) (19) and increasing amount of IFIXα1. We found that IFIXα1 activates $p21^{CIP1}$ promoter in a dose-dependent manner in both cell lines (Fig. 5C). This modest induction (2~3 fold) of $p21^{CIP1}$ promoter activity was similar to that observed by either IFN-γ (26) or another HIN-200 protein, IFI16 (84). This result indicates IFIXα1 can transcriptionally activate $p21^{CIP1}$ gene. p53 is a major transcriptional activator that binds $p21^{CIP1}$ promoter (19). It is possible that IFIXα1 activates $p21^{CIP1}$ transcription by increasing p53 binding to the promoter. To test this possibility, we employed chromatin-immunoprecipitation (ChIP) assay using anti-p53 or anti-GFP antibody (as a negative control). As shown in Fig. 5D, an increase of p53 binding to the $p21^{CIP1}$ promoter is observed in the IFIXα1 stable MCF-7 cell lines (X-1 and X-2) as compared with the basal levels of p53 binding in the vector control cells. These results strongly suggest that IFIXα1 activates $p21^{CIP1}$ transcription by increasing p53 binding to the promoter.

IFIXα1 promotes p53 nuclear accumulation

Since nuclear p53 is active in transcriptional activation, it is possible that increased p53-mediated transcription correlates with increased p53 nuclear localization. As shown in Fig. 5E, p53 is predominantly nuclear and co-localized with IFIXα1 in the IFIXα1 stable MCF-7 cell line, X-2 (16). In contrast, p53 staining appears to be diffused throughout the entire cells in the vector (V) control cell. The IgG staining serves as a negative control. To further confirm this observation, we transiently transfected a vector expressing GFP-p53 fusion protein (73) into the IFIXα1 stable cell lines or the vector control cells. Twenty-four h after transfection, we determined the percentage of GFP-positive

cells with GFP-p53 present in both cytoplasmic and nuclear compartments (C+N) or primarily nuclear compartment (N). Consistent with that observed in the stable cell lines (Fig. 5E), the majority of GFP-p53 is localized in the nuclear compartment of the IFIXα1 stable cell lines, X-1 and X-2, as compared with that in the vector control cells (Fig. 5F). These data indicate IFIXα1 promotes p53 nuclear localization.

The HIN domain is sufficient to induce p53

To determine the functional domain responsible for the p53 induction, we co-transfected H1299 cells with p53 and increasing amount of IFIXα1, IFIX-HIN, or IFIX-N. As expected, we observed a dose dependent increase of p53 in cells transfected with IFIXα1 (Fig. 6A). Consistently, the endogenous $p21^{CIP1}$ is also increased in a dose dependent manner. Interestingly, the HDM2 binding competent mutant, IFIX-HIN, is sufficient to induce both p53 and $p21^{CIP1}$ (Fig. 6B), but not the HDM2 binding deficient mutant IFIX-N (Fig. 6C). This result is further confirmed by a northern blot analysis in which the p53-induced $p21^{CIP1}$ mRNA levels are increased by IFIXα1 and IFIX-HIN, but not IFIX-N (Fig. 6D). Our previous observation that IFIXγ1, which lacks the HIN domain, was unable to induce $p21^{CIP1}$ (16) supports the requirement of HIN domain for $p21^{CIP1}$ induction. Together, these data suggest that the HIN domain of IFIXα1 is sufficient to induce p53 and activates the p53-mediated transcription of $p21^{CIP1}$.

HDM2 is required for the p53 induction and activation by IFIXα1.

Given that IFIXα1 binds and destabilizes HDM2 (Fig. 1 and 3A), our data support a model that IFIXα1 functions as a positive regulator of p53 by negatively regulating HDM2. This model predicts that HDM2 is required for the p53 induction by IFIXα1. To test this possibility, we co-transfected p53-/- MEF and

p53-/-, mdm2-/- double knockout (DKO) MEF with GFP-p53 and increasing amount of IFIXα1. As expected, p53 is induced by IFIXα1 in p53-/- MEF in a dose dependent manner (Fig. 7A). However, IFIXα1 fails to do so in DKO MEF. This result strongly suggests that HDM2 is required for the induction of p53 by IFIXα1. To further confirm this observation, p53-/- MEF and DKO MEF were co-transfected with PG13-LUC, p53, and increasing amount of IFIXα1. As shown in Fig. 7B, IFIXα1 activates p53-mediated transcription in a dose-dependent manner in p53-/- MEF but not in DKO MEF. Notably, in the absence of IFIXα1, p53 drastically enhances p53-mediated transcription in DKO MEF because p53 is stabilized in the absence of HDM2. It is consistent with the observation that the p53 levels are higher in DKO MEF than that in p53-/- MEF (Fig. 7A). Together, these results suggest that IFIXα1 induces p53 indirectly through targeting HDM2.

IFIXα1 down regulates HDM2 independent of p53

In spite of HDM2 mRNA induction by IFIXα1 (Fig. 4E), little change on the HDM2 protein levels was seen in the p53-expressing MCF-7 cells (Fig. 1D, right panel), H1299 transfected with p53 (Fig. 6A), and the p53-expressing HCT116 (Fig. 8D, left panel). In addition, although IFIXα1 depletion by siRNA reduces p53 in MCF-7 cells (Fig. 4C), it has little effect on the HDM2 expression (data not shown). These observations can be explained by the combination of two opposite effects on HDM2 by IFIXα1. Namely, the negative effect of IFIXα1 on HDM2 protein stability leads to stabilization of p53. In turn, p53 positively regulates HDM2. The net result of these two opposing effect may be responsible for the apparent little change on the HDM2 levels. If so, the negative effect on HDM2 by IFIXα1 would be pronounced in cells without functional p53. Indeed, as shown in Fig. 8A, the HDM2 protein levels were greatly reduced in the IFIXα1 stable MDA-MB-468 cells (expressing mutant p53), i.e., X-1 and X-2 (16), as compared with the vector (V). We also noted that a lack of HDM2 reduction by EGFP-IFIXα1

or EGFP-IFIXβ1 transfection in 293T cells as compared with the EGFP vector transfection (Fig. 1A-B, right panels). It could be explained by the constitutive expression of the HDM2 gene driven by a CMV promoter. In essence, it resembles the comparable levels of the endogenous HDM2 in the p53-expressing MCF-7 cell lines with or without IFIXα1 (Fig. 1D, right panel). For the IFIXα1 knockdown experiment, we chose a low IFIXα1 expresser, i.e., MDA-MB-468 (X-1). IFIX siRNA, but not the control (NS) siRNA transfection, reverses the HDM2 down regulation in MDA-MB-468 (X-1) (Fig. 8B). This result clearly indicates IFIXα1 is directly responsible for the HDM2 reduction. In addition, IFIXα1 expression has little effect on the HDM2 mRNA levels in the IFIXα1 stable MDA-MB-468 cell lines (Fig. 8C). This result not only shows that the elevated levels of HDM2 mRNA observed in the IFIXα1 stable MCF-7 cells are indeed p53 dependent (Fig. 4E); but also effectively rules out the possibility that transcriptional repression is responsible for HDM2 down regulation by IFIXα1. To further confirm the p53-independent down regulation of HDM2 by IFIXα1, we employed HCT116 and its p53-null derivative, HCT116 (p53-/-), in which both p53 alleles were deleted by homologous recombination (8). Both cell lines were transfected with either EGFP-IFIXα1 or the EGFP control vector followed by FACS to enrich the GFP-positive cells for western blot analysis. As shown in Fig. 8D (left panel), IFIXα1 expression increases p53 but has a little effect on HDM2 levels, which is similar to that observed in MCF-7 cells (Fig. 1D, right panel). In contrast, IFIXα1 expression results in a drastic reduction of HDM2 in HCT116 (p53-/-) cells (Fig. 8D, right panel). HDM2 reduction by IFIXα1 is also observed in two other cell lines that lack wild type p53, i.e., H1299 and 293 (Fig. 8E-F). Importantly, the IFIXα1-mediated HDM2 down regulation can be abrogated in the presence of a proteasome inhibitor, MG132 (Fig. 8E-F). These results suggest that IFIXα1 down regulates HDM2 post-translationally through a proteasome-mediated degradation. Further confirmation of the above results came from the HDM2 half-life study in the IFIXα1 stable and the vector control cells. We found the

HDM2 half-life is shorter in IFIXα1 stable MDA-MB-468 (X-1 and X-2) cells than that in the vector control cells (data not shown).

Since IFIX-HIN alone induces p53 (Fig. 6B), it is possible that, like IFIXα1, IFIX-HIN does so by targeting HDM2. To test this possibility, we transfected 293 cells with EGFP empty vector or EGFP-IFIX-HIN followed by FACS. The GFP-positive cells were analyzed for HDM2 expression by WB. As shown in Fig. 8G, IFIX-HIN alone is sufficient to reduce the endogenous HDM2 as compared with that transfected with EGFP vector. As expected, MG132 treatment stabilizes HDM2 expression. In contrast, MG132 has little effect on the expression of IFIXα1 (Fig. 8E-F) or IFIX-N (data not shown). Interestingly, MG132 treatment increases EGFP-IFIX-HIN expression (Fig. 8G). This result suggests that IFIX-HIN is relatively unstable and is susceptible for degradation by proteasome.

IFIXα1 mediates the down regulation of HDM2 by IFN

IFIXα1 is IFN-inducible protein (16). We show that the IFN-induced IFIXα also interacts with HDM2 (Fig. 1E). It is possible that this protein-protein interaction also leads to HDM2 down regulation. We chose Raji (a human Burkitt's lymphoma cell line in which p53 is mutated (18)) because IFIX expression can be readily induced by IFN-α (16). At 72 h of treatment, the induction of endogenous IFIXα correlates well with a significant decrease of HDM2 (Fig. 9A). As a positive control for the IFN-α responsiveness, the same membrane was probed with an antibody against a known IFN-inducible protein, PKR (36). The PKR levels increase in response to IFN-α treatment, indicating IFN pathway is activated (Fig. 9A). However, it remains possible that other HIN-200 genes inducible by IFN-α may contribute to HDM2 down regulation. We then analyzed the expression of HIN-200 proteins in the IFN-α treated Raji cells. Except for AIM2 (the anti-AIM2 antibody is not available), we found the expression

of IFI16 is also induced by IFN-α in normal growth condition with 10% FCS (Fig. 9A). The expression of MNDA was not detected with or without IFN-α treatment in Raji cells (data not shown). Interestingly, we found IFIXα, but not IFI16, can also be induced by IFN-α under low serum (0.2% FCS) condition (Fig. 9B, left panel). Importantly, under this condition, the IFN-α-induced IFIXα expression remains correlated with HDM2 down regulation. Thus, the low serum condition provides us a unique opportunity to determine the role of IFIXα in IFN-α-induced HDM2 down regulation. To assure the specificity of IFIX siRNA, a mixture of four IFIX siRNAs (see Materials and Methods) was transfected into Raji cells followed by IFN-α treatment. We show that IFIX siRNAs transfection reduces IFIXα, but it has little effect on IFI16 expression (Fig. 9B, right panel). Importantly, IFIXα depletion by IFIX siRNAs increases the expression of HDM2 as compared with that transfected with NS siRNA (Fig. 9B, right panel). This result indicates that IFIXα plays an essential role in the IFN-induced HDM2 down regulation.

DISCUSSION

In this report, we present evidence to suggest that IFIXα1 functions as a negative regulator of HDM2. As such, IFIXα1 positively regulates p53. IFIXα1 increases p53 abundance by stabilizing p53 leading to increased p53-mediated transcriptional activity.

Emerging evidence has suggested a crosstalk between IFN signaling pathway and p53 tumor suppressor pathway. For example, it was shown that IFNα/β transcriptionally activates p53 (75). In contrast, IFN-inducible proteins regulate p53 post-transcriptionally. For instance, PKR not only activates p53 transcription (86), but also binds to the C-terminus of p53 and phosphorylates serine 392 (12). In turn,

PKR up regulates p53-mediated gene transcription (11). IFI16 binds to p53 and is able to augment the transcriptional activation of a p53 reporter gene (24, 40). This physical interaction may contribute to the ability of IFI16 to sensitize cells to p53-dependent apoptosis induced by γ-irradiation (24). p202*a* was shown to be associated with a p53 protein complex through the p53 binding protein 1 (53BP1) leading to the inhibition of p53 transcriptional activity (13). Although IFIXα1 co-localizes with p53 in the nucleus (Fig. 5E), we have not found a physical association between IFIXα1 and p53 despite our intensive efforts to look for such an interaction (data not shown). Additional experiment such as gel-filtration analysis is needed to verify this observation. However, it remains possible that IFIXα1-HDM2 and p53-HDM2 may exist as mutually exclusive complexes. Therefore, unlike PKR, IFI16, and p202*a*, p53 binding may not be necessary for IFIXα1 to stabilize p53 and activates the p53-mediated transcription. Our data suggest that p53 induction and stabilization are the result of HDM2 down regulation by IFIXα1. These results suggest that HDM2, but not p53, is the primary target of IFIXα1. This conclusion is confirmed by the observation that p53 can only be stabilized and activated by IFIXα1 in p53-/- MEF but not in DKO MEF (Fig. 7).

Due to the HDM2-p53 auto-regulatory loop, the IFIXα1-mediated HDM2 down regulation is especially clear in the absence of p53 (Fig. 8). The fact that the HDM2 reduction can be rescued by MG132 (Fig. 8E-F) suggests that IFIXα1- or IFN-α-mediated HDM2 down regulation is through proteasome-mediated degradation. It is known that the E3 ligase activity of RING domain also serves to ubiquitinate HDM2 itself (21, 34). We show here that the RING domain is required for the IFIXα1-mediated HDM2 destabilization (Fig. 3C). We therefore hypothesize that IFIXα1 increases the E3 ligase activity resulting in increased levels of ubiquitinated HDM2. The observation that HDM2 is highly ubiquitinated in the IFIXα1-transfected cells (Fig. 3D) supports this hypothesis. The mechanism underlying the increased

ubiquitination of HDM2 by IFIXα1 is not clear. However, it is possible that IFIXα1, when binding to HDM2, may simultaneously compromise the binding of certain HDM2 interacting proteins that negatively regulate the ubiquitination of HDM2, e.g., p14ARF (67, 81), MDMX (29, 71), TSG101 (47), and HAUSP (48). It is conceivable that disruption of these interactions by IFIXα1 may restore the E3 ligase activity of HDM2 resulting in an increase of ubiquitination. Alternatively, post-translational modifications such as sumoylation, acetylation, and phosphorylation are also known to regulate the E3 ligase activity of HDM2 (9, 55). Thus, it is also possible that IFIXα1 binding may alter certain modifications of HDM2 and tip the balance to favoring ubiquitination.

The nuclear localization of IFIX-N is somewhat expected since a putative NLS, ^{134}LGPQKRKK, resides within the N-terminal region of IFIXα1 (16). However, unlike IFIXγ1, which forms nuclear specks (16), IFX-N localizes throughout the nucleus (Fig. 2D). This result suggests the unique C-terminal 52 amino acid region of IFIXγ1 may be responsible for the nuclear speck localization. On the other hand, the attenuated nuclear localization of IFIX-HIN (Fig. 2D) suggests the N-terminal NLS is required for the exclusive nuclear localization of IFIXα1. It also suggests that other NLS(s) exists to direct IFIX-HIN to the nucleus. Two highly charged regions, e.g., ^{259}LKRKFIKKR and ^{306}RRAKKIPK, reside within the HIN domain may represent such NLSs. Alternatively, it is possible that IFIX-HIN may be shuttled into the nucleus by interacting with other nuclear protein.

Like IFIXα1, IFIX-HIN alone is able to induce p53 and p21^{CIP1} (Fig. 6B). This result is consistent with our previous finding that p21^{CIP1} induction was observed in cells expressing IFIXα1 and IFIXβ1 but not IFIXγ1, which lacks the HIN domain (16). Thus, the N-terminal PYD domain and the C-terminal domain appear to be dispensable for the destabilization of HDM2 by IFIXα1. Together with the

observation that IFIX-HIN down regulates HDM2 (Fig. 8G), these data raise the possibility that IFIX-HIN alone may be sufficient to destabilize HDM2. Although experiments have been performed to test this possibility, the instability of IFIX-HIN (Fig. 8G) has become a challenge in this effort. Perhaps, an exclusively nucleus localized IFIX-HIN by tagging its own NLS or a heterologous NLS may help to solve the stability issue. Nevertheless, given that IFIX-HIN is the signature motif of HIN-200 proteins, it is possible that other HIN-200 family proteins may possess a similar activity to destabilize HDM2.

In addition to IFN's role in innate and adaptive immunity (5), the pro-apoptosis, anti-angiogenesis, and anti-proliferation activities of IFN have been the basis for treating human malignancies (31, 66). The anti-tumor activity of IFN is likely attributed to the tumor suppressor functions of certain IFN-inducible proteins (31, 45). HIN-200 genes have been implicated as tumor suppressors by virtue of their loss or reduced expression in human malignancies (for recent reviews see (2, 51)). IFIXα1, a novel member of the human HIN-200 gene family, is down regulated in breast cancer and its expression is associated with growth inhibition and tumor suppression (16). Here, we present a mechanism for the IFIXα1-mediated anti-tumor activity. Our data suggest IFIXα1 destabilizes HDM2. IFIXα1 does so by binding to HDM2 and promoting its ubiquitination and degradation. Consequently, p53 is stabilized and the p53-responsive gene such as $p21^{CIP1}$ activated leading to growth inhibition. Therefore, the IFN-IFIXα1-HDM2-p53-$p21^{CIP1}$ pathway may contribute to the overall IFN-mediated anti-tumor activity in certain cancers.

ACKNOWLEDGMENTS

This work was supported by a Susan Komen Breast Cancer Foundation grant and an Institutional Research grant from the University of Texas M. D. Anderson Cancer Center (to DHY), CA095441 (to HL) from NIH, and Cancer Center Core grant CA16672. YD is a recipient of a post-doctoral fellowship from the Department of Defense (DAMD17-02-1-0451).

The authors would like to thank Dr. Mong-Hong Lee for critical reading of this manuscript and Dr. Yanping Zhang for helpful discussion. The authors also thank Drs. Mien-Chie Hung, Mong-Hong Lee, Li-Kuo Su, Naoto Ueno, Bert Vogelstein, Geoffrey Wahl, and Yanping Zhang for their generous gift of reagents used in this study.

REFERENCES

1. **Albrecht, M., D. Choubey, and T. Lengauer.** 2005. The HIN domain of IFI-200 proteins consists of two OB folds. Biochem. Biophys. Res. Commun. **327:**679-687.

2. **Asefa, B., K. D. Klarmann, N. G. Copeland, D. J. Gilbert, N. A. Jenkins, and J. R. Keller.** 2004. The interferon-inducible negative regulator of cell growth. Blood Cells Mol. Dis. **32:**155-167.

3. **Azzimonti, B., M. Pagano, M. Mondini, M. De Andrea, G. Valente, G. Monga, M. Tommasino, P. Aluffi, S. Landolfo, and M. Gariglio.** 2004. Altered patterns of the interferon-inducible gene IFI16 expression in head and neck squamous cell carcinoma: immunohistochemical study including correlation with retinoblastoma protein, human papillomavirus infection and proliferation index. Histopatholgy **45:**560-572.

4. **Barak, Y., T. Juven, R. Haffner, and M. Oren.** 1993. mdm2 expression is induced by wild type p53 activity. EMBO J. **12:**461-468.

5. **Biron, C. A., and G. C. Sen.** 2001. Interferons and other cytokines, p. 321-351, 4th ed. Lippincott Williams & Wilkins.

6. **Bochkarev, A., and E. Bochkareva.** 2004. From RPA to BRCA2: lessons from single-stranded DNA binding by the OB-fold. Curr. Opin. Struct. Biol. **14:**36-42.

7. **Brooks, C. L., and W. Gu.** 2004. Dynamics in the p53-Mdm2 ubiquitination pathway. Cell Cycle **3:**895-899.

8. **Bunz, F., A. Dutriaux, C. Lengauer, T. Waldman, S. Zhou, J. P. Brown, J. M. Sedivy, K. W. Kinzler, and B. Vogelstein.** 1998. Requirement for p53 and p21 to sustain G2 arrest after DNA damage. Science **282:**1497-1501.

9. **Buschmann, T., D. Lerner, C. G. Lee, and Z. Ronai.** 2001. The Mdm-2 amino terminus is required for Mdm2 binding and SUMO-1 conjugation by the E2 SUMO-1 conjugating enzyme Ubc9. J. Biol. Chem. **276:**40389-40395.

10. **Chen, J., V. Marechal, and A. J. Levine.** 1993. Mapping of the p53 and mdm-2 interaction domains. Mol. Cell. Biol. **13:**4107-4114.

11. **Cuddihy, A. R., S. Li, N. W. Tam, A. H. Wong, Y. Taya, N. Abraham, J. C. Bell, and A. E. Koromilas.** 1999. Double-stranded-RNA-activated protein kinase PKR enhances transcriptional activation by tumor suppressor p53. Mol. Cell. Biol. **19:**2475-2484.

12. **Cuddihy, A. R., A. H. Wong, N. W. Tam, S. Li, and A. E. Koromilas.** 1999. The double-stranded RNA activated protein kinase PKR physically associates with the tumor suppressor p53 protein and phosphorylates human p53 on serine 392 in vitro. Oncogene **18:**2690-2702.

13. **Datta, B., B. Li, D. Choubey, G. Nallur, and P. Lengyel.** 1996. p202, an interferon-inducible modulator of transcription, inhibits transcriptional activation by the p53 tumor suppressor protein, and a segment from the p53-binding protein 1 that binds to p202 overcomes this inhibition. J. Biol. Chem. **271:**27544-27555.

14. **Deb, S. P.** 2003. Cell cycle regulatory functions of the human oncoprotein MDM2. Mol. Cancer Res.: MCR **1:**1009-1016.

15. **DeYoung, K. L., M. E. Ray, Y. A. Su, S. L. Anzick, R. W. Johnstone, J. A. Trapani, P. S. Meltzer, and J. M. Trent.** 1997. Cloning a novel member of the human interferon-inducible gene family associated with control of tumorigenicity in a model of human melanoma. Oncogene **15:**453-457.

16. **Ding, Y., L. Wang, L. K. Su, J. A. Frey, R. Shao, K. K. Hunt, and D. H. Yan.** 2004. Antitumor activity of IFIX, a novel interferon-inducible HIN-200 gene, in breast cancer. Oncogene **23:**4556-4566.

17. **Doggett, K. L., J. A. Briggs, M. F. Linton, S. Fazio, D. R. Head, J. Xie, Y. Hashimoto, J. Laborda, and R. C. Briggs.** 2002. Retroviral mediated expression of the human myeloid nuclear antigen in a null cell line upregulates Dlk1 expression. J. Cell. Biochem. **86:**56-66.

18. **Duthu, A., B. Debuire, J. Romano, J. C. Ehrhart, M. Fiscella, E. May, E. Appella, and P. May.** 1992. p53 mutations in Raji cells: characterization and localization relative to other Burkitt's lymphomas. Oncogene **7:**2161-2167.

19. **el-Deiry, W. S., T. Tokino, V. E. Velculescu, D. B. Levy, R. Parsons, J. M. Trent, D. Lin, W. E. Mercer, K. W. Kinzler, and B. Vogelstein.** 1993. WAF1, a potential mediator of p53 tumor suppression. Cell **75:**817-825.

20. **Fakharzadeh, S. S., S. P. Trusko, and D. L. George.** 1991. Tumorigenic potential associated with enhanced expression of a gene that is amplified in a mouse tumor cell line. EMBO J. **10:**1565-4569.

21. **Fang, S., J. P. Jensen, R. L. Ludwig, K. H. Vousden, and A. M. Weissman.** 2000. Mdm2 is a RING finger-dependent ubiquitin protein ligase for itself and p53. J. Biol. Chem. **275:**8945-8951.

22. **Finlay, C. A.** 1993. The mdm-2 oncogene can overcome wild-type p53 suppression of transformed cell growth. Mol. Cell. Biol. **13:**301-306.

23. **Fischer, P. M., and D. P. Lane.** 2004. Small-molecule inhibitors of the p53 suppressor HDM2: have protein-protein interactions come of age as drug targets? Trends Pharmacol. Sci. **25:**343-346.

24. **Fujiuchi, N., J. A. Aglipay, T. Ohtsuka, N. Maehara, F. Sahin, G. H. Su, S. W. Lee, and T. Ouchi.** 2004. Requirement of IFI16 for the maximal activation of p53 induced by ionizing radiation. J. Biol. Chem. **279:**20339-20344.

25. **Gariglio, M., B. Azzimonti, M. Pagano, G. Palestro, M. De Andrea, G. Valente, G. Voglino, L. Navino, and S. Landolfo.** 2002. Immunohistochemical expression analysis of the human interferon-inducible gene IFI16, a member of the HIN200 family, not restricted to hematopoietic cells. J. Interferon Cytokine Res. **22:**815-821.

26. **Gooch, J. L., R. E. Herrera, and D. Yee.** 2000. The role of p21 in interferon gamma-mediated growth inhibition of human breast cancer cells. Cell Growth Differ. **11:**335-342.

27. **Grossman, S. R., M. E. Deato, C. Brignone, H. M. Chan, A. L. Kung, H. Tagami, Y. Nakatani, and D. M. Livingston.** 2003. Polyubiquitination of p53 by a ubiquitin ligase activity of p300. Science **300:**342-344.

28. **Grossman, S. R., M. Perez, A. L. Kung, M. Joseph, C. Mansur, Z. X. Xiao, S. Kumar, P. M. Howley, and D. M. Livingston.** 1998. p300/MDM2 complexes participate in MDM2-mediated p53 degradation. Mol. Cell **2:**405-415.

29. **Gu, J., H. Kawai, L. Nie, H. Kitao, D. Wiederschain, A. G. Jochemsen, J. Parant, G. Lozano, and Z. M. Yuan.** 2002. Mutual dependence of MDM2 and MDMX in their functional inactivation of p53. J. Biol. Chem. **277:**19251-19254.

30. **Gudas, J. M., H. Nguyen, R. C. Klein, D. Katayose, P. Seth, and K. H. Cowan.** 1995. Differential expression of multiple MDM2 messenger RNAs and proteins in normal and tumorigenic breast epithelial cells. Clin. Cancer Res. **1:**71-80.

31. **Gutterman, J. U.** 1994. Cytokine therapeutics: lessons from interferon alpha. Proc. Natl. Acad. Sci. USA **91:**1198-1205.

32. **Hiller, S., A. Kohl, F. Fiorito, T. Herrmann, G. Wider, J. Tschopp, M. G. Grutter, and K. Wuthrich.** 2003. NMR structure of the apoptosis- and inflammation-related NALP1 pyrin domain. Structure **11:**1199-1205.

33. **Honda, R., H. Tanaka, and H. Yasuda.** 1997. Oncoprotein MDM2 is a ubiquitin ligase E3 for tumor suppressor p53. FEBS Lett. **420:**25-27.

34. **Honda, R., and H. Yasuda.** 2000. Activity of MDM2, a ubiquitin ligase, toward p53 or itself is dependent on the RING finger domain of the ligase. Oncogene **19:**1473-1476.

35. **Iwakuma, T., and G. Lozano.** 2003. MDM2, an introduction. Mol. Cancer Res.: MCR **1:**993-1000.

36. **Jagus, R., B. Joshi, and G. N. Barber.** 1999. PKR, apoptosis and cancer. Inter. J. Biochem. Cell Biol. **31:**123-138.

37. **Jin, A., K. Itahana, K. O'Keefe, and Y. Zhang.** 2004. Inhibition of HDM2 and activation of p53 by ribosomal protein L23. Mol. Cell. Biol. **24:**7669-7680.

38. **Jin, Y., H. Lee, S. X. Zeng, M. S. Dai, and H. Lu.** 2003. MDM2 promotes p21waf1/cip1 proteasomal turnover independently of ubiquitylation. EMBO J. **22:**6365-6377.

39. **Joazeiro, C. A., and A. M. Weissman.** 2000. RING finger proteins: mediators of ubiquitin ligase activity. Cell **102:**549-552.

40. **Johnstone, R. W., W. Wei, A. Greenway, and J. A. Trapani.** 2000. Functional interaction between p53 and the interferon-inducible nucleoprotein IFI 16. Oncogene **19:**6033-6042.

41. **Jones, S. N., A. E. Roe, L. A. Donehower, and A. Bradley.** 1995. Rescue of embryonic lethality in Mdm2-deficient mice by absence of p53. Nature **378:**206-208.

42. **Klein, C., and L. T. Vassilev.** 2004. Targeting the p53-MDM2 interaction to treat cancer. Brit. J. Cancer **91:**1415-1419.

43. **Kulaeva, O. I., S. Draghici, L. Tang, J. M. Kraniak, S. J. Land, and M. A. Tainsky.** 2003. Epigenetic silencing of multiple interferon pathway genes after cellular immortalization. Oncogene **22:**4118-4127.

44. **Lai, Z., K. V. Ferry, M. A. Diamond, K. E. Wee, Y. B. Kim, J. Ma, T. Yang, P. A. Benfield, R. A. Copeland, and K. R. Auger.** 2001. Human mdm2 mediates multiple mono-ubiquitination of p53 by a mechanism requiring enzyme isomerization. J. Biol. Chem. **276:**31357-31367.

45. **Lengyel, P.** 1993. Tumor-suppressor genes: news about the interferon connection. Proc. Natl. Acad. Sci. USA **90:**5893-5895.

46. **Levy, D. E., and A. Garcia-Sastre.** 2001. The virus battles: IFN induction of the antiviral state and mechanisms of viral evasion. Cytokine Growth Factor Rev. **12:**143-156.

47. **Li, L., J. Liao, J. Ruland, T. W. Mak, and S. N. Cohen.** 2001. A TSG101/MDM2 regulatory loop modulates MDM2 degradation and MDM2/p53 feedback control. Proc. Natl. Acad. Sci. USA **98:**1619-1624.

48. **Li, M., C. L. Brooks, N. Kon, and W. Gu.** 2004. A dynamic role of HAUSP in the p53-Mdm2 pathway. Mol. Cell **13:**879-886.

49. **Liepinsh, E., R. Barbals, E. Dahl, A. Sharipo, E. Staub, and G. Otting.** 2003. The death-domain fold of the ASC PYRIN domain, presenting a basis for PYRIN/PYRIN recognition. J. Mol. Biol. **332:**1155-1163.

50. **Liu, Y., M. Encinas, J. X. Comella, M. Aldea, and C. Gallego.** 2004. Basic helix-loop-helix proteins bind to TrkB and p21(Cip1) promoters linking differentiation and cell cycle arrest in neuroblastoma cells. Mol. Cell. Biol. **24:**2662-2672.

51. **Ludlow, L. E. A., R. W. Johnstone, and C. J. Clarke.** 2005. The HIN-200 family: More than interferon-inducible genes? Exp. Cell Res. **308:**1-17.

52. **Marchetti, A., F. Buttitta, S. Girlando, P. Dalla Palma, S. Pellegrini, P. Fina, C. Doglioni, G. Bevilacqua, and M. Barbareschi.** 1995. mdm2 gene alterations and mdm2 protein expression in breast carcinomas. J. Pathol. **175:**31-38.

53. **Martin, K. J., E. Graner, Y. Li, L. M. Price, B. M. Kritzman, M. V. Fournier, E. Rhei, and A. B. Pardee.** 2001. High-sensitivity array analysis of gene

expression for the early detection of disseminated breast tumor cells in peripheral blood. Proc. Natl. Acad. Sci. USA **98:**2646-2651.

54. **McCann, A. H., A. Kirley, D. N. Carney, N. Corbally, H. M. Magee, G. Keating, and P. A. Dervan.** 1995. Amplification of the MDM2 gene in human breast cancer and its association with MDM2 and p53 protein status. Brit. J. Cancer **71:**981-985.

55. **Meek, D. W., and U. Knippschild.** 2003. Posttranslational modification of MDM2. Mol. Cancer Res.: MCR **1:**1017-1026.

56. **Moll, U. M., and O. Petrenko.** 2003. The MDM2-p53 interaction. Mol. Cancer Res.: MCR **1:**1001-1008.

57. **Moller, M. B.** 2003. Molecular control of the cell cycle in cancer: biological and clinical aspects. Dan. Med. Bull. **50:**118-138.

58. **Montes de Oca Luna, R., D. S. Wagner, and G. Lozano.** 1995. Rescue of early embryonic lethality in mdm2-deficient mice by deletion of p53. Nature **378:**203-206.

59. **Mori, Y., J. Yin, A. Rashid, B. A. Leggett, J. Young, L. Simms, P. M. Kuehl, P. Langenberg, S. J. Meltzer, and O. C. Stine.** 2001. Instabilotyping: comprehensive identification of frameshift mutations caused by coding region microsatellite instability. Cancer Res. **61:**6046-6049.

60. **Oliner, J. D., J. A. Pietenpol, S. Thiagalingam, J. Gyuris, K. W. Kinzler, and B. Vogelstein.** 1993. Oncoprotein MDM2 conceals the activation domain of tumour suppressor p53. Nature **362:**857-860.

61. **Picksley, S. M., and D. P. Lane.** 1993. The p53-mdm2 autoregulatory feedback loop: a paradigm for the regulation of growth control by p53? Bioessays **15:**689-690.

62. **Pradhan, A., A. Mijovic, K. Mills, P. Cumber, N. Westwood, G. J. Mufti, and F. V. Rassool.** 2004. Differentially expressed genes in adult familial myelodysplastic syndromes. Leukemia **18:**449-459.

63. **Raffaella, R., D. Gioia, M. De Andrea, P. Cappello, M. Giovarelli, P. Marconi, R. Manservigi, M. Gariglio, and S. Landolfo.** 2004. The interferon-inducible IFI16 gene inhibits tube morphogenesis and proliferation of primary, but not HPV16 E6/E7-immortalized human endothelial cells. Exp. Cell Res. **293:**331-345.

64. **Reed, J. C., K. Doctor, A. Rojas, J. M. Zapata, C. Stehlik, L. Fiorentino, J. Damiano, W. Roth, S. Matsuzawa, R. Newman, S. Takayama, H. Marusawa, F. Xu, G. Salvesen, A. Godzik, R. G. Group, and G. S. L. Members.** 2003. Comparative analysis of apoptosis and inflammation genes of mice and humans. Genome Res. **13:**1376-1388.

65. **Romeo, G., G. Fiorucci, M. V. Chiantore, Z. A. Percario, S. Vannucchi, and E. Affabris.** 2002. IRF-1 as a negative regulator of cell proliferation. J. Interferon Cytokine Res. **22:**39-47.

66. **Sandoval, R., J. Xue, M. Pilkinton, D. Salvi, H. Kiyokawa, and O. R. Colamonici.** 2004. Different requirements for the cytostatic and apoptotic effects of type I interferons. Induction of apoptosis requires ARF but not p53 in osteosarcoma cell lines. J. Biol. Chem. **279:**32275-32280.

67. **Sharpless, N. E., and R. A. DePinho.** 1999. The INK4A/ARF locus and its two gene products. Curr. Opin. Genet. Dev. **9:**22-30.

68. **Sheikh, M. S., Z. M. Shao, A. Hussain, and J. A. Fontana.** 1993. The p53-binding protein MDM2 gene is differentially expressed in human breast carcinoma. Cancer Res. **53:**3226-3228.

69. **Shiraishi, T., and P. E. Nielsen.** 2004. Down-regulation of MDM2 and activation of p53 in human cancer cells by antisense 9-aminoacridine-PNA (peptide nucleic acid) conjugates. Nucleic Acids Res. **32:**4893-4902.

70. **Silverman, R. H.** 2003. Implications for RNase L in prostate cancer biology. Biochemistry **42:**1805-1812.

71. **Stad, R., N. A. Little, D. P. Xirodimas, R. Frenk, A. J. van der Eb, D. P. Lane, M. K. Saville, and A. G. Jochemsen.** 2001. Mdmx stabilizes p53 and Mdm2 via two distinct mechanisms. EMBO Rep. **2:**1029-1034.

72. **Stehlik, C., and J. C. Reed.** 2004. The PYRIN connection: novel players in innate immunity and inflammation. J. Exp. Med. **200:**551-558.

73. **Stommel, J. M., N. D. Marchenko, G. S. Jimenez, U. M. Moll, T. J. Hope, and G. M. Wahl.** 1999. A leucine-rich nuclear export signal in the p53 tetramerization domain: regulation of subcellular localization and p53 activity by NES masking. EMBO J. **18:**1660-1672.

74. **Stommel, J. M., and G. M. Wahl.** 2005. A new twist in the feedback loop: Stress-activated MDM2 destabilization is required for p53 activation. Cell Cycle **4:**e11-e17.

75. **Takaoka, A., S. Hayakawa, H. Yanai, D. Stoiber, H. Negishi, H. Kikuchi, S. Sasaki, K. Imai, T. Shibue, K. Honda, and T. Taniguchi.** 2003. Integration of interferon-alpha/beta signalling to p53 responses in tumour suppression and antiviral defence. Nature **424:**516-523.

76. **Theobald, D. L., R. M. Mitton-Fry, and D. S. Wuttke.** 2003. Nucleic acid recognition by OB-fold proteins. Ann. Rev. Biophys. Biomol. Struct. **32:**115-133.

77. **Tokino, T., S. Thiagalingam, W. S. el-Deiry, T. Waldman, K. W. Kinzler, and B. Vogelstein.** 1994. p53 tagged sites from human genomic DNA. Hum. Mol. Genet. **3:**1537-1542.

78. **Varambally, S., S. M. Dhanasekaran, M. Zhou, T. R. Barrette, C. Kumar-Sinha, M. G. Sanda, D. Ghosh, K. J. Pienta, R. G. Sewalt, A. P. Otte, M. A. Rubin, and A. M. Chinnaiyan.** 2002. The polycomb group protein EZH2 is involved in progression of prostate cancer. Nature **419:**624-629.

79. **Vilcek, J., and M. Feldmann.** 2004. Historical review: Cytokines as therapeutics and targets of therapeutics. Trends Pharmacol. Sci. **25:**201-209.

80. **Wang, H., L. Nan, D. Yu, S. Agrawal, and R. Zhang.** 2001. Antisense anti-MDM2 oligonucleotides as a novel therapeutic approach to human breast cancer: in vitro and in vivo activities and mechanisms. Clin. Cancer Res. **7:**3613-3624.

81. **Weber, J. D., L. J. Taylor, M. F. Roussel, C. J. Sherr, and D. Bar-Sagi.** 1999. Nucleolar Arf sequesters Mdm2 and activates p53. Nature Cell Biol. **1:**20-26.

82. **Wei, W., C. J. Clarke, G. R. Somers, K. S. Cresswell, K. A. Loveland, J. A. Trapani, and R. W. Johnstone.** 2003. Expression of IFI 16 in epithelial cells and lymphoid tissues. Histochem. Cell Biol. **119:**45-54.

83. **Wen, Y., D. H. Yan, B. Wang, B. Spohn, Y. Ding, R. Shao, Y. Zou, K. Xie, and M. C. Hung.** 2001. p202, an interferon-inducible protein, mediates multiple antitumor activities in human pancreatic cancer xenograft models. Cancer Res. **61:**7142-7147.

84. **Xin, H., J. Curry, R. W. Johnstone, B. J. Nickoloff, and D. Choubey.** 2003. Role of IFI 16, a member of the interferon-inducible p200-protein family, in prostate epithelial cellular senescence. Oncogene **22:**4831-4840.

85. **Yang, H. Y., Y. Y. Wen, C. H. Chen, G. Lozano, and M. H. Lee.** 2003. 14-3-3 sigma positively regulates p53 and suppresses tumor growth. Mol. Cell. Biol. **23:**7096-7107.

86. **Yeung, M. C., and A. S. Lau.** 1998. Tumor suppressor p53 as a component of the tumor necrosis factor-induced, protein kinase PKR-mediated apoptotic pathway in human promonocytic U937 cells. J. Biol. Chem. **273:**25198-25202.

87. **Zhang, Z., H. Wang, M. Li, S. Agrawal, X. Chen, and R. Zhang.** 2004. MDM2 is a negative regulator of p21WAF1/CIP1, independent of p53. J. Biol. Chem. **279:**16000-16006.

FIGURE LEGENDS

Fig. 1. IFIXα1 interacts with HDM2. A. HDM2 interacts with EGFP-IFIXα1 and β1. 293T cells were transfected with 2.5 μg CMV-HDM2 and 2.5 μg EGFP-vector (Vector), or 2.5 μg EGFP-IFIXα1 (α1), EGFP-IFIXβ1(β1). Forty-eight h post-transfection, cell extracts (500 μg) were immunoprecipitated (IP) with a monoclonal anti-HDM2 antibody, and western blot (WB) was performed using a polyclonal anti-GFP or anti-HDM2 antibody. **B.** A reciprocal experiment that used anti-GFP antibody for IP and WB with anti-IFIX or anti-HDM2 antibodies. **C.** HDM2 interacts with FLAG-tagged IFIXα1. 293T cells were transfected with 5 μg CMV-HDM2 and 5 μg FLAG-vector (V) or Flag-IFIXα1 (α1). Forty-eight h post-transfection, cell extracts (500 μg) were IP using anti-FLAG (M2, Sigma), anti-IFIX, or anti-HDM2 antibodies and WB using anti-IFIX, anti-FLAG, and anti-IFIXα antibody, respectively. **D.** IFIXα1 interacts with HDM2 in the IFIXα1 stable cell lines. The cell lysate (600 μg) isolated from the IFIXα1 stable cell line (X-1 and X-2) or the empty vector (V) stable cells derived from MCF-7 cells were IP using anti-HDM2 antibody and WB with anti-IFIXα or anti-HDM2 antibody. **E.** IFN-α treatment increased the IFIXα and HDM2 interaction. Cell lysate (800 μg) isolated from Raji or U937 cells treated with (+) or without (-) IFN-α (2000 u/ml) or IFN-γ (1000 u/ml), respectively, for 48 h followed by immunoprecipitation (IP) with anti-HDM2 or IgG antibody and western blot (WB) with anti-HDM2 and anti-IFIXα antibodies.

Fig. 2. Mapping the IFIXα1-HDM2 interacting domains. A. The HDM2 (1-441) mutant interacts with IFIXα1. 293T cells were transfected with HDM2 or HDM2 (1-441), and EGFP empty vector (V) or EGFP-IFIXα1 (α1) followed by IP with anti-HDM2 antibody and WB with either anti-HDM2 or anti-GFP antibody. **B-C.** The 150-230 region of HDM2 interacts with IFIXα1. 293T cells were co-transfected with HDM2 or HDM2 (Δ150-230) and EGFP empty vector (V) or EGFP-IFIXα1 (α1) (**B**) or

FLAG empty vector (V) or FLAG-IFIXα1 (α1) (**C**) followed by IP/WB with antibodies as indicated. The HDM2 band is indicated by an arrowhead. The untransfected 293T cells serve as controls (C). **D-F**. The HIN domain of IFIXα1 interacts with HDM2. **D.** Cellular localization of IFIX-N and IFIX-HIN. Plasmid encoding EGFP-fused with IFIX-N (EGFP-IFIX-N) or IFIX-HIN (EGFP-IFIX-HIN) was transfected into MCF-7 cells. Green fluorescence (GFP), nuclear staining (DAPI), and phase contrast are shown. EGFP-IFIX-N is exclusively localized in the nucleus. The localization of EGFP-IFIX-HIN is predominantly nuclear, i.e., N > C (92/110 or 83.6%) and N = C (18/110 or 16.4%). Magnification: 400X. **E**. The HIN domain of IFIXα1 interacts with HDM2. 293T cells transfected with HDM2 and EGFP empty vector (V), EGFP-IFIXα1 (α1), EGFP-IFIX-N (N), or EGFP-IFIX-HIN (HIN) followed by IP with anti-GFP or anti-HDM2 antibody and WB with anti-HDM2 antibody or anti-GFP antibody. Untransfected 293T cells are indicated (C). **F**. A summary of HDM2 binding by IFIXα1, IFIXβ1, IFIX-N, and IFIX-HIN.

Fig. 3. The E3 ligase activity of HDM2 is required for the destabilization by IFIXα1. A. IFIXα1 destabilizes HDM2. H1299 cells were co-transfected with HDM2 (0.7 μg) and 1.3 μg of either the empty vector (V), FLAG-IFIXα1 (IFIXα1), or FLAG-IFIX-N (IFIX-N). Twenty-four h post-transfection, cells were treated with cyclohexamide (CHX) (100 μg/ml). Cell lysates were isolated at 0, 15, and 30 min after CHX treatment for WB using antibodies against HDM2, IFIXα, and α-tubulin. **B**. The amount of HDM2 protein at 0 time point was arbitrarily set at 1. The % of HDM2 protein remained was determined using a BioRad software. **C**. The RING domain of HDM2 is required for the destabilization by IFIXα1. HDM2 (1-441) (0.7 μg) was co-transfected into H1299 cells with 1.3 μg of either the empty vector (V) or FLAG-IFIXα1 (IFIXα1). CHX-chase assay and WB were carried out as described in (**A**). **D**. IFIXα1 induces ubiquitination of HDM2. H1299 cells were co-transfected with

HDM2 (1.5 μg), HA-Ubiqutin (1 μg), and IFIXα1 (α1) (0 (-), 1.5, and 3.5 μg). Cells were treated with MG132 (10 μM) 6 h prior to harvest at 48 h post-transfection. Cell lysate (0.9 mg) was IP using anti-HDM2 antibody and WB using anti-HDM2 or anti-IFIXα antibody.

Fig. 4. IFIXα1 stabilizes p53 protein. A. Increased p53 protein levels in IFIXα1 stable MCF-7 cell lines. Total cell lysates isolated from the IFIXα1 stable (X-1 and X-2) and the vector control (V) cell lines derived from MCF-7 were analyzed by WB using antibodies against p53, IFIXα, and α-tubulin. **B.** Increased p53 protein levels in the IFIXα1 transiently transfected MCF-7 cells. MCF-7 cells were transfected with EGFP vector (EGFP) or EGFP-IFIXα1. 48 h post-transfection, the EGFP-positive cells were collected by FACS. Cell lysates were analyzed by WB using antibodies against p53, IFIXα, and α-tubulin. **C.** IFIXα1 knockdown by siRNA reduces p53 expression. The IFIXα1 stable MCF-7 cell line, X-1, was transfected with siRNA specific to IFIXα (IFIX) (100 nM) or non-specific scramble siRNA (NS) (100 nM). Forty-eight h after transfection, the expression of p53, IFIXα1, or α-tubulin were analyzed by WB. **D.** IFIXα1 knockdown by siRNA reduces $p21^{CIP1}$ expression. The IFIXα1 stable MCF-7 cell line, X-1, was transfected with siRNA specific to IFIXα (IFIX) (100 nM) or non-specific scramble siRNA (NS) (100 nM). Forty-eight h after transfection, the expression of $p21^{CIP1}$, IFIXα1, or α-tubulin were analyzed by WB. **E.** IFIXα1 induces the steady-state HDM2 mRNA but has little effect on p53 mRNA levels in MCF-7 cells. Total RNA (10 μg) isolated from the parental MCF-7 (C) and the stable cell lines transfected with the empty vector (V) or IFIXα1 expression vector (X-1 and X-2) were analyzed by northern blot using HDM2, p53, or IFIXα1 cDNA as a probe. The 18S and 28S rRNAs are shown as loading controls. **F.** IFIXα1 expression increases p53 stability. The vector control (V) and the IFIXα1 stable MCF-7 (X-1 and X-2) cells were treated with cyclohexamide (CHX) (100 μg/ml) for the time indicated. Cell lysates were analyzed for the expression of p53 and α-tubulin.

Fig. 5. IFIXα1 activates p53-mediated transcription and promotes p53 nuclear localization. A. IFIXα1 augments the p53-mediated transcriptional activity. H1299 cells were transfected with 0.3 μg of PG13-LUC or MG15-LUC with or without p53 (0.01 μg) and IFIXα1 (0.845 and 1.69 μg). pRL-TK (0.05 μg) was co-transfected to normalize transfection efficiency. Cells were harvested 24 h after transfection and the luciferase activity was measured using dual luciferase assay (Promega). The relative luciferase activity was obtained by setting the normalized activity of PG13-LUC or MG15-LUC at 1. **B.** IFIXα1 enhances p53 DNA binding activity. Nuclear extract (7.5 μg) was incubated with ^{32}P-labeled oligonucleotide containing p53-binding sites prior to electrophoretic mobility shift assay according to manufacturer's instruction (p53 Nushift kit, Geneka) (left panel). MCF-7 cells treated with (+) or without (-) ultraviolet light (UV) (20 j/m^2) serve as a positive control. Nuclear extract isolated from X-1 cells was incubated with (+) or without (-) the anti-p53 antibody in the binding reactions to indicate the specific p53/DNA complex (arrow). The nuclear extracts used in the mobility shift assay were analyzed for the expression of p53 and IFIXα1 by WB (right panel). **C.** IFIXα1 activates p21^{CIP1} promoter. MCF-7 and HCT116 cells were transfected with wwp-LUC (0.5 μg) and increasing amount of IFIXα1 (0, 0.75, 1.5 μg). pRL-TK (0.1 μg) was co-transfected to normalize transfection efficiency. The luciferase activity was determined using an illuminometer and normalized with the dual luciferase protocol (Promega). The normalized luciferase activity of wwp-LUC without IFIXα1 was set as one. **D.** Increased p53 binding to the p21^{CIP1} promoter in IFIXα1 stable cells. ChIP assay was performed in the vector control (V) and the IFIXα1 stable MCF-7 (X-1 and X-2) cells. The primer pair that specifically amplifies a 320-bp region of p21^{CIP1} promoter was used to analyze the DNA immunoprecipitated by either anti-p53 antibody or a control anti-GFP antibody. The input DNA used for ChIP assay was likewise amplified to indicate equal loading. **E.** The IFIXα1-induced p53 is localized in the nucleus. The

vector control (V) and the IFIXα1 stable MCF-7 (X-2) cells were fixed and treated with rabbit polyclonal antibody against IFIXα, a monoclonal antibody against p53, or a control mouse IgG followed by incubation with secondary anti-rabbit Fc antibody conjugated with FITC (green) and anti-mouse Fc antibody conjugated with Texas red (red). Nuclei were stained by DAPI (blue). Magnification: 400X. **F.** The GFP-p53 fusion protein is preferentially localized in the nucleus of the IFIXα1 stable cells. GFP-p53 was transfected into the vector control (V) and the IFIXα1 stable MCF-7 (X-1 and X-2) cells. 24 h after transfection, the number of cells in which GFP-p53 localized in both nucleus and cytoplasm (C+N) or predominantly in the nucleus (N) was counted. Two independent experiments were performed, V: C+N (69, 51.1%; 30, 58%), N (66, 48.9%; 21, 42%), total 135 and 51 GFP-positive cells counted; X-1: C+N (65, 34.2%; 48, 38%), N (125, 65.8%; 78, 62%), total 190 and 126 GFP-positive cells counted; and X-2: C+N (21, 19.3%; 28, 23%), N (88, 80.7%; 94, 77%), total 109 and 122 GFP-positive cells counted.

Fig. 6. IFIX-HIN is sufficient to induce p53 and p21^{CIP1}. H1299 cells were transfected with p53 (0.1 μg) and increasing amount (0.5, 1.0, and 1.8 μg) of the FLAG-tagged IFIXα1 (**A**), IFIX-HIN (**B**), or IFIX-N (**C**), followed by WB using antibodies against p53, HDM2, FLAG, p21^{CIP1}, and α-tubulin at 24 h after transfection. **D.** IFIXα1 induces p21^{CIP1} mRNA expression. H1299 cells were co-transfected with p53 (0.5 μg) and 5.5 μg of FLAG-tagged empty vector (V), IFIXα1 (α1), IFIX-HIN (HIN), or IFIX-N (N). Twenty-four h post-transfection, total RNA (10 μg) isolated from these cells were analyzed by northern blot using p21^{CIP1} or IFIX cDNA as a probe. The 18S and 28S rRNA serve as loading control.

Fig. 7. Mdm2 is required for p53 induction and p53-mediated transcription by IFIXα1. A. Mdm2 is required for the increased p53 protein expression by IFIXα1. p53-/- MEF or DKO MEF was transfected with GFP-p53 (0.1 μg), and increasing amount of IFIXα1 (0, 1, or 2 μg). Twenty-four h

post-transfection, cell lysate was analyzed by WB using antibodies against p53, IFIXα1, or α-tubulin. **B.** Mdm2 is required for the p53-mediated transcriptional activation by IFIXα1. PG13-LUC (0.3 μg) was co-transfected with p53 (0.1 μg) with or without increasing amount of IFIXα1 (0.845 μg and 1.69 μg) into the p53-/- MEF or DKO MEF. pRL-TK (0.05 μg) was co-transfected to normalize transfection efficiency. Cells were harvested 24 h after transfection and the luciferase activity was measured using dual luciferase assay. The relative luciferase activity was obtained by setting the normalized activity of PG13-LUC alone at one.

Fig. 8. IFIXα1 down regulates HDM2 independent of p53. A. Inverse relationship between IFIXα1 and HDM2 expression. Cell lysates isolated from IFIXα1 stable cell lines (X-1 and X-2) and the vector control cell lines (V) derived from MDA-MB-468 were analyzed by western blot using antibodies against HDM2, p53, IFIXα, and α-tubulin. **B.** IFIXα1 is responsible for HDM2 down regulation. MDA-MB-468 (X-1) cells were transfected with IFIX siRNA (100 nM) or non-specific scramble siRNA (NS) (100 nM). Forty-eight h after transfection, the expression of HDM2, IFIXα1, p53, or α-tubulin were analyzed by western blot. **C.** IFIXα1 expression has little effect on both the steady-state mRNA levels of HDM2 and p53 in MDA-MB-468 cells. Total RNA (10 μg) isolated from the parental MDA-MB-468 (C) and the stable cell lines transfected with the empty vector (V) or IFIXα1 expression vector (X-1 and X-2) were analyzed by northern blot using HDM2, p53, or IFIXα1 cDNA as a probe. The 18S and 28S rRNAs are shown as loading controls. **D.** IFIXα1 decreases HDM2 expression in p53-null cells. HCT116 and HCT116 (p53-/-) cells were transfected with EGFP vector or EGFP-IFIXα1. 48 h after transfection, the GFP-positive cells were collected by FACS. Cell lysates of the GFP-positive cells were analyzed by western blot using antibodies against HDM2, p53, IFIXα1, and α-tubulin. **E-F.** MG132 treatment reverses the IFIXα1-mediated HDM2 down regulation. H1299 (**E**) or 293 (**F**) cells were

transfected with EGFP vector or EGFP-IFIXα1. MG132 (10 μM) treatment started 5 h prior to harvest at 48 h after transfection. The GFP-positive cells were collected by FACS followed by western blot using antibodies against HDM2, IFIXα1, and α-tubulin. The untransfected cells with or without MG132 serve as positive controls for HDM2 stabilization by MG132. **G**. IFIX-HIN down regulates HDM2 expression. 293 cells were transfected with EGFP empty vector (EGFP) or EGFP-IFIX-HIN. MG132 (10 μM) treatment started at 5 h before harvest. The GFP-positive cells were collected by FACS followed by western blot using antibodies against HDM2, EGFP, and α-tubulin.

Fig. 9. IFIXα1 mediates the IFN-α-induced HDM2 down regulation. A. IFN-α treatment decreases the HDM2 protein levels. Raji cells were treated with or without IFN-α (2000 u/ml) for 72 h followed by WB using the antibodies against HDM2, IFI16, IFIXα, PKR, and α-tubulin. **B**. IFIX siRNA transfection reverses the IFN-α-mediated down regulation of HDM2. Raji cells growing in 0.2% FCS DMEM/F12 medium with or without IFN-α treatment (2000 u/ml) for 72 h was analyzed by western blot using antibodies against HDM2, IFIXα, IFI16, and α-tubulin (left panel). The protein expression was likewise analyzed by western blot in the Raji cells transfected with either IFIX siRNA (100 nM) or the non-specific scramble (NS) siRNA (100 nM) in 0.2% FCS DMEM/F12 medium followed by IFN-α treatment (2000 u/ml) for 72 h (right panel).

Fig. 1

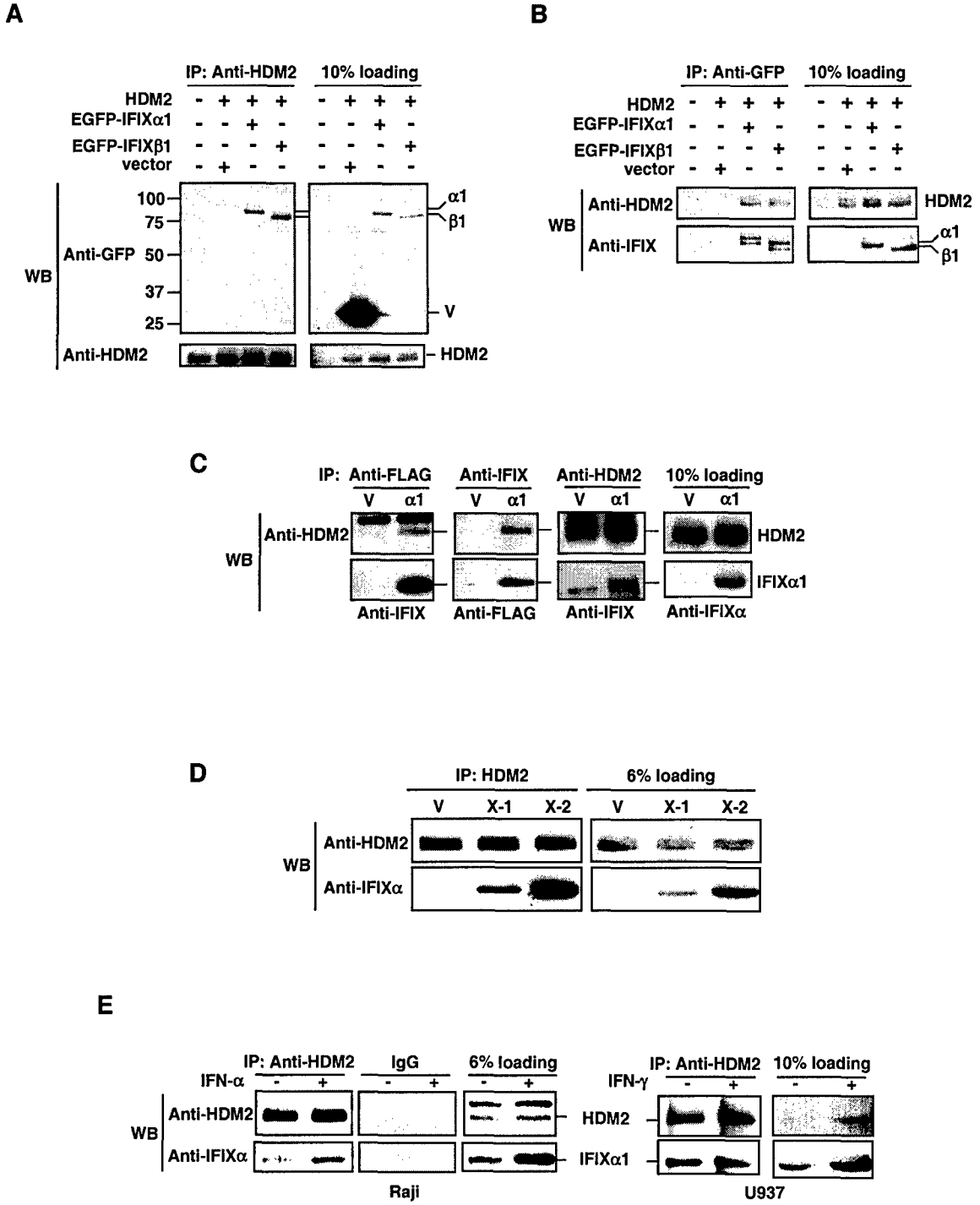
A
IP: Anti-HDM2
10% loading
HDM2
EGFP-IFIXα1
EGFP-IFIXβ1
vector
100
75
50
37
25
WB
Anti-GFP
Anti-HDM2
α1
β1
V
HDM2
B
IP: Anti-GFP
10% loading
HDM2
EGFP-IFIXα1
EGFP-IFIXβ1
vector
WB
Anti-HDM2
Anti-IFIX
HDM2
α1
β1
C
IP: Anti-FLAG
Anti-IFIX
Anti-HDM2
10% loading
V
α1
WB
Anti-HDM2
Anti-IFIX
Anti-FLAG
Anti-IFIX
Anti-IFIXα
HDM2
IFIXα1
D
IP: HDM2
6% loading
V
X-1
X-2
WB
Anti-HDM2
Anti-IFIXα
E
IP: Anti-HDM2
IgG
6% loading
IFN-α
WB
Anti-HDM2
Anti-IFIXα
Raji
IP: Anti-HDM2
10% loading
IFN-γ
HDM2
IFIXα1
U937

Fig. 2

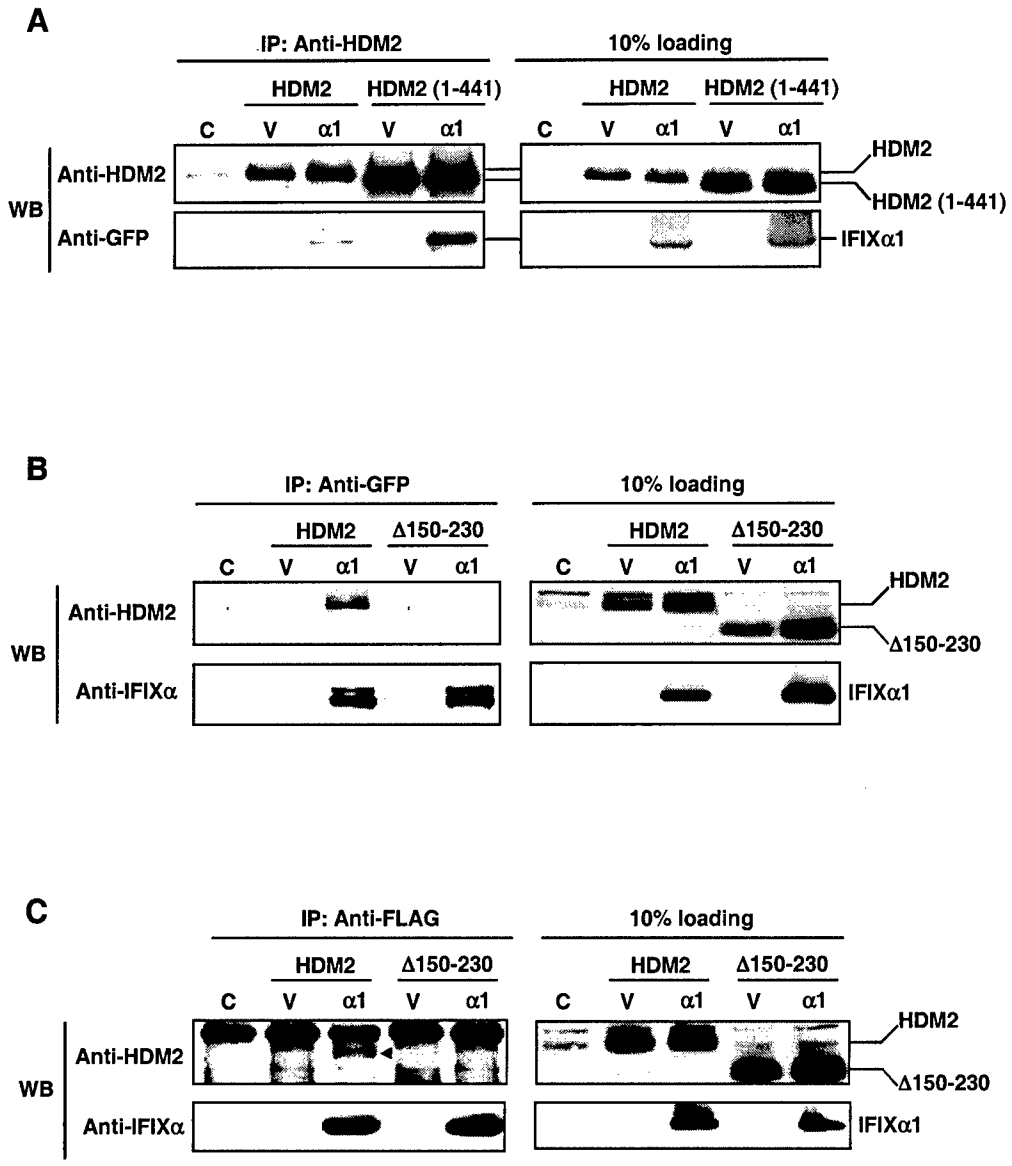
A
IP: Anti-HDM2
10% loading
HDM2
HDM2 (1-441)
C V α1 V α1
WB
Anti-HDM2
Anti-GFP
HDM2
HDM2 (1-441)
IFIXα1
B
IP: Anti-GFP
10% loading
HDM2
Δ150-230
C V α1 V α1
WB
Anti-HDM2
Anti-IFIXα
HDM2
Δ150-230
IFIXα1
C
IP: Anti-FLAG
10% loading
HDM2
Δ150-230
C V α1 V α1
WB
Anti-HDM2
Anti-IFIXα
HDM2
Δ150-230
IFIXα1

Fig. 2 (Cont'd)

D

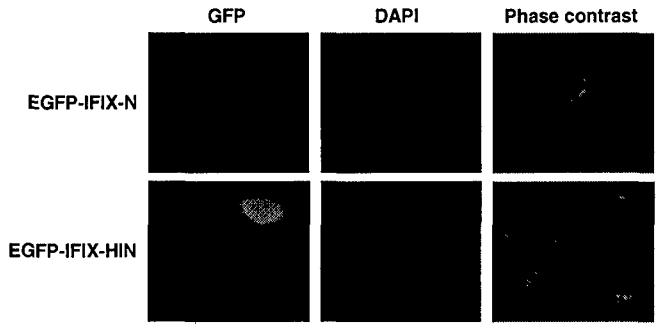

E

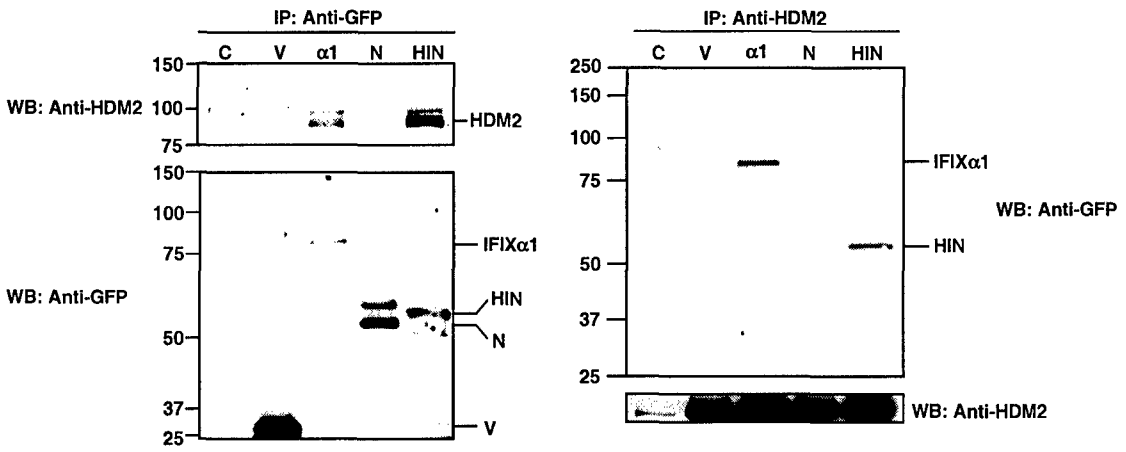

F

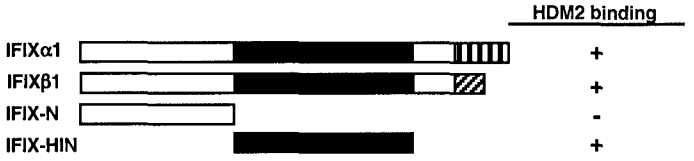

Fig. 3

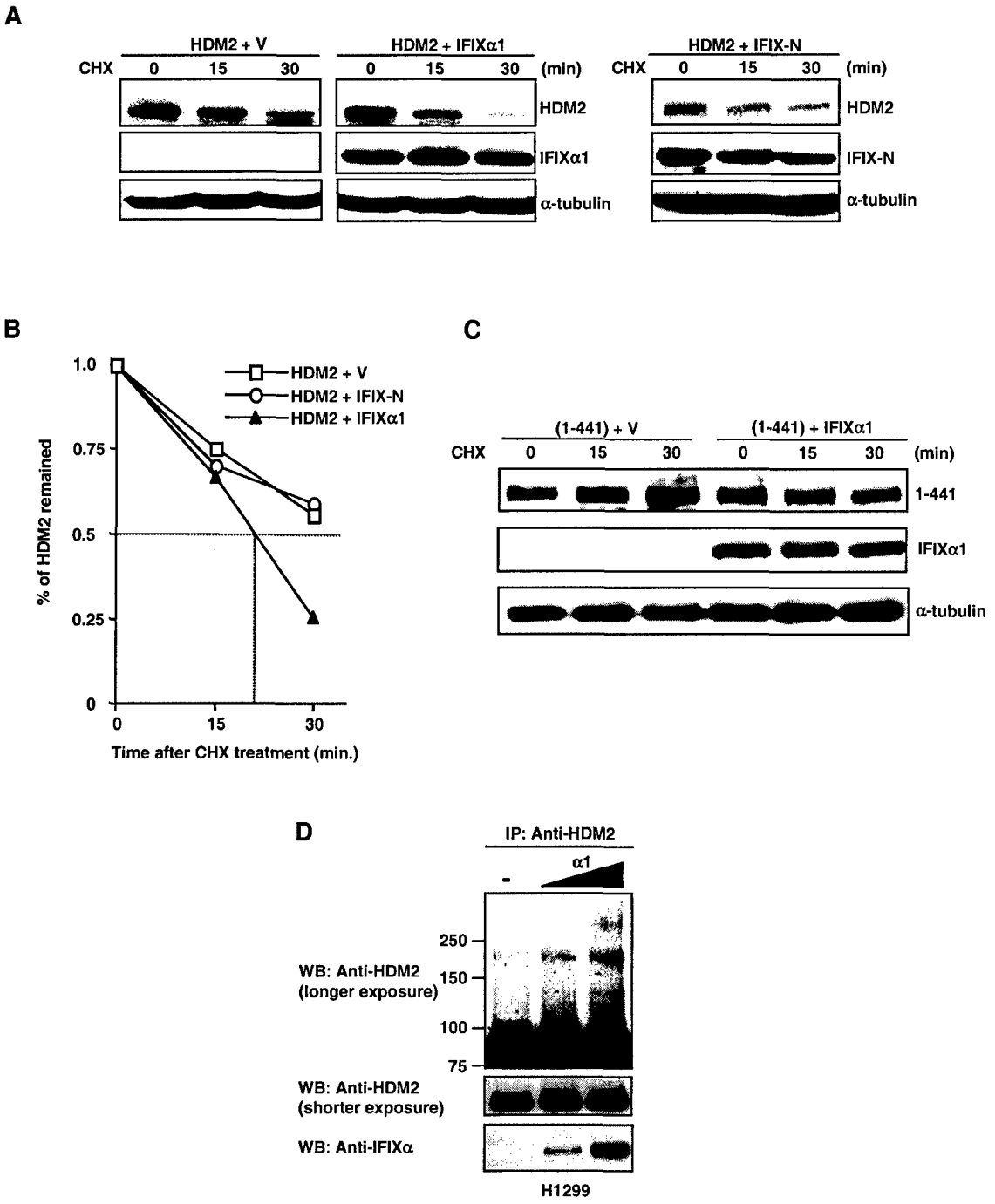
A
HDM2 + V
HDM2 + IFIXα1
HDM2 + IFIX-N
CHX
0
15
30
(min)
HDM2
IFIXα1
IFIX-N
α-tubulin
B
HDM2 + V
HDM2 + IFIX-N
HDM2 + IFIXα1
% of HDM2 remained
1.0
0.75
0.5
0.25
0
Time after CHX treatment (min.)
C
(1-441) + V
(1-441) + IFIXα1
1-441
IFIXα1
α-tubulin
D
IP: Anti-HDM2
-
α1
250
150
100
75
WB: Anti-HDM2
(longer exposure)
WB: Anti-HDM2
(shorter exposure)
WB: Anti-IFIXα
H1299

Fig. 4

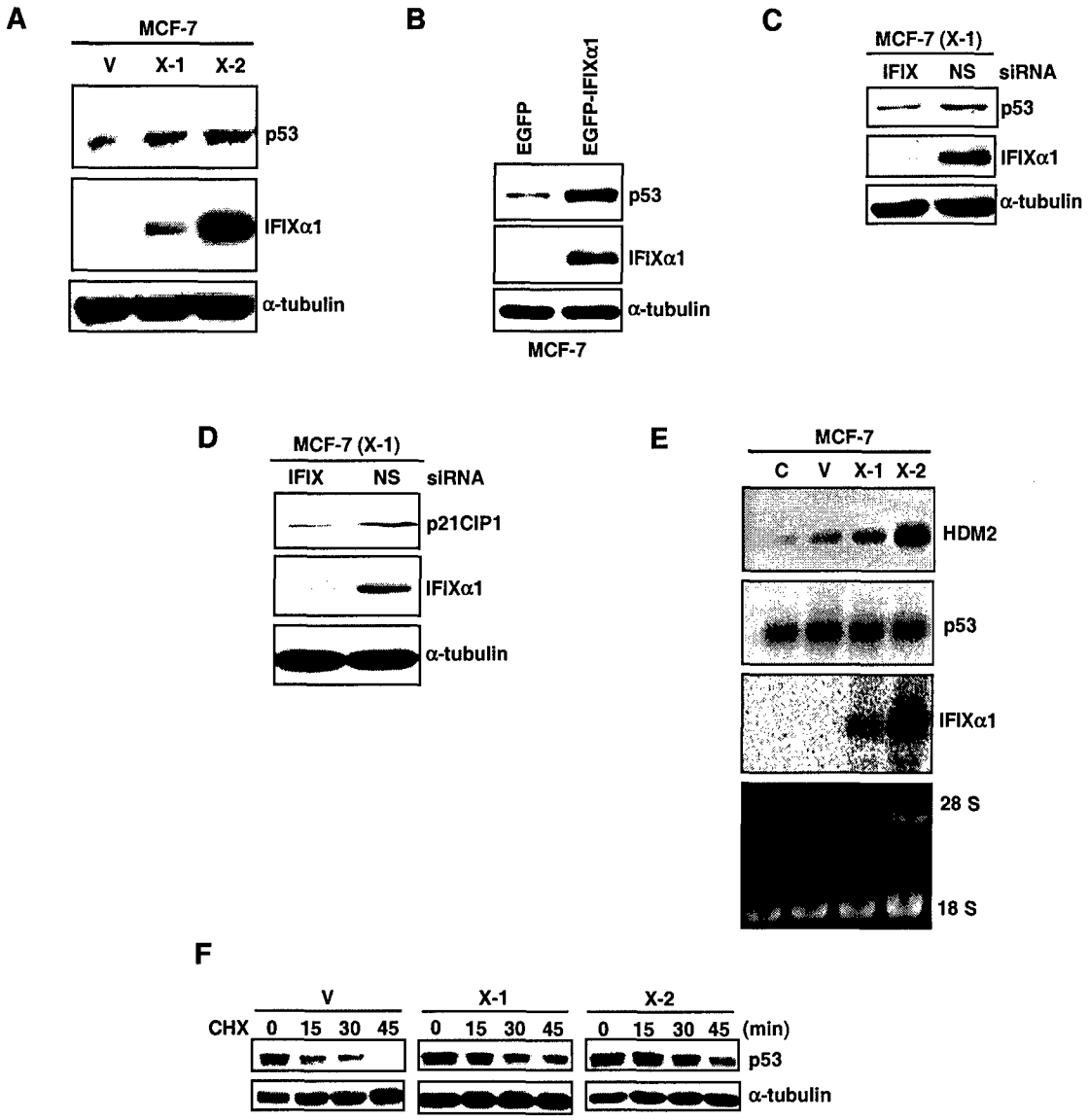
A
MCF-7
V
X-1
X-2
p53
IFIXα1
α-tubulin
B
EGFP
EGFP-IFIXα1
p53
IFIXα1
α-tubulin
MCF-7
C
MCF-7 (X-1)
IFIX
NS
siRNA
p53
IFIXα1
α-tubulin
D
MCF-7 (X-1)
IFIX
NS
siRNA
p21CIP1
IFIXα1
α-tubulin
E
MCF-7
C
V
X-1
X-2
HDM2
p53
IFIXα1
28 S
18 S
F
V
X-1
X-2
CHX
0
15
30
45
(min)
p53
α-tubulin

Fig. 5

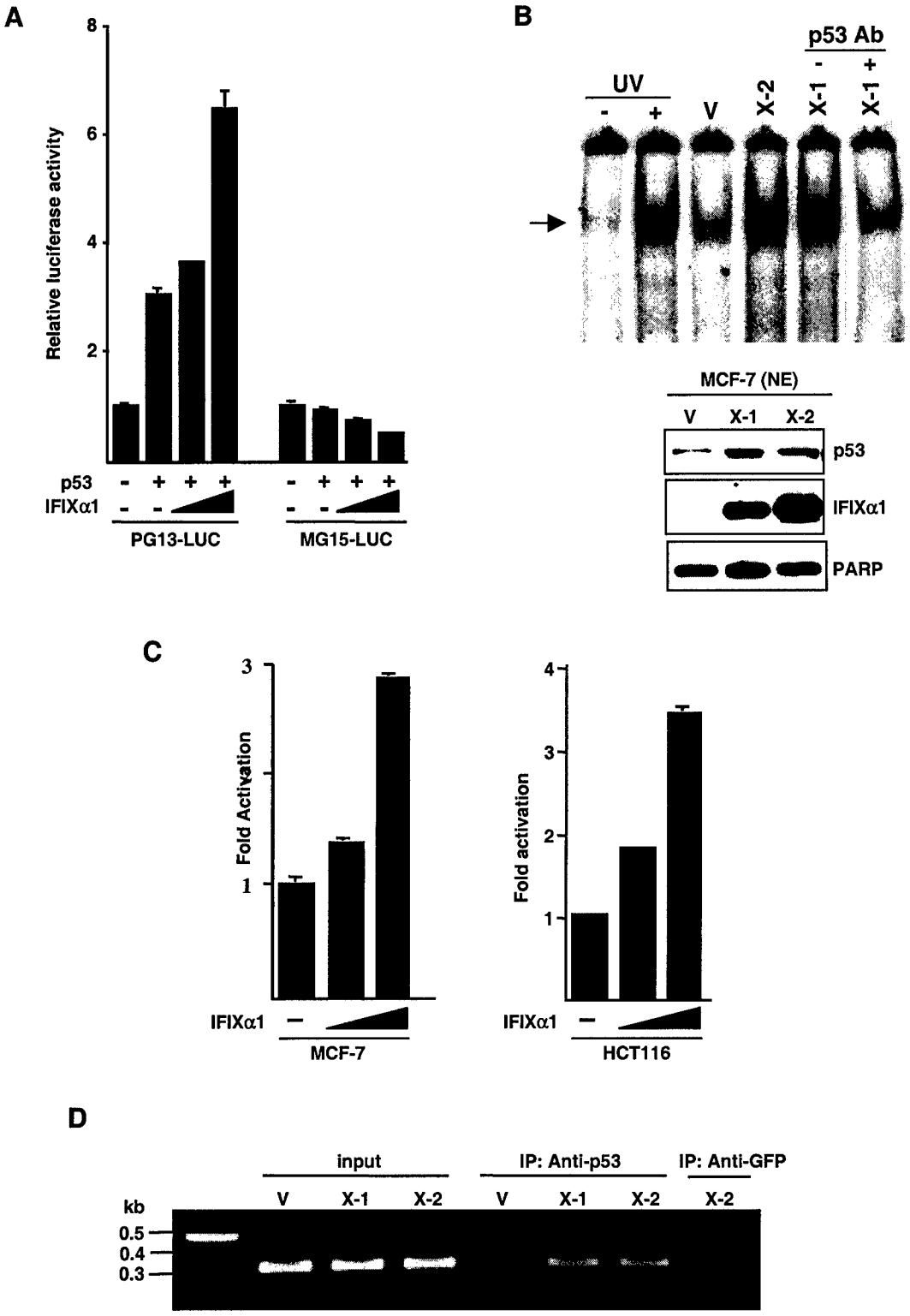
A
Relative luciferase activity
8
6
4
2
p53
IFIXα1
PG13-LUC
MG15-LUC
B
p53 Ab
UV
V
X-2
X-1
X-1
MCF-7 (NE)
V
X-1
X-2
p53
IFIXα1
PARP
C
Fold Activation
3
1
IFIXα1
MCF-7
Fold activation
4
3
2
1
IFIXα1
HCT116
D
input
IP: Anti-p53
IP: Anti-GFP
V
X-1
X-2
V
X-1
X-2
X-2
kb
0.5
0.4
0.3

Fig. 5

E

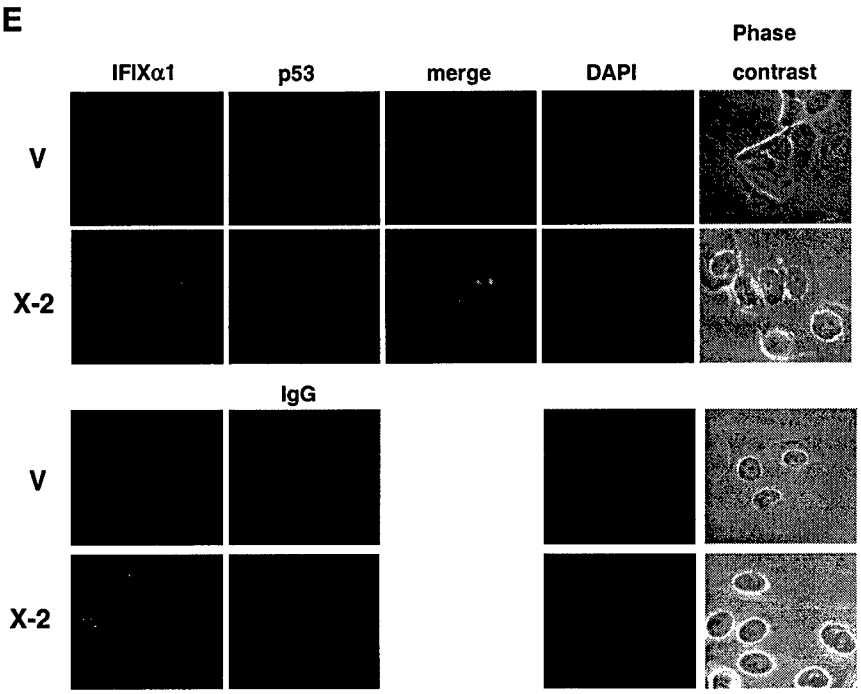
IFIXα1
p53
merge
DAPI
Phase contrast
V
X-2
IgG
V
X-2

F

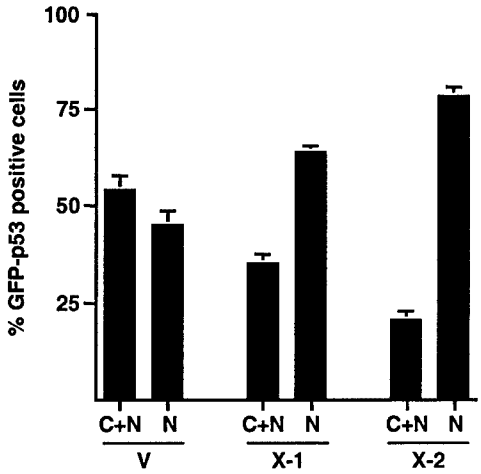
% GFP-p53 positive cells
100
75
50
25
C+N
N
C+N
N
C+N
N
V
X-1
X-2

Fig. 6

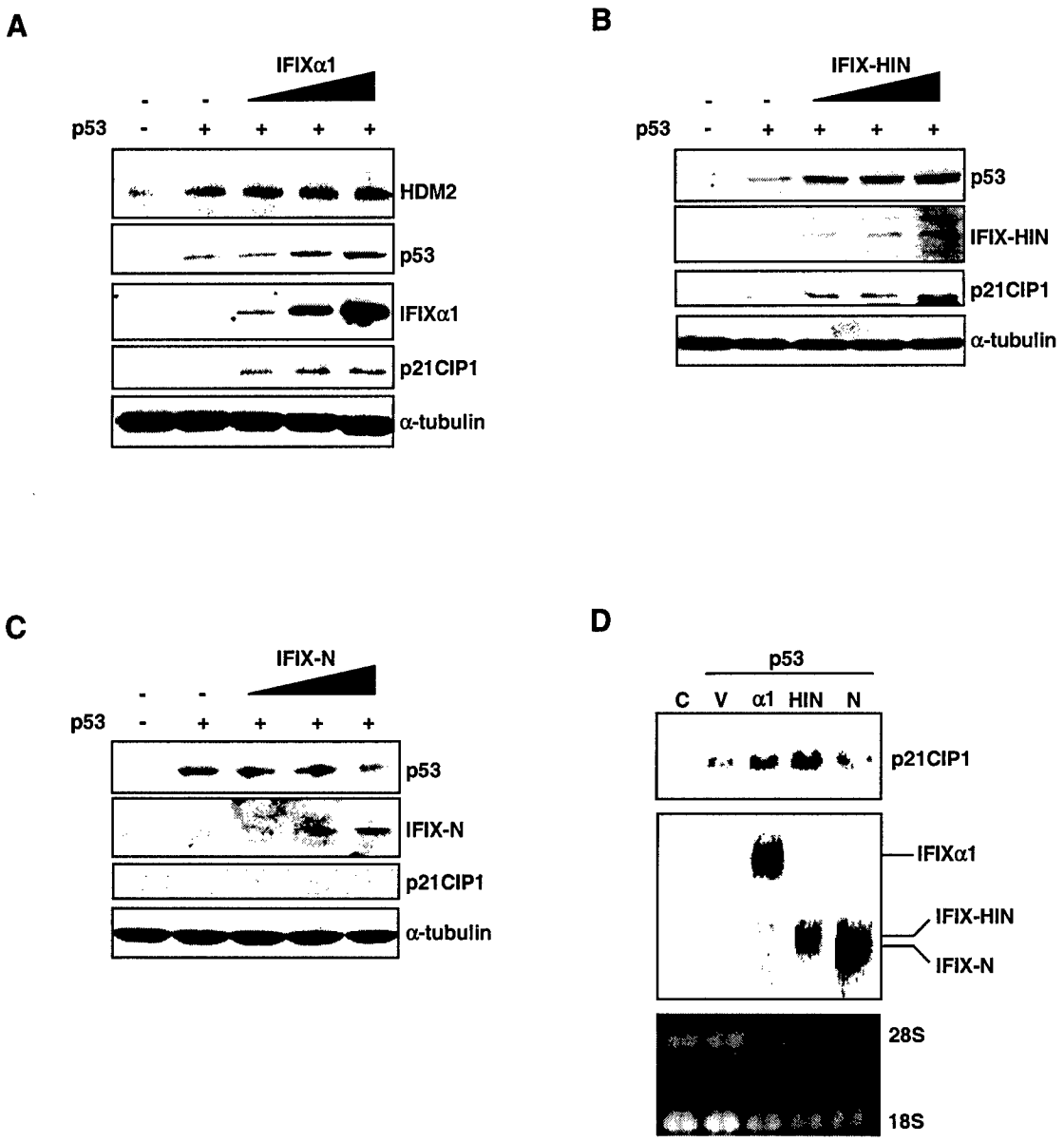
A
IFIXα1
p53
HDM2
p53
IFIXα1
p21CIP1
α-tubulin
B
IFIX-HIN
p53
p53
IFIX-HIN
p21CIP1
α-tubulin
C
IFIX-N
p53
p53
IFIX-N
p21CIP1
α-tubulin
D
p53
C V α1 HIN N
p21CIP1
IFIXα1
IFIX-HIN
IFIX-N
28S
18S

Fig. 7

A

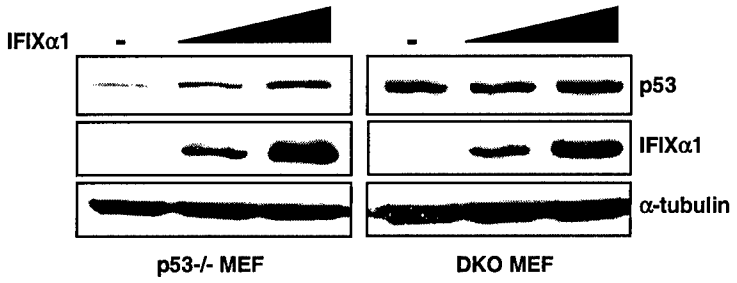
IFIXα1
-
-
p53
IFIXα1
α-tubulin
p53-/- MEF
DKO MEF

B

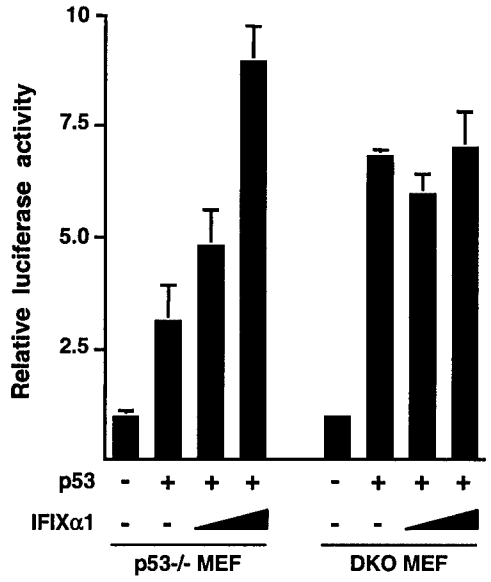
Relative luciferase activity
10
7.5
5.0
2.5
p53 - + + + - + + +
IFIXα1 - - - -
p53-/- MEF
DKO MEF

Fig. 8

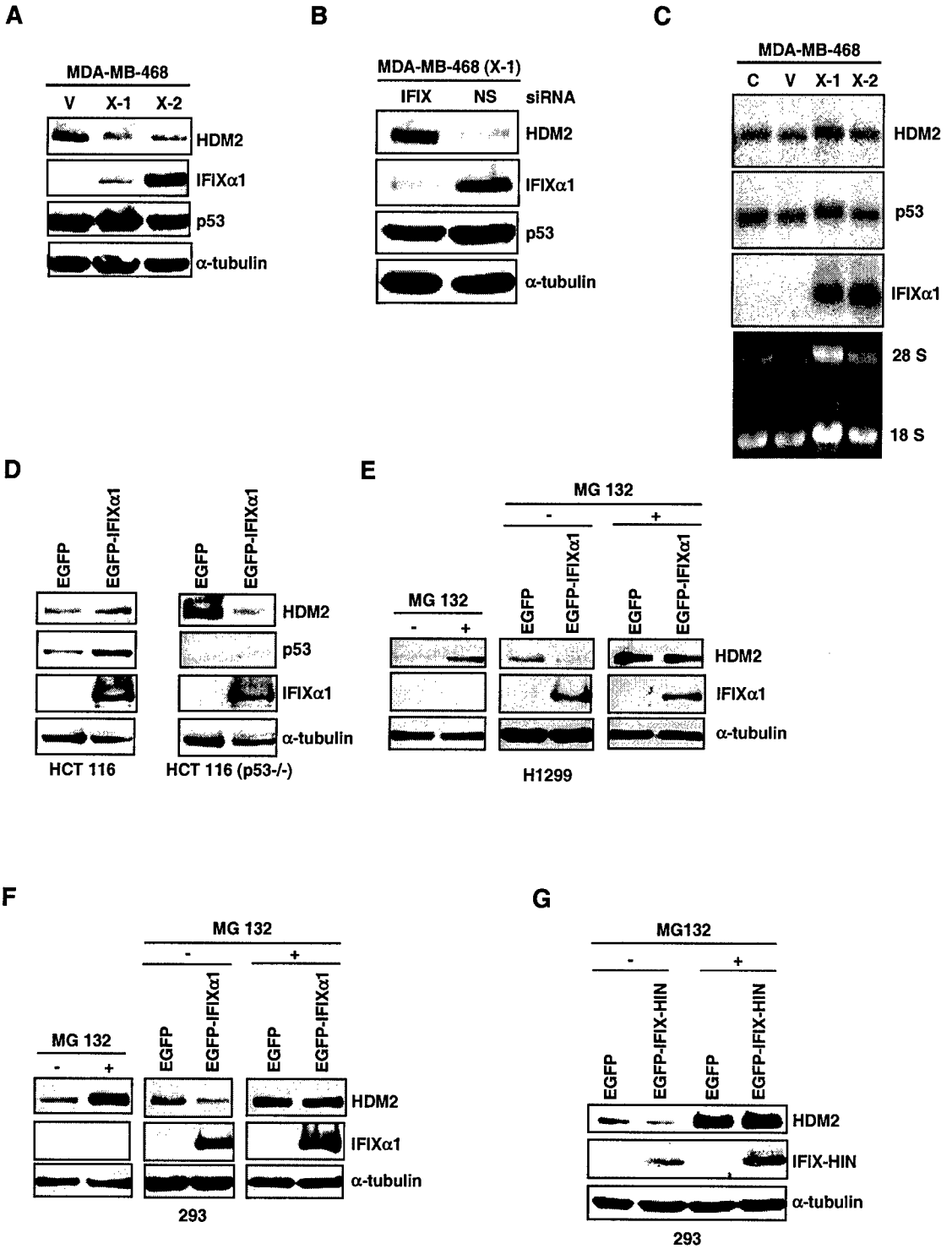
A
MDA-MB-468
V X-1 X-2
HDM2
IFIXα1
p53
α-tubulin
B
MDA-MB-468 (X-1)
IFIX NS siRNA
HDM2
IFIXα1
p53
α-tubulin
C
MDA-MB-468
C V X-1 X-2
HDM2
p53
IFIXα1
28 S
18 S
D
EGFP
EGFP-IFIXα1
HDM2
p53
IFIXα1
α-tubulin
HCT 116
HCT 116 (p53-/-)
E
MG 132
-
+
EGFP
EGFP-IFIXα1
HDM2
IFIXα1
α-tubulin
H1299
F
MG 132
EGFP
EGFP-IFIXα1
HDM2
IFIXα1
α-tubulin
293
G
MG132
EGFP
EGFP-IFIX-HIN
HDM2
IFIX-HIN
α-tubulin
293

Fig. 9

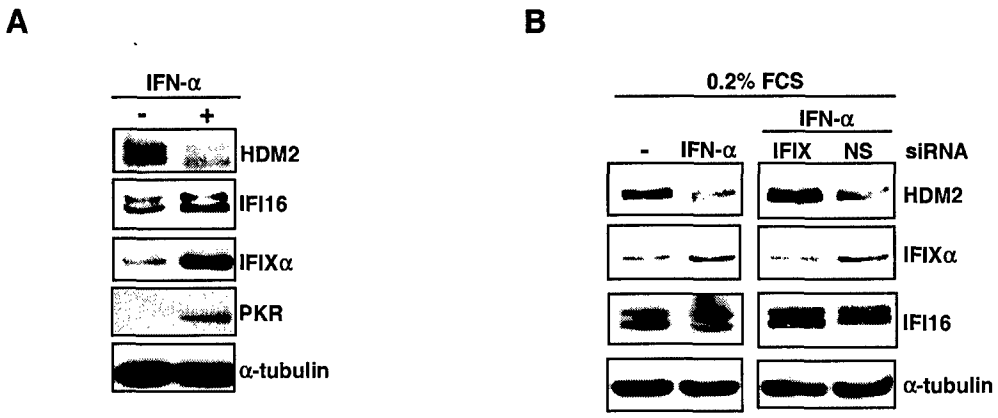
A
IFN-α
-
+
HDM2
IFI16
IFIXα
PKR
α-tubulin
B
0.2% FCS
IFN-α
-
IFN-α
IFIX
NS
siRNA
HDM2
IFIXα
IFI16
α-tubulin